

Summary of Seismic and Accident Load Conditions for Primary Components and Piping

Non-Proprietary Version

January 2009

**©2009 Mitsubishi Heavy Industries, Ltd.
All Rights Reserved**

Revision History

Revision	Page	Description
0	All	Original Issue

© 2009
MITSUBISHI HEAVY INDUSTRIES, LTD.
All Rights Reserved

This document has been prepared by Mitsubishi Heavy Industries, Ltd. (MHI) in connection with the U.S. Nuclear Regulatory Commission's (NRC) licensing review of MHI's US-APWR nuclear power plant design. No right to disclose, use or copy any of the information in this document, other than that by the NRC and its contractors in support of the licensing review of the US-APWR, is authorized without the express written permission of MHI.

This document contains technology information and intellectual property relating to the US-APWR and it is delivered to the NRC on the express condition that it not be disclosed, copied or reproduced in whole or in part, or used for the benefit of anyone other than MHI without the express written permission of MHI, except as set forth in the previous paragraph.

This document is protected by the laws of Japan, U.S. copyright law, international treaties and conventions, and the applicable laws of any country where it is being used.

Mitsubishi Heavy Industries, Ltd.
16-5, Konan 2-chome, Minato-ku
Tokyo 108-8215 Japan

Abstract

The purpose of this technical report is to present the seismic and accident loads for the US-APWR primary components and piping and the analysis methods used to produce them.

This report describes the development of the models, the modeling method and assumptions, the analysis approach, and the following analysis results:

Table of Contents

List of Tables	ii
List of Figures	iii
List of Acronyms	vi
1.0 INTRODUCTION	1-1
2.0 ANALYSIS PROCESS	2-1
2.1 Seismic Analysis	2-1
2.2 Accident Analysis	2-1
3.0 SEISMIC DESIGN CONDITION	3-1
3.1 Coupled RCL-Buildings Model	3-1
3.2 Seismic Motion and Site Conditions	3-1
4.0 DESIGN CONDITION OF ACCIDENT ANALYSIS	4-1
4.1 Consideration of Accident Design Conditions	4-1
4.2 Method of Accident Analysis	4-3
4.2.1 Blowdown Analysis	4-3
4.2.1.1 LOCA Blowdown	4-3
4.2.1.2 Main Steam Line Break Blowdown	4-4
4.2.2 Asymmetric Compartment Pressurization Analysis	4-5
4.2.2.1 Break Conditions	4-5
4.2.2.2 Nodalization Schemes	4-5
4.2.2.3 Calculated Pressure Response	4-5
5.0 DESCRIPTION OF RCL ANALYSIS	5-1
5.1 Model Development of RCL	5-1
5.2 Seismic Analysis of Coupled RCL-Building Model	5-2
5.3 Accident Analysis of RCL	5-5
5.3.1 Forcing Function of Dynamic Analysis	5-5
5.3.2 RCL Dynamic Analysis	5-6
5.4 Nozzle Loads from Piping Reaction Force	5-7
6.0 ANALYSIS OF REACTOR EQUIPMENT	6-1
6.1 Introduction	6-1
6.2 Seismic Loads	6-1
6.3 Hydraulic Loads in LOCA Events	6-2
6.4 Reactor Internals Dynamic Response Model	6-3
6.5 Response Analysis	6-4

Table of Contents (Cont'd)

7.0	ANALYSIS OF PRESSURIZER	7-1
7.1	Seismic Analysis	7-1
7.2	Accident Analysis	7-1
8.0	SUMMARY OF PRIMARY COMPONENTS LOADS	8-1
8.1	RCL Member Forces and Support Loads	8-1
8.2	Loads Related to RV and Reactor Equipment Dynamic Response	8-1
8.3	Component Loads of PZR	8-2
9.0	COMPUTER PROGRAM	9-1
10.0	CONCLUSION	10-1
11.0	REFERENCES	11-1

List of Tables

Table 3-1	Soil Spring Constants and Damping Coefficients	3-2
Table 8-1	List of Tables and Figures of RCL Seismic and Accident Loads	8-3
Table 8-2	Seismic Loads of Inlet and Outlet Nozzle on RV, SG, RCP	8-4
Table 8-3	Seismic Reaction Forces of Support Points	8-4
Table 8-4	Seismic Member Forces of MCP	8-5
Table 8-5	Seismic Loads of Nozzles on RV, SG, MCP	8-6
Table 8-6	Accident Loads of Inlet and Outlet Nozzle on RV, SG, RCP	8-6
Table 8-7	Accident Reaction Force of Support Points	8-7
Table 8-8	Accident Member Force of MCP	8-8
Table 8-9	Accident Loads of Nozzles on RV, SG, MCP	8-10
Table 8-10	Seismic and Accident Loads on Lower Reactor Internal Assembly	8-10
Table 8-11	Seismic and Accident Loads on Upper Reactor Internal Assembly	8-11
Table 8-12	Seismic and Accident Loads on Radial Support Keys	8-12
Table 8-13	Seismic and Accident Loads between Vessel / Reactor Internals Interface Loads	8-12
Table 8-14	Seismic and Accident Loads on RV Head Nozzles and IHP Lug	8-13
Table 8-15	Seismic and Accident Loads on CRDM	8-13
Table 8-16	Seismic Loads of PZR Component	8-14
Table 8-17	Seismic Loads of PZR Nozzles	8-14
Table 8-18	Accident Loads of PZR Nozzles	8-15

List of Figures

Figure 2-1	Seismic Analysis Process	2-2
Figure 2-2	Accident Analysis Process	2-3
Figure 3-1	Lumped Mass Stick Model for Buildings (R/B, PCCV, CIS)	3-3
Figure 3-2	Coupled Stick Mass Model for RCL and Buildings	3-4
Figure 3-3	US-APWR Horizontal CSDRS	3-5
Figure 3-4	US-APWR Vertical CSDRS	3-5
Figure 3-5	Artificial Time Histories Plots (H1)	3-6
Figure 3-6	Artificial Time Histories Plots (H2)	3-7
Figure 3-7	Artificial Time Histories Plots (V)	3-8
Figure 4-1	Blowdown Analysis Model for Cases 1: Cold Leg 14 inches Break (B-Loop)	4-6
Figure 4-2	Blowdown Analysis Model for Case 2: Hot Leg 10 inches Break (B-Loop)	4-7
Figure 4-3	Blowdown Analysis Model for Intact A, C & D Loops (for all cases)	4-8
Figure 4-4	Blowdown Analysis Model for Downcomer Region (all cases)	4-9
Figure 4-5	Blowdown Analysis Model for Core Region (all cases)	4-10
Figure 4-6	Pressure at Break Region of Case 1	4-11
Figure 4-7	Flow Rate at Break Region of Case 1	4-11
Figure 4-8	Pressure at RV Outlet Nozzle of Case 1	4-12
Figure 4-9	Pressure at RV Inlet Nozzle of Case 1	4-12
Figure 4-10	Differential Pressure Between Core and Downcomer of Case 1	4-13
Figure 4-11	Differential Pressure Between Downcomer 0 degree and 180 degree of Case 1	4-13
Figure 4-12	Pressure at Break Region of Case 2	4-14
Figure 4-13	Flow Rate at Break Region of Case 2	4-14
Figure 4-14	Pressure at RV Outlet Nozzle of Case 2	4-15
Figure 4-15	Pressure at RV Inlet Nozzle of Case 2	4-15
Figure 4-16	Differential Pressure Between Core and Downcomer of Case 2	4-16
Figure 4-17	Differential Pressure Between Downcomer 0 degree and 180 degree of Case 2	4-16
Figure 4-18	Main Steam Line Break Blowdown Analysis Model	4-17
Figure 4-19	Pressure at Steam Outlet Nozzle of Case 1	4-18
Figure 4-20	Fluid Density at Steam Outlet Nozzle of Case 1	4-18
Figure 4-21	Flow Rate at Steam Outlet Nozzle of Case 1	4-19
Figure 4-22	Nodalization Scheme for SG Compartment Analysis	4-20
Figure 4-23	Nodalization Scheme for SG Compartment Analysis	4-21

List of Figures (Cont'd)

Figure 4-24	Nodalization Scheme for SG Compartment Analysis	4-22
Figure 4-25	Nodalization Scheme for SG Compartment Analysis	4-23
Figure 4-26	Nodalization Scheme for SG Compartment Analysis	4-24
Figure 4-27	Nodalization Diagram for SG Compartment Analysis	4-25
Figure 4-28	Nodalization Diagram for SG Compartment Analysis	4-26
Figure 4-29	Pressure Transient at The Node V70	4-27
Figure 4-30	Pressure Transient at The Node V68	4-27
Figure 5-1	US-APWR RCL	5-8
Figure 5-2	Stick Mass Model for RV with Internals	5-9
Figure 5-3	Stick Mass Model for SG with Internals	5-10
Figure 5-4	Stick Mass Model for RCP with Internals	5-11
Figure 5-5	RCL Piping Model	5-12
Figure 5-6	RV Support and FE Structural Model	5-13
Figure 5-7	Spring Model of SG Upper Shell Support	5-14
Figure 5-8	Spring Model of SG Intermediate Shell Support	5-15
Figure 5-9	Stick Mass Spring Model for RCL	5-16
Figure 5-10	RCL Model for Accident Analysis	5-17
Figure 5-11	SG Lower Support and RCP Tie Rod	5-18
Figure 6-1	Horizontal Hydraulic Loads on RV during LOCA	6-5
Figure 6-2	Vertical Hydraulic Loads on RV during LOCA	6-5
Figure 6-3	RV and Internals Dynamic Analysis Model	6-6
Figure 6-4	Model Details Inside The Core Barrel and Lower Plenum	6-7
Figure 6-5	Horizontal Displacement of RV during LOCA	6-8
Figure 6-6	Vertical Displacement of RV during LOCA	6-8
Figure 7-1	Stick Mass Model for PZR	7-2
Figure 7-2	Spring Model of PZR Upper Supports	7-3
Figure 7-3	ISRS for PZR	7-4
Figure 8-1	RV Nozzle Load	8-16
Figure 8-2	SG Nozzle Load	8-16
Figure 8-3	RCP Nozzle Load	8-17
Figure 8-4	Reaction Force of SG Support Points	8-18
Figure 8-5	Reaction Force of RCP Lower Support Points	8-19
Figure 8-6	MCP Member Forces	8-20

List of Figures (Cont'd)

Figure 8-7	RV Nozzles	8-21
Figure 8-8	SG Nozzles	8-22
Figure 8-9	RCP Nozzle	8-23
Figure 8-10	MCP Nozzles	8-24
Figure 8-11	RV and Reactor Internals	8-25
Figure 8-12	Locations of Stress Evaluation on Lower Reactor Internal Assembly	8-26
Figure 8-13	Locations of Stress Evaluation on Upper Reactor Internal Assembly	8-27
Figure 8-14	CRDM Assembly	8-28
Figure 8-15	Axial Force vs Elevation on CRDM (SSE+LOCA)	8-29
Figure 8-16	Shear Force vs Elevation on CRDM (SSE+LOCA)	8-29
Figure 8-17	Bending Moment vs Elevation on CRDM (SSE+LOCA)	8-30
Figure 8-18	Horizontal UCP Acceleration during SSE	8-31
Figure 8-19	Horizontal LCSP Acceleration during SSE	8-31
Figure 8-20	Horizontal UCP Acceleration during LOCA	8-32
Figure 8-21	Horizontal LCSP Acceleration during LOCA	8-32
Figure 8-22	Reaction Force of PZR Lower Elements	8-33
Figure 8-23	PZR Nozzles	8-34

List of Acronyms

The following list defines the acronyms used in this document.

ASME	American Society of Mechanical Engineers
CIS	Containment Internal Structure
CRDM	Control Rod Drive Mechanism
CSDRS	Certified Seismic Design Response Spectra
CVCS	Chemical and Volume Control System
DCD	Design Control Document
DOFs	Degrees of Freedom
DVI	Direct Vessel Injection
FEs	Finite Elements
FW	Feedwater
ISRS	In-Structure Response Spectra
LBB	Leak-before-break
LOCA	Loss of Coolant Accident
MCP	Main Coolant Piping
MS	Main Steam
PCCV	Prestressed Concrete Containment Vessel
PGA	Peak Ground Acceleration
PZR	Pressurizer
R/B	Reactor Building
RCL	Reactor Coolant Loop
RCP	Reactor Coolant Pump
RCS	Reactor Coolant System
RG	Regulatory Guide
RHR	Residual Heat Removal
RV	Reactor Vessel
SG	Steam Generator
SI	Safety Injection
SRP	Standard Review Plan
SRSS	Square Root of the Sum of the Squares
SSE	Safe Shutdown Earthquake
SSI	Soil-structure Interaction

1.0 INTRODUCTION

This technical report describes the methods and results of the analysis methods used to determine the seismic and accident loads for the US-APWR primary system components. These loads will be used as design inputs for stress analysis as described in Subsection 3.9.3 of the US-APWR design control document (DCD).

Section 2.0 describes the steps in the analysis process used to develop the seismic and accident loads for the primary system components and piping.

Section 3.0 describes the seismic motion and site conditions used as input for the analysis of the primary system components and piping. The seismic analysis is based on the technical report MUAP-08005, Rev.0, "Dynamic Analysis of the Coupled RCL-R/B-PCCV-CIS" (Reference 1).

Section 4.0 defines the accident design conditions including postulated accidents associated with level C and D service conditions and analyses of associated loads including initial boundary conditions, modeling, and results. The analysis of asymmetric compartment pressurization loads is included.

Section 5.0 presents an integrated analysis of the reactor coolant loop (RCL) subject to the seismic and accident loads developed in the preceding sections of the report. The RCL model and methods of dynamic analysis are described.

Sections 6.0 and 7.0 describe the analysis to define the dynamic responses of the reactor vessel (RV) and pressurizer (PZR), respectively, to the seismic and postulated accident loads.

Section 8.0 provides a summary of the seismic and accident loads for the component nozzles, supports points, and members of the main coolant system. It provides the loads at the locations to be included in the design stress analyses.

Section 9.0 describes the computer codes used in the analyses described in the report.

Finally, Section 10.0 presents the overall conclusions of the report.

Seismic and accident loads are applied the stress analysis and evaluation in accordance with American Society of Mechanical Engineers (ASME) Code, Section III (Reference 2) which requires stress evaluation on Level C and D Service conditions. Summary of stress analysis and related information of primary components and piping will be provided technical reports in a separate.

2.0 ANALYSIS PROCESS

2.1 Seismic Analysis

The seismic analysis process depicted in Figure 2-1 shows the steps used to generate the safe shutdown earthquake (SSE) loads in the primary components, piping, and the support structure.

2.2 Accident Analysis

The accident analysis process depicted in Figure 2-2 shows the steps used to generate the RCL pipe rupture forces in the primary components, loop piping, and the support structures.

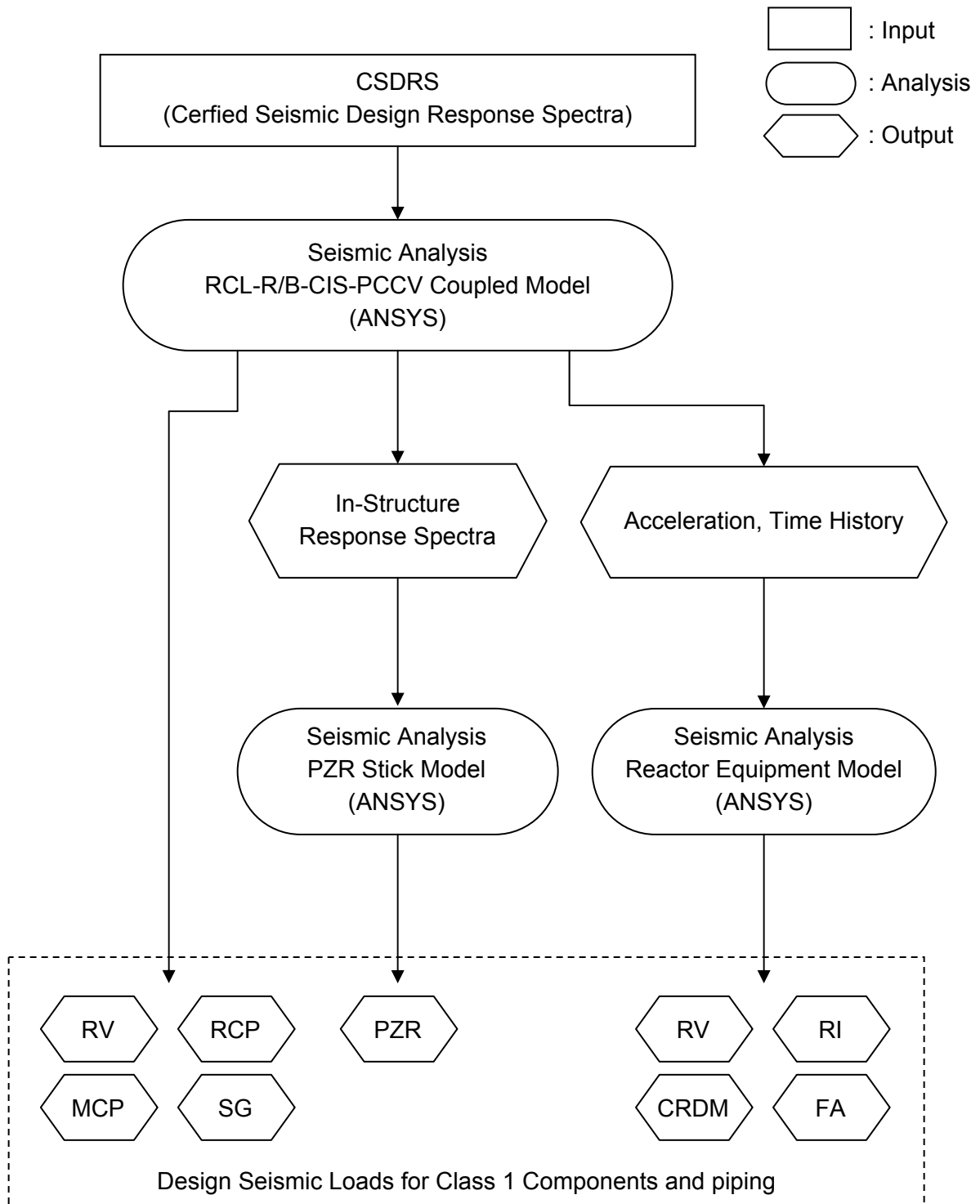
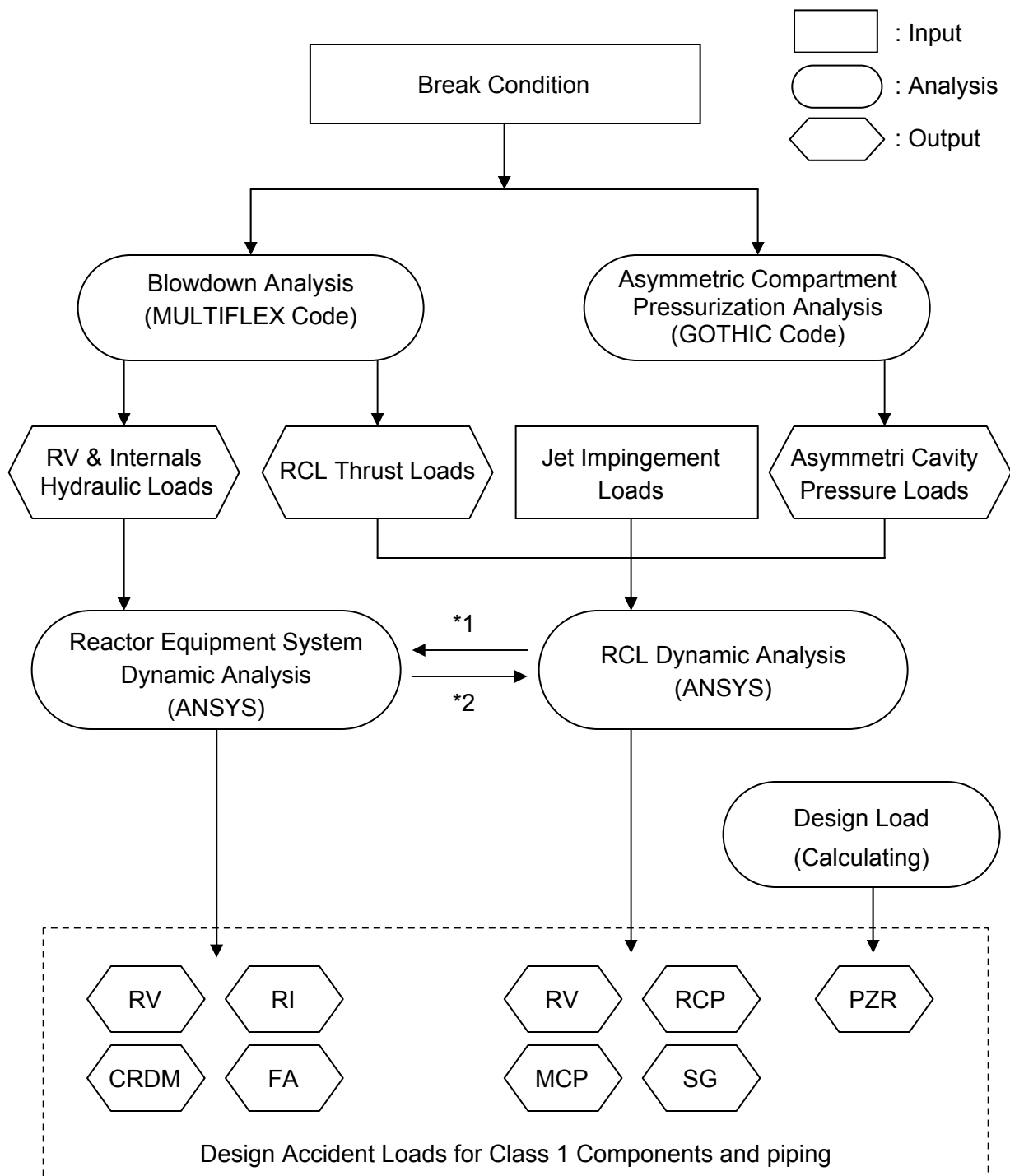


Figure 2-1 Seismic Analysis Process



*1 : Reactor Coolant Loop Force from RCL is provided for RV LOCA Analysis

*2 : RV Displacement is provided for RCL Dynamic Analysis

Figure 2-2 Accident Analysis Process

3.0 SEISMIC DESIGN CONDITION

This section provides the seismic design conditions for the US-APWR primary components and piping system. The seismic analysis is based on the coupled model of the RCL and the building structures, including the reactor building (R/B), the prestressed concrete containment vessel (PCCV), and containment internal structures (CIS).

3.1 Coupled RCL-Buildings Model

The seismic design evaluation of the coupled model of RCL and the building structures was developed using a lumped mass stick model representing the stiffness and mass characteristics of RCL components and the piping system coupled with the building structures. The building structures (R/B, PCCV, and CIS) are also represented as a lumped mass stick model rigidly connected to the basemat as shown in Figure 3-1. These models of the building structures are described in Appendix 3H of the US-APWR DCD. The effects of soil-structure interaction (SSI) are included in the analysis utilizing frequency-independent lumped soil springs and damping. The resulting analytical model represents all six degrees of freedom (DOFs).

Figure 3-2 shows the complete lumped mass coupled model of RCL and the building structures. The detailed descriptions of RCL model are described more fully in Section 5.

3.2 Seismic Motion and Site Conditions

The seismic input of ground motion is represented in the US-APWR DCD as the Certified Seismic Design Response Spectra (CSDRS). The CSDRS are sufficiently broad banded and expected to envelope the seismic design ground motion at a wide range of sites in the central and eastern United States. The CSDRS are similar to the standard shapes of the Regulatory Guide (RG) 1.60 (Reference 3) spectra with an enhanced high frequency content anchored to a peak ground acceleration (PGA) of 0.3 g as shown in Figures 3-3 and 3-4. Figures 3-5 through 3-7 present the acceleration, velocity and displacement time histories used in the seismic analysis.

The site-independent seismic conditions of US-APWR standard plant are performed by the following four kinds of frequency independent SSI impedance parameters, based on the assumption that the subgrade conditions are relatively uniform up to a depth of one equivalent foundation diameter below the bottom of the combined R/B and PCCV mat foundation. The following values for shear wave V_s , density γ and Poisson's ratio ν are assigned to the uniform elastic half-space to simulate the general subgrade conditions:

- Soft soil site, $V_s = 1,000$ ft/s, $\gamma = 110$ pcf, $\nu = 0.40$
- Rock site (Medium 1), $V_s = 3,500$ ft/s, $\gamma = 130$ pcf, $\nu = 0.35$
- Rock site (Medium 2), $V_s = 6,500$ ft/s, $\gamma = 140$ pcf, $\nu = 0.35$
- Hard rock site, $V_s = 8,000$ ft/s, $\gamma = 160$ pcf, $\nu = 0.30$

The soil spring constants and damping coefficients for each site condition, which are attached at the base bottom of the building stick model, are evaluated in Table 3-1.

Table 3-1 Soil Spring Constants and Damping Coefficients

Type of Spring			Soft	Medium 1	Medium 2	Hard Rock
			Subgrade Vs=1,000 (ft/s)	Subgrade Vs=3,500 (ft/s)	Subgrade Vs=6,500 (ft/s)	Subgrade Vs=8,000 (ft/s)
NS	Horizontal	Spring Const. ($\times 10^8$ lb/in)	1.89	26.4	98.2	Fixed Base Assumption
		Damping Coef. ($\times 10^7$ lb·s/in)	0.948	3.78	7.56	
	Rotational	Spring Const. ($\times 10^{14}$ lb·in/rad)	7.83	105.	389.	
		Damping Coef. ($\times 10^{13}$ lb·in·s/rad)	3.81	12.3	24.9	
EW	Horizontal	Spring Const. ($\times 10^8$ lb/in)	2.05	28.6	106.	
		Damping Coef. ($\times 10^7$ lb·s/in)	1.02	4.09	8.16	
	Rotational	Spring Const. ($\times 10^{14}$ lb·in/rad)	4.57	61.0	227.	
		Damping Coef. ($\times 10^{13}$ lb·in·s/rad)	1.68	6.46	13.0	
UD	Vertical	Spring Const. ($\times 10^8$ lb/in)	2.62	35.0	130.	
		Damping Coef. ($\times 10^7$ lb·s/in)	3.23	12.3	24.6	
	Torsional	Spring Const. ($\times 10^{14}$ lb·in/rad)	7.24	105.	389.	
		Damping Coef. ($\times 10^{13}$ lb·in·s/rad)	1.54	6.54	13.2	

Note:

The points located at the upper level of basemat (RE00, IC00, CV00) are considered as the fixed end points when a fixed base assumption is adopted.

Security-Related Information - Withheld Under 10 CFR 2.390

Figure 3-1 Lumped Mass Stick Model for Buildings (R/B, PCCV, CIS)

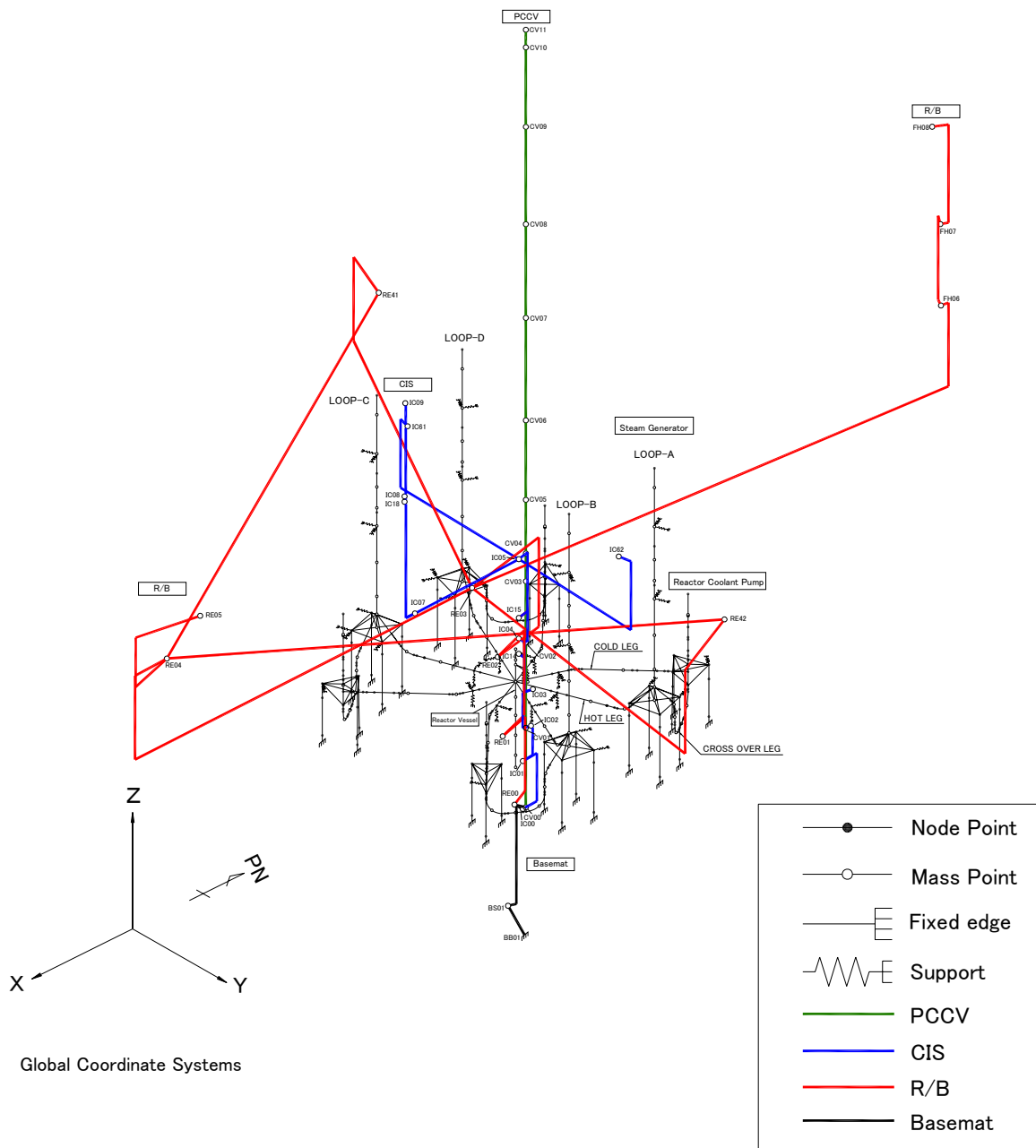
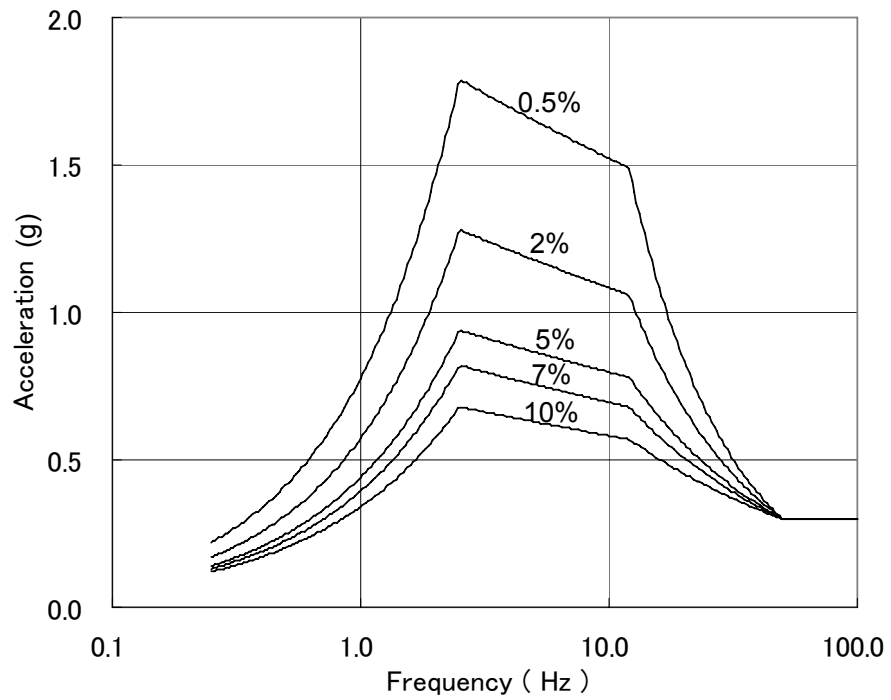
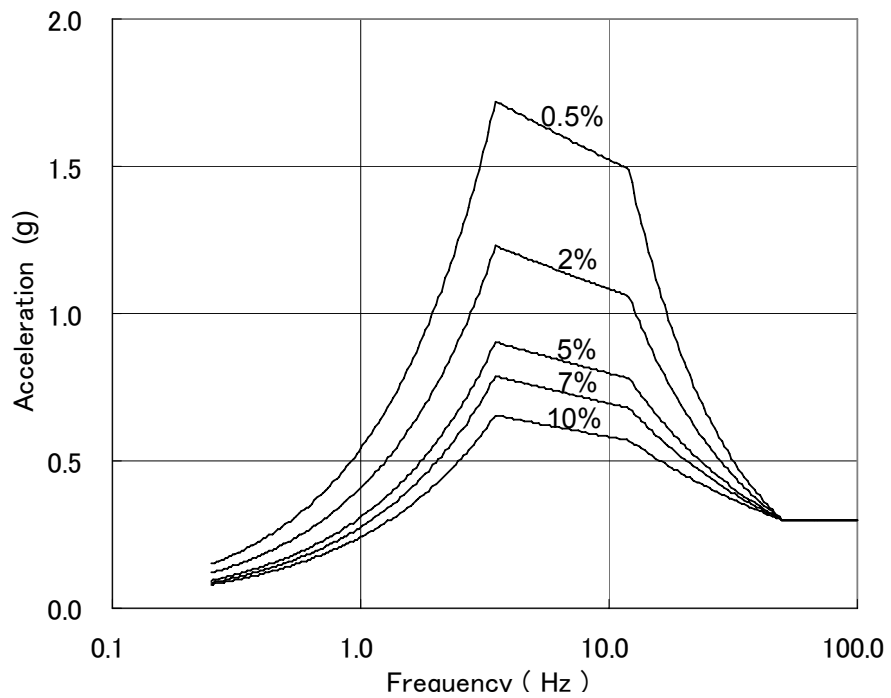


Figure 3-2 Coupled Stick Mass Model for RCL and Buildings



Note: spectra for damping 0.5, 2, 5, 7, 10%.

Figure 3-3 US-APWR Horizontal CSDRS



Note: spectra for damping 0.5, 2, 5, 7, 10%.

Figure 3-4 US-APWR Vertical CSDRS

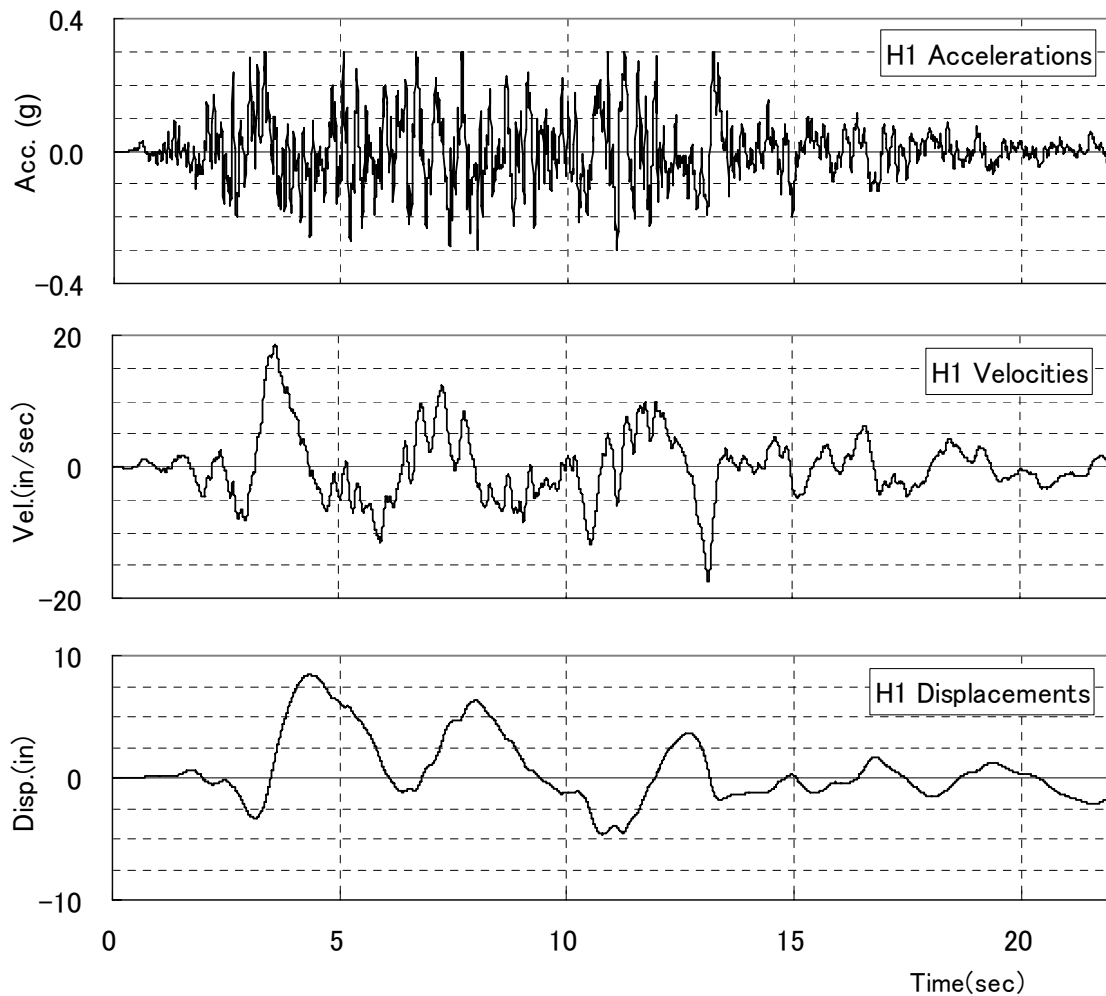


Figure 3-5 Artificial Time Histories Plots (H1)

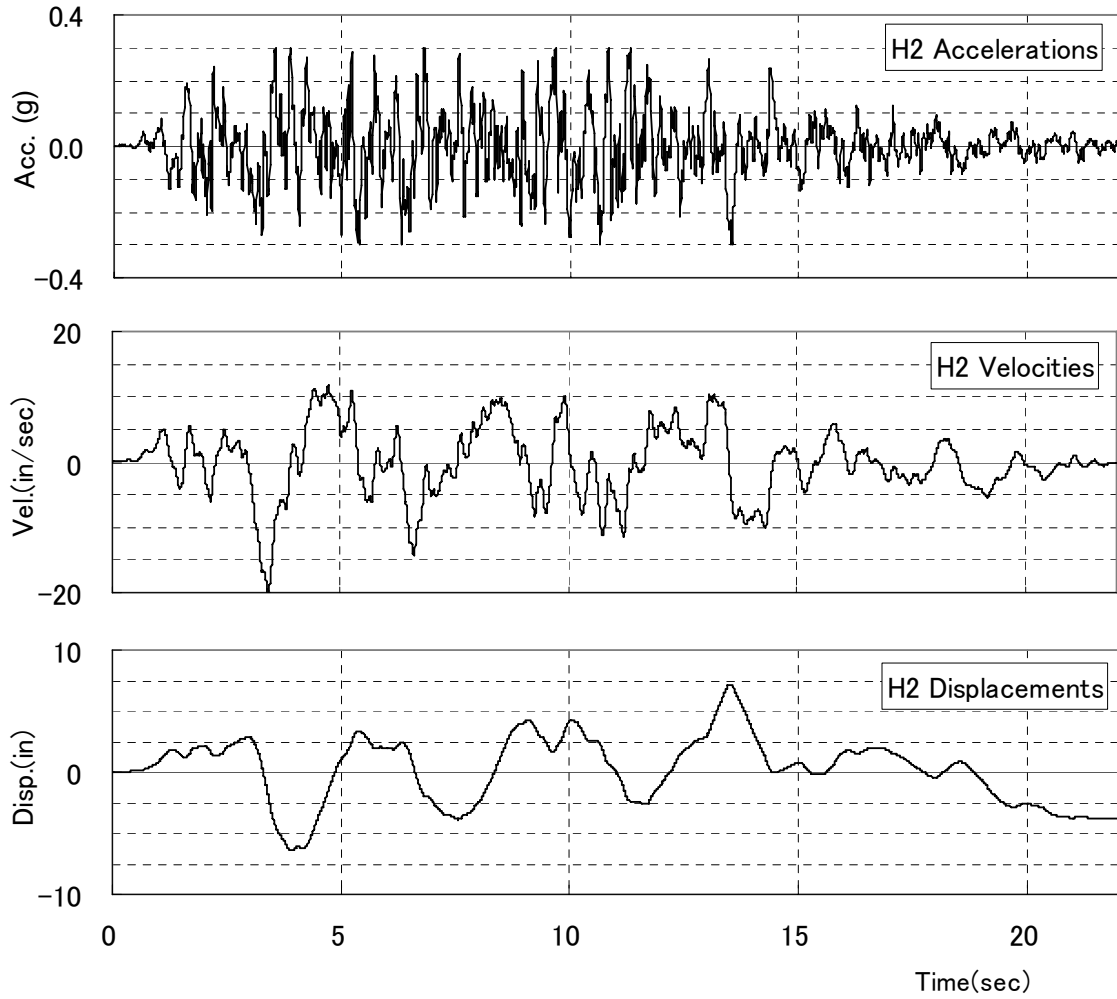


Figure 3-6 Artificial Time Histories Plots (H2)

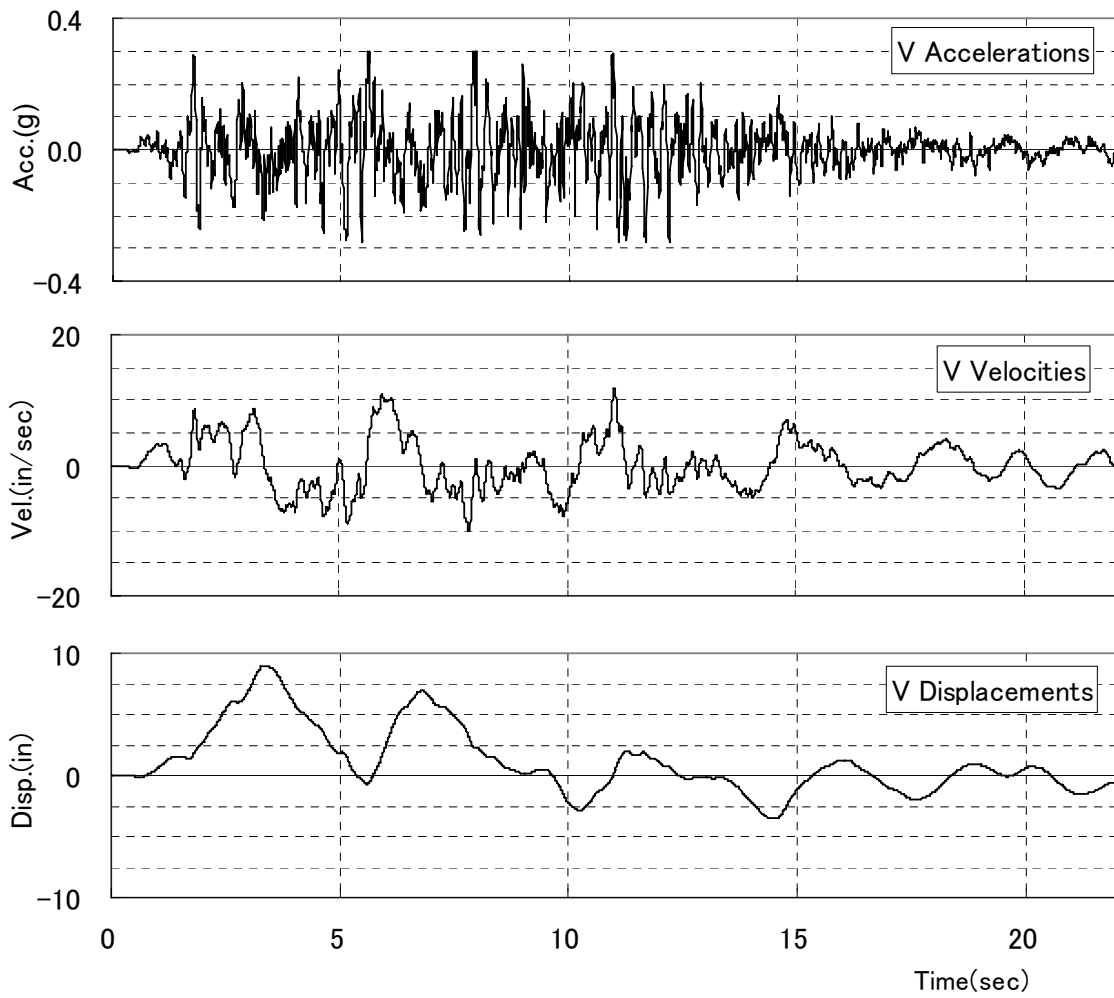


Figure 3-7 Artificial Time Histories Plots (V)

4.0 DESIGN CONDITION OF ACCIDENT ANALYSIS

4.1 Consideration of Accident Design Conditions

DCD 3.9.1 identifies the following events as Level C and D service conditions.

• Level C

- Small Loss of Coolant Accident (LOCA)
- Small Main Steam (MS) Line Break
- Complete Loss of Flow
- Small Feedwater (FW) Line Break
- Steam Generator (SG) Tube Rupture

• Level D

- Large LOCA
- Large Main Steam Line Break
- Large Feedwater Line Break
- Reactor Coolant Pump (RCP) Locked Rotor
- Control Rod Ejection

US-APWR has applied the leak-before-break (LBB) methodology. As a result the main coolant piping (MCP) break and surge line break dynamic evaluations are eliminated. The postulated pipe break events that are evaluated for the reactor coolant system (RCS) loop components are as follows.

- Hot Leg Branch Line break at the 10 inch Schedule 160 Residual Heat Removal (RHR)/ Safety Injection (SI) line nozzle
- Cold Leg Branch Line break at the 14 inch Schedule 160 accumulator line nozzle
- Feedwater Line break at the SG FW nozzle
- Main Steam Line break at the SG MS nozzle

Following portions must be protected against mechanical loads of the LOCA and secondary side pipe rupture (MS line break and FW line break).

a. LOCA

(a) Intact loop including branch piping and support components.

(b) Intact leg main coolant pipe of affected loop, SG support components and RCP support components in order to maintain the flow path.

- (e) Intact leg safety injection line connected to intact leg of affected loop in order to maintain safety injection.
 - (f) MS line and main FW line in order to prevent simultaneous rupture of secondary side.
- b. All of primary side must be protected against secondary side pipe rupture.

4.2 Method of Accident Analysis

4.2.1 Blowdown Analysis

The blowdown analysis was performed to provide the hydraulic transient input for each postulated pipe break event except FW line break accident. The thrust force due to pipe break at FW nozzle was needed in the dynamic analysis of RCS loop described in the section 5.3.1, but it was calculated according to the simplified method given in Appendix B of ANSI/ANS-58.2-1988 (Reference 6).

4.2.1.1 LOCA Blowdown

(1) Introduction

As shown in Figure 2-2, the blowdown analysis of a postulated pipe break accident provides the hydraulic transient input for primary coolant system stress evaluation. The blowdown analysis was performed using the MULTIFLEX hydraulic depressurization analysis code that is described in detail in Section 9.0, Computer Programs. The specification of the procedures, methodology and result for this blowdown analysis are described below.

(2) Condition

(a) Analysis Cases

The sizes and locations of the break for each of the analysis cases are:

Case 1	Cold Leg Accumulator Line 14 inches Nozzle Break, and
Case 2	Hot Leg RHR and SIS Line 10 inches Nozzle Break

which are consistent with the description in subsection 4.1.

(b) Initial Condition

The initial condition for blowdown analysis was at 102% power in accordance with NUREG-0800 Standard Review Plan (SRP) 3.6.2. (Reference 5)

(c) Analysis Model

Figure 4-1 shows the loop nodal diagram for the cold leg accumulator line 14B nozzle break for case 1. Figure 4-2 shows the loop nodal diagram for the hot leg RHR and SIS line 10B pipe break for case 2. Figure 4-3 shows the intact loop nodal diagram. Figure 4-4 shows the downcomer nodal diagram. Figure 4-5 shows the nodal diagram for the inside of the core barrel.

(3) Result

The blowdown hydraulic analysis for each case was performed for 500 milliseconds. Figures 4-6 through 4-17 show the results of the blowdown analysis for each case. These figures show the pressure and mass flow rate at the break region, the pressure at RV outlet and inlet nozzles, the differential pressure between the core and the downcomer regions, and the differential pressure between the downcomer regions at 0° and 180°.

4.2.1.2 Main Steam Line Break Blowdown

(1) Introduction

The blowdown analysis of the postulated steam line break accident also provides the break flow transient for jet force evaluation from the secondary coolant system after the pipe break. The blowdown analysis was performed using the M-RELAP5 code that is described in section 9.0 Computer Programs. The specification of the procedures, methodology and results for this blowdown analysis are described below:

(2) Condition

(a) Analysis Cases

The size and location of the break for the analysis case is:

Case 1: Main steam line break at the MS nozzle on the SG,
which is consistent with the description in subsection 4.1.

(b) Initial Condition

The initial condition for blowdown analysis was at 0% power in accordance with NUREG-0800 SRP 3.6.2. (Reference 5)

(c) Analysis Model

Figure 4-18 shows the SG nodal diagram which includes the break location at the Steam Line piping nozzle for case 1.

(d) Result

The blowdown analysis was performed for 3.0 seconds. Figures 4-19 through 4-21 show the results of the blowdown analysis including the pressure, fluid density, and mass flow rate at the steam outlet nozzle.

4.2.2 Asymmetric Compartment Pressurization Analysis

The asymmetric pressurization due to a postulated piping break was performed to provide the load conditions for components. The asymmetric pressurization analysis was performed by using the GOTHIC code. An overview of the GOTHIC code is described in section 9.0.

4.2.2.1 Break Conditions

- The analysis cases break sizes and locations, consistent with the description in subsection 4.1, are : RHR pump inlet line 10 inches break
- ACC injection line 14 inches break
- Feedwater line 16 inches break

Because the MS nozzle is located at open space without surrounding walls, the asymmetric pressurization due to MS nozzle break is not generated. Therefore MS nozzle break was excluded from the piping postulated break.

4.2.2.2 Nodalization Schemes

A separate GOTHIC evaluation model was prepared for the SG compartment. In this model, the compartment was divided into nodes, with paths defined to model the transfer of mass and energy between nodes during the analyzed transient. The compartment nodalization scheme was selected so that nodal boundaries are basically at the location of flow obstructions or geometry changes within the compartment. These discontinuities create pressure differentials across nodal boundaries. Annular configurations were nodalized circumferentially when asymmetric pressure distribution was presumed.

The nodalization scheme for US-APWR the SG compartment pressure analysis is shown in Figure 4-22 to Figure 4-26. The SG compartment was azimuthally divided into 4 sectors around the SG and the RCP, and vertically divided into 8 sectors for the SG region, and 6 sectors for the RCP region. The region close to FW line nozzle was divided in smaller nodes. The vertical nodal boundaries are basically at the location of flow obstructions (gratings) or geometry changes. The GOTHIC nodalization for the SG compartment analysis is shown in Figure 4-27 and Figure 4-28. A total of 99 nodes, including the containment atmosphere and other compartment nodes, are used for the SG compartment analyses.

The flow area of each vent path was conservatively estimated considering the flow obstruction by main components including margin. The friction length was conservatively estimated considering the length of the estimated flow line plus margin. The loss coefficient was conservatively estimated considering the effect of obstruction, contraction and expansion plus margin.

4.2.2.3 Calculated Pressure Response

The calculated pressure transients at typical nodes in the case of FW line nozzle break are shown in Figure 4-29 and Figure 4-30. The selected nodes are close to the break point and connecting with the SG. The node including the break point is V70. The load to the SG due to the asymmetric pressurization was calculated with the pressure transient data and area of all nodes contacting the SG.

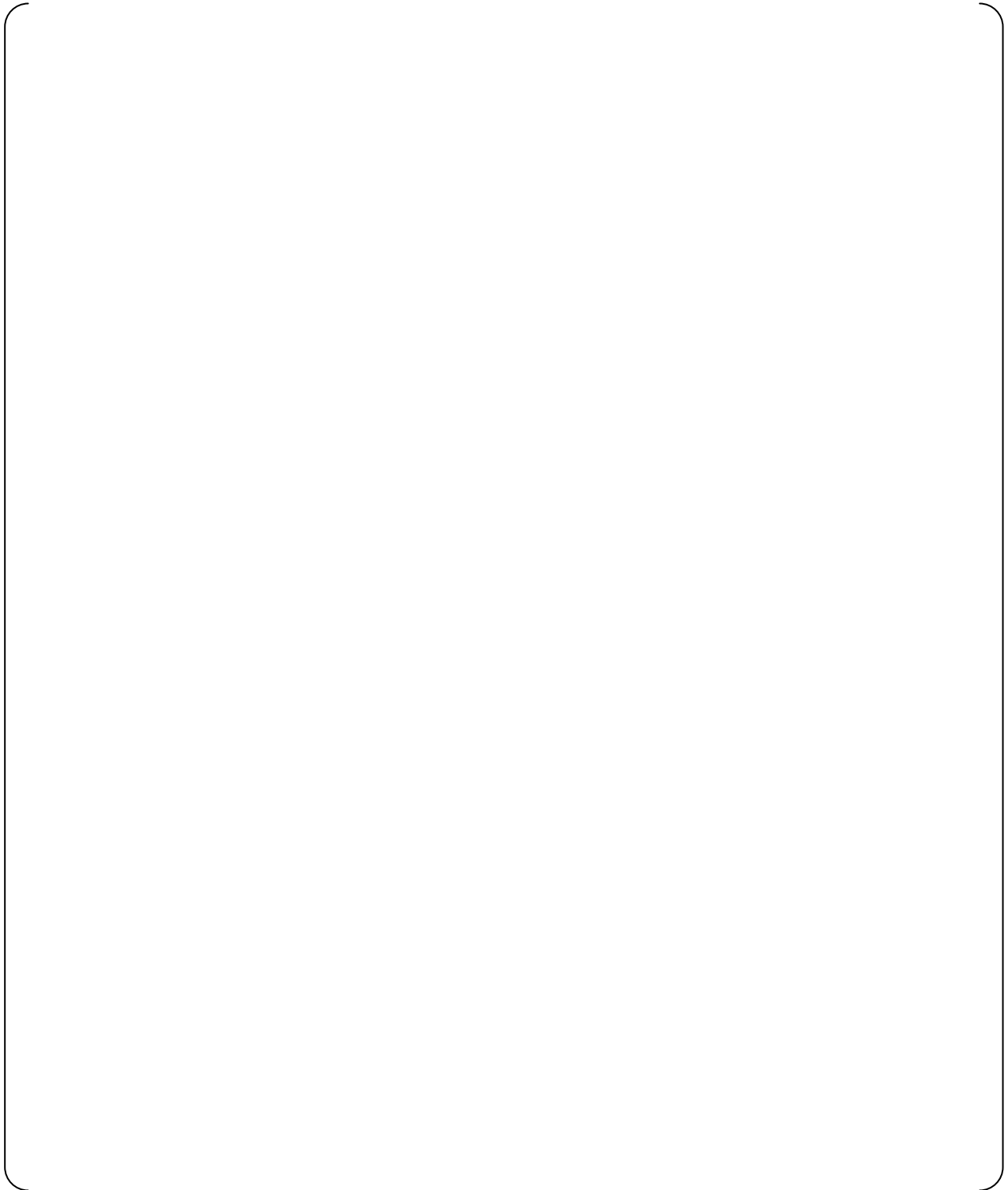


Figure 4-1 Blowdown Analysis Model for Cases 1: Cold Leg 14 inches Break (B-Loop)

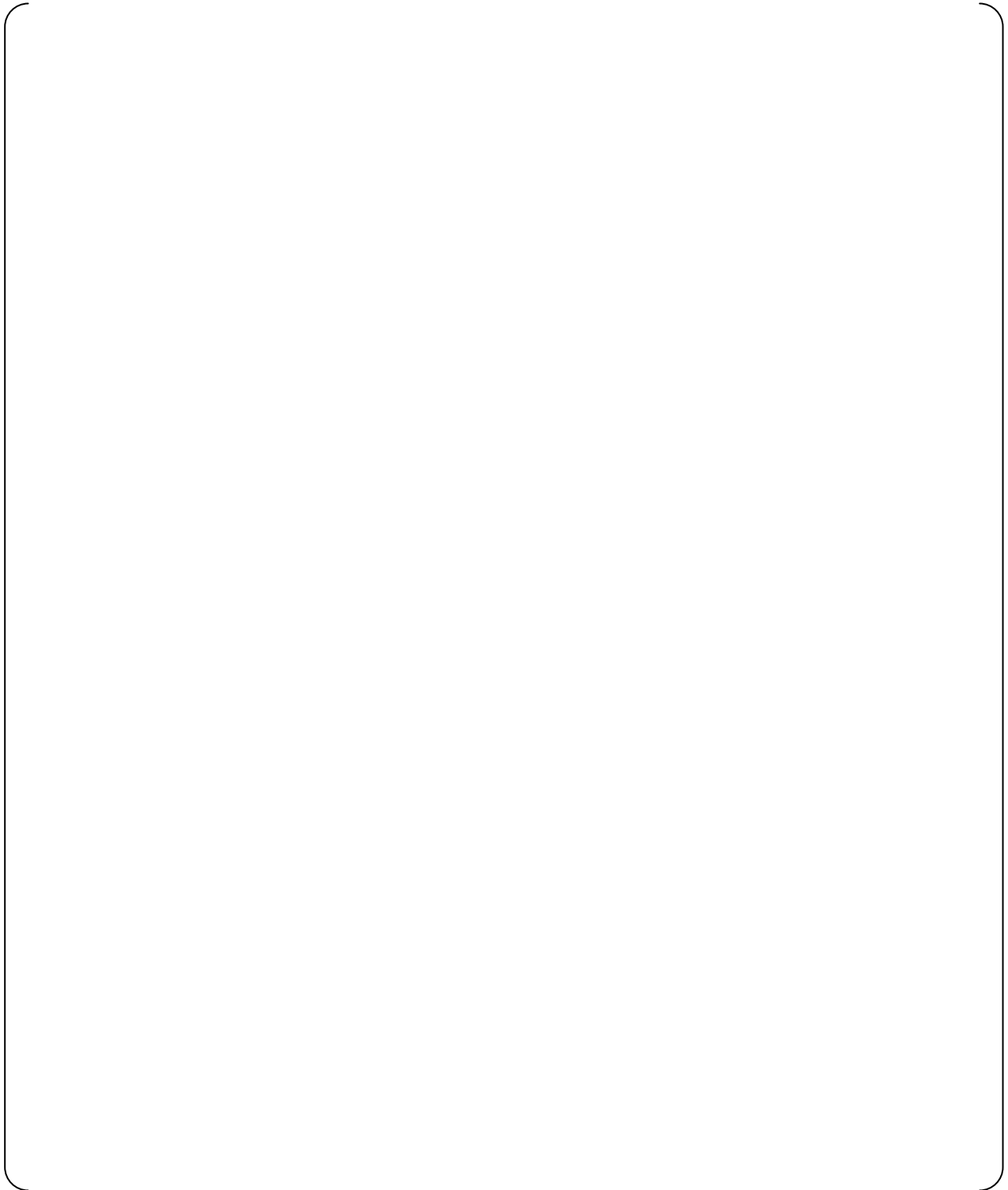


Figure 4-2 Blowdown Analysis Model for Case 2: Hot Leg 10 inches Break (B-Loop)

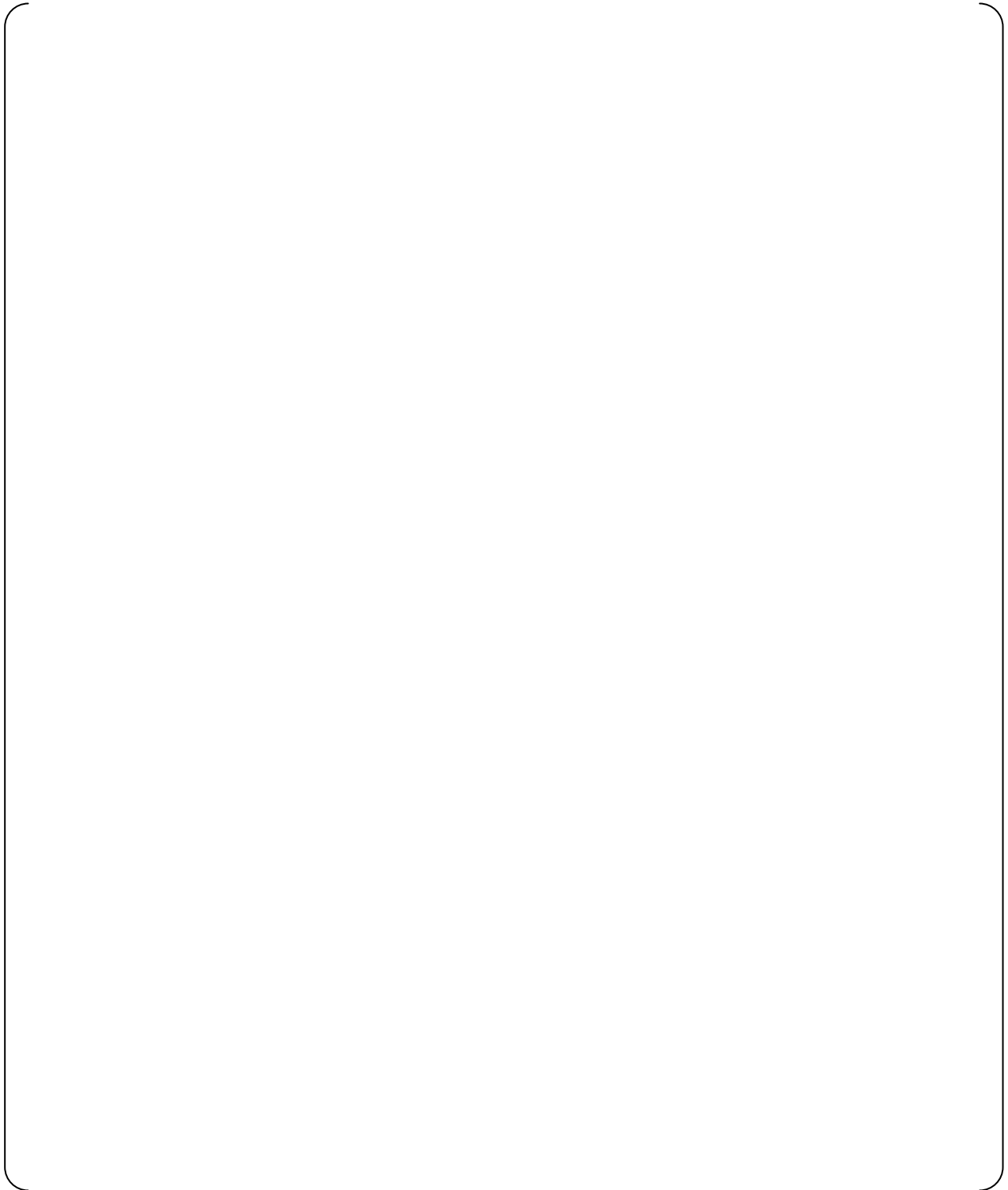


Figure 4-3 Blowdown Analysis Model for Intact A, C & D Loops (for all cases)

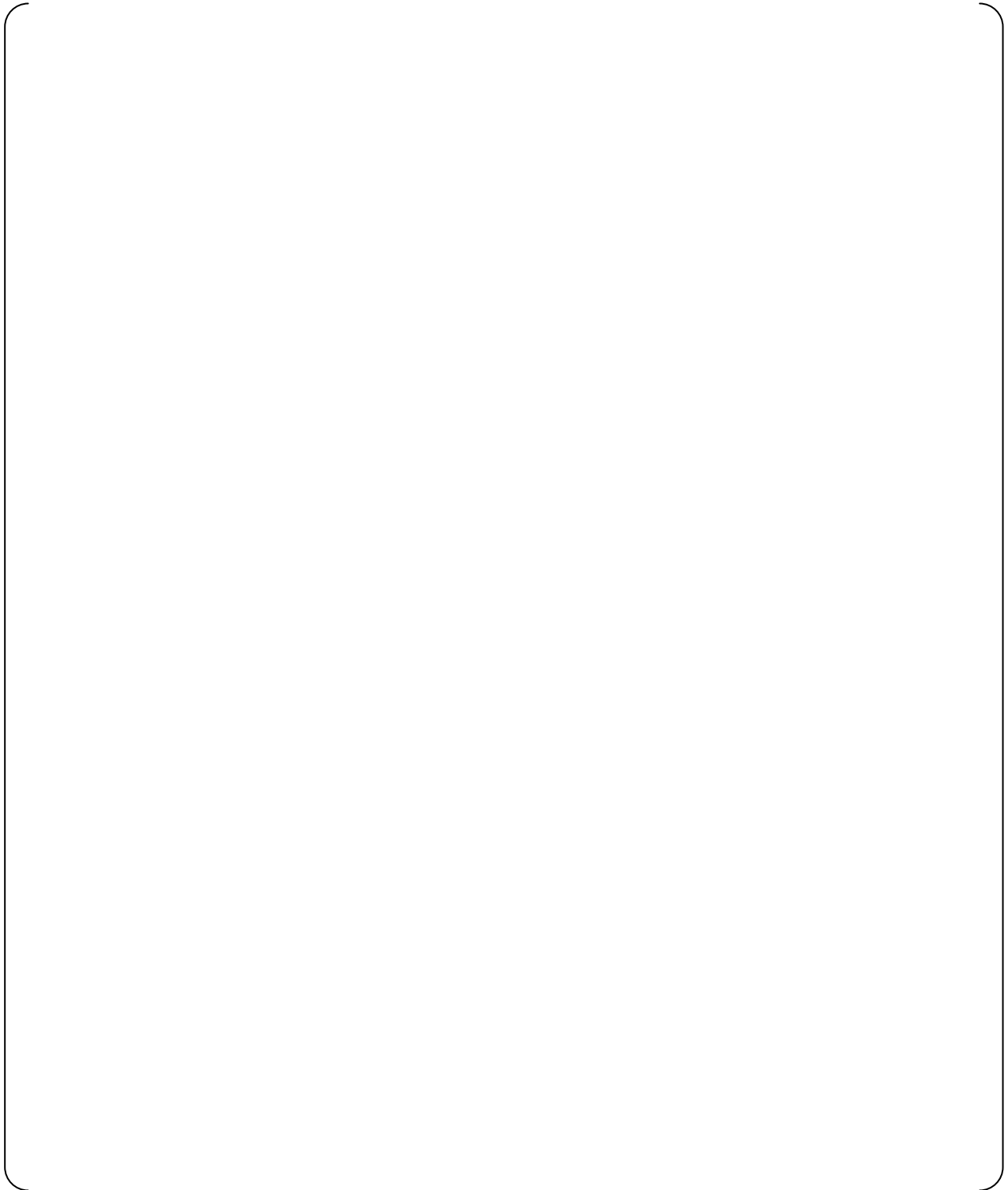


Figure 4-4 Blowdown Analysis Model for Downcomer Region (all cases)

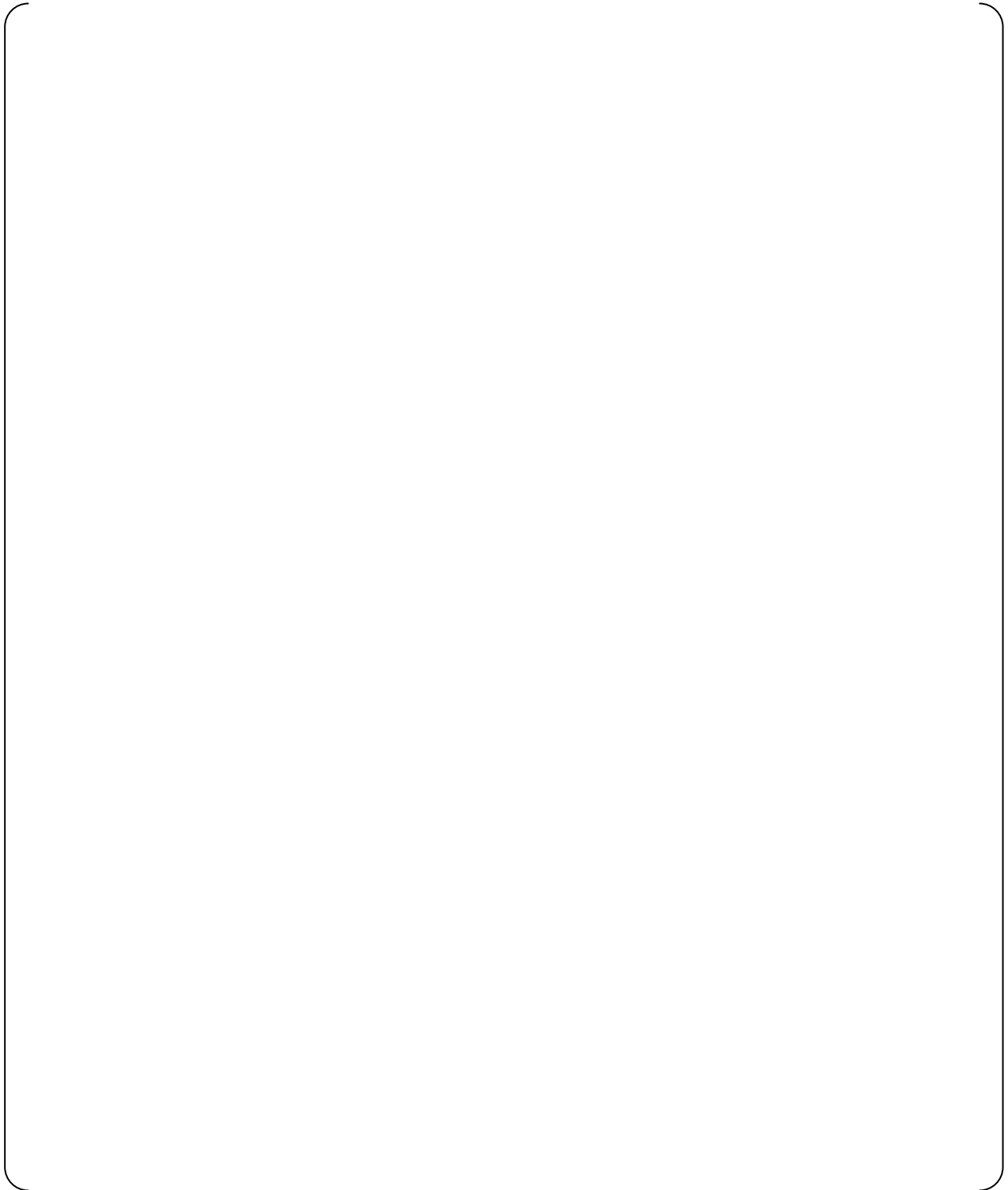


Figure 4-5 Blowdown Analysis Model for Core Region (all cases)



Figure 4-6 Pressure at Break Region of Case 1



Figure 4-7 Flow Rate at Break Region of Case 1



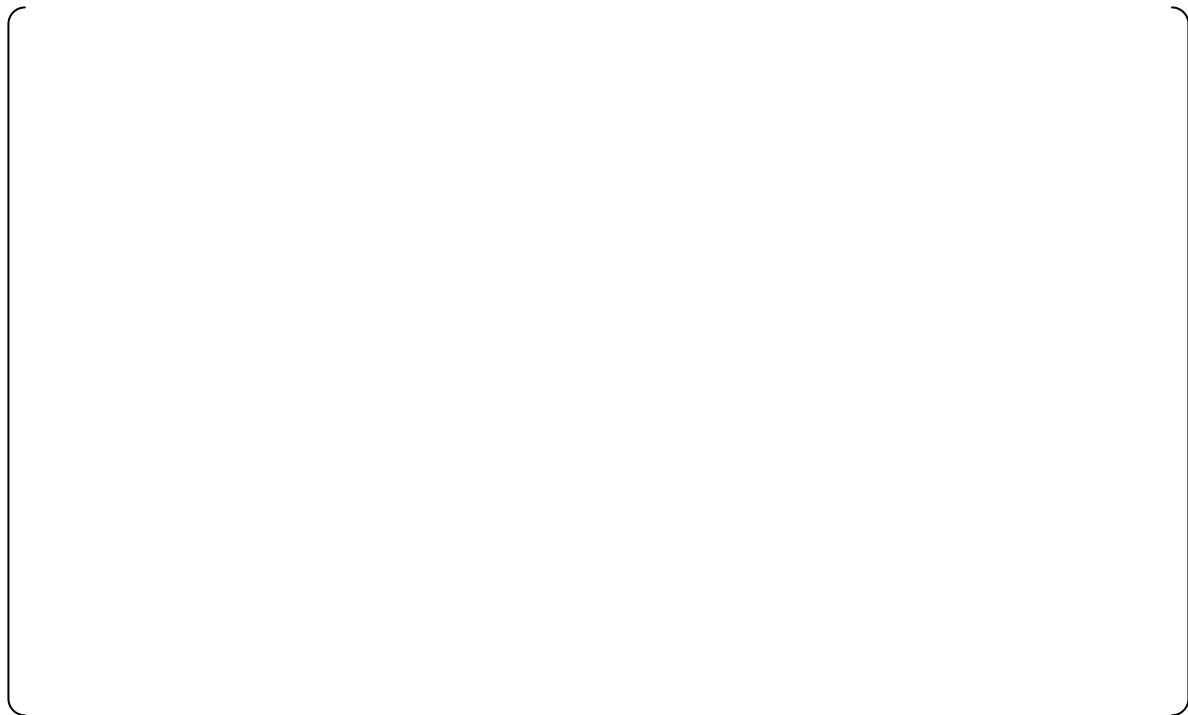
Figure 4-8 Pressure at RV Outlet Nozzle of Case 1



Figure 4-9 Pressure at RV Inlet Nozzle of Case 1



Figure 4-10 Differential Pressure Between Core and Downcomer of Case 1



**Figure 4-11 Differential Pressure Between Downcomer 0 degree
and 180 degree of Case 1**



Figure 4-12 Pressure at Break Region of Case 2



Figure 4-13 Flow Rate at Break Region of Case 2



Figure 4-14 Pressure at RV Outlet Nozzle of Case 2



Figure 4-15 Pressure at RV Inlet Nozzle of Case 2



Figure 4-16 Differential Pressure Between Core and Downcomer of Case 2



Figure 4-17 Differential Pressure Between Downcomer 0 degree and 180 degree of Case 2

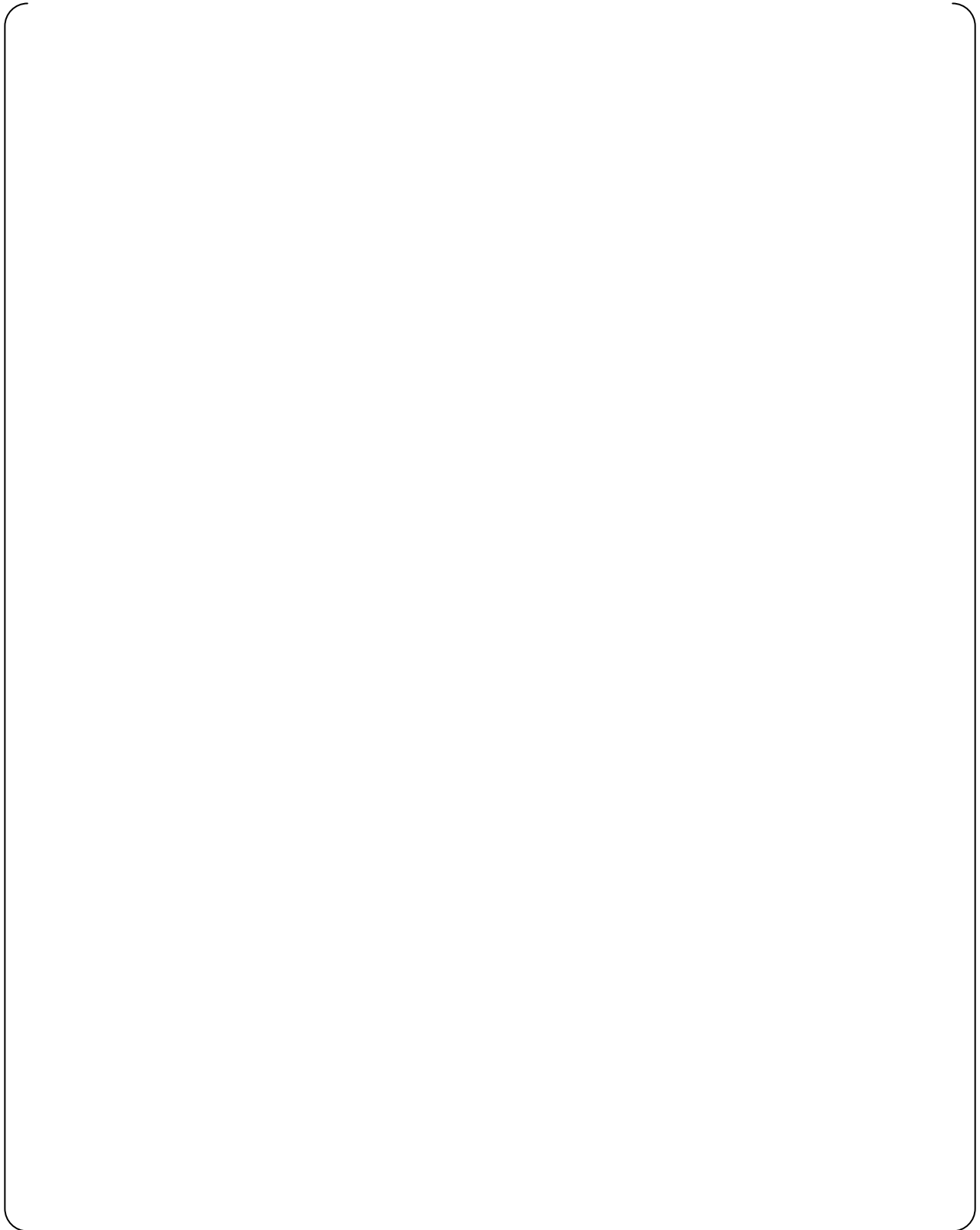


Figure 4-18 Main Steam Line Break Blowdown Analysis Model



Figure 4-19 Pressure at Steam Outlet Nozzle of Case 1



Figure 4-20 Fluid Density at Steam Outlet Nozzle of Case 1



Figure 4-21 Flow Rate at Steam Outlet Nozzle of Case 1

Security-Related Information - Withheld Under 10 CFR 2.390

Figure 4-22 Nodalization Scheme for SG Compartment Analysis

Security-Related Information - Withheld Under 10 CFR 2.390

Figure 4-23 Nodalization Scheme for SG Compartment Analysis

Security-Related Information - Withheld Under 10 CFR 2.390

Figure 4-24 Nodalization Scheme for SG Compartment Analysis

Security-Related Information - Withheld Under 10 CFR 2.390

Figure 4-25 Nodalization Scheme for SG Compartment Analysis

Security-Related Information - Withheld Under 10 CFR 2.390

Figure 4-26 Nodalization Scheme for SG Compartment Analysis

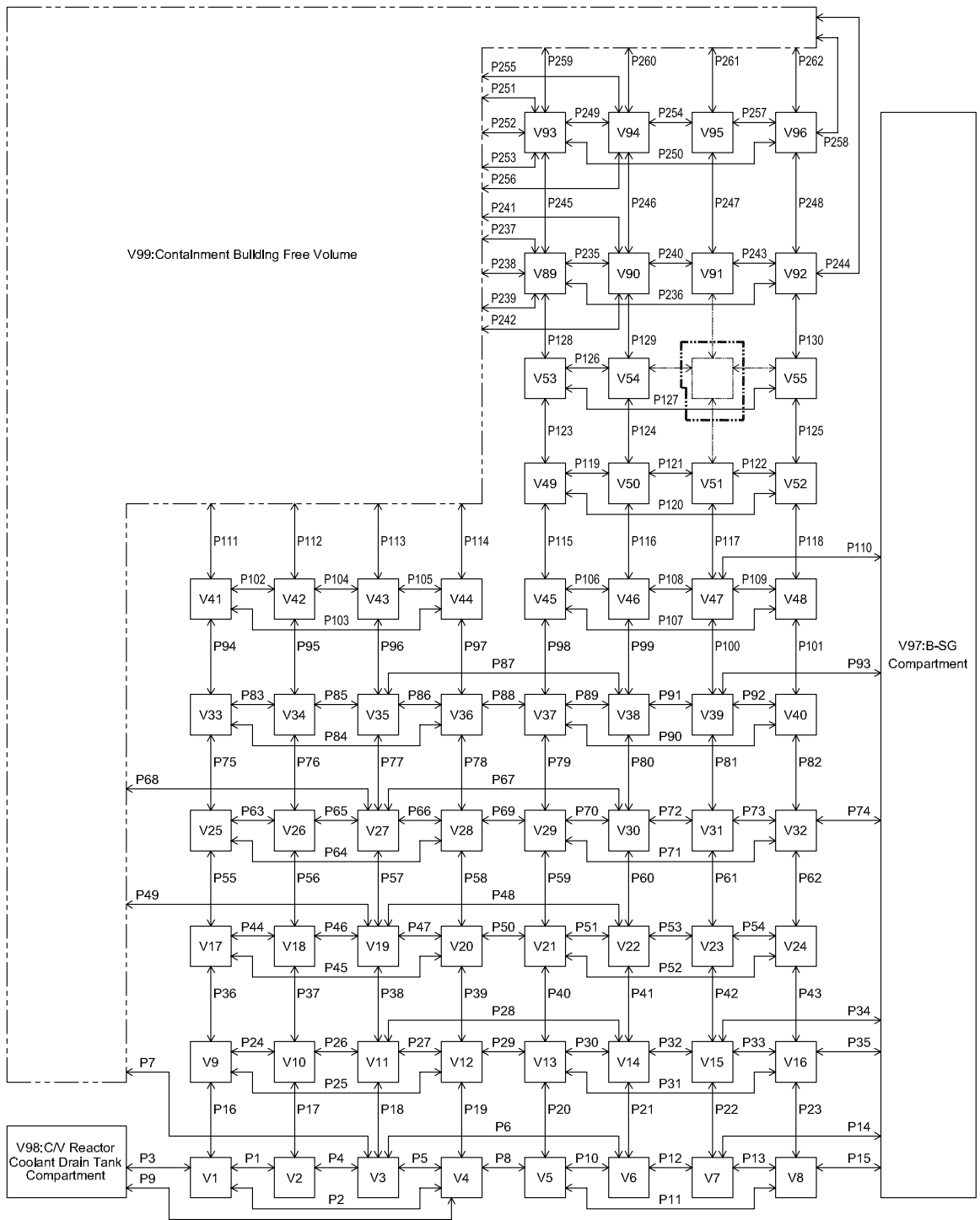


Figure 4-27 Nodalization Diagram for SG Compartment Analysis

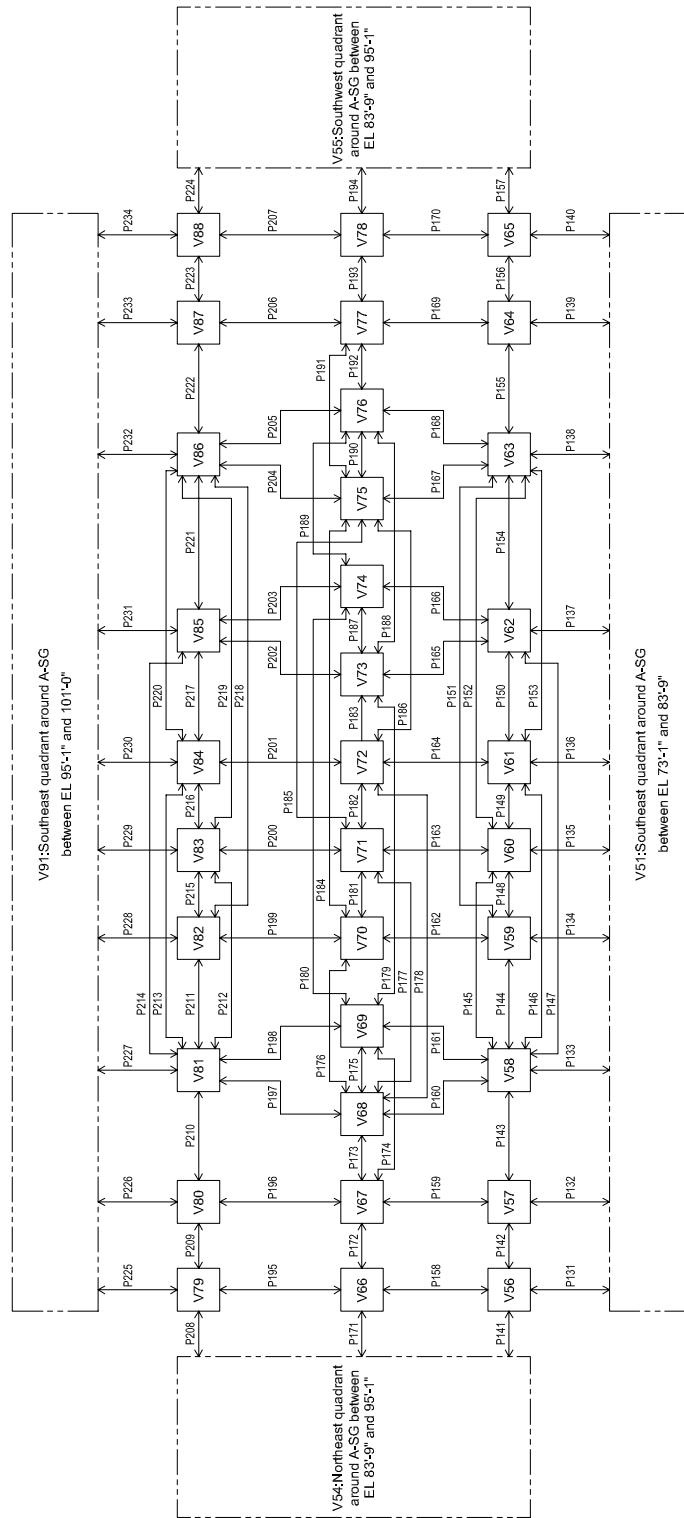


Figure 4-28 Nodalization Diagram for SG Compartment Analysis



Figure 4-29 Pressure Transient at The Node V70



Figure 4-30 Pressure Transient at The Node V68

5.0 DESCRIPTION OF RCL ANALYSIS

5.1 Model Development of RCL

Figure 5-1 shows a schematic of the US-APWR RCL. The US-APWR is a four loop plant with four safety trains. Each RCL connecting to the RV includes the SG, RCP, and the loop piping. The loop piping consists of hot leg, crossover leg and cold leg piping in which the coolant flows from the RV to SG, from the SG to RCP, and from RCP back to RV, respectively.

The RCL analysis model consists of the RV, SG, RCP, MCP, and component supports, as applicable, for each loop. The RCL piping and support system was modeled with three-dimensional finite elements (FEs) representing the components, pipes, and supports as beam elements, masses, and springs with imposed boundary conditions.

The RCL of the US-APWR has four loops, which are modeled as combination of RV, SG, RCP and MCP. These combined system models include both the translational and rotational stiffness, mass characteristics of RCL piping and components, and the stiffness of supports. The analytical models of the individual components of RCL are shown in Figures 5-2, 5-3, 5-4 and 5-5. Detailed model characteristics related to nodal coordinates, mass, material properties and stiffness of the components are described in the technical report MUAP-08005 Rev.0, (Reference 1).

The RV support system consists of eight steel support pads which are integrated with the inlet and outlet nozzle forgings. The support pads are placed on brackets, which are supported by an embedded steel structure on the primary shield wall. The supports allow radial thermal growth of RCS and RV. Figure 5-6 shows RV support configuration and the FE model of the support ring utilized to obtain the support stiffness coefficients.

The SG support system consists of an upper shell support structure, an intermediate shell support structure, and a lower support structure. The upper and intermediate shell supports are lateral restraints (snubbers) attached to structural steel brackets, while the lower support structure is constructed entirely of structural steel and provides both vertical and lateral support. Four pinned-end columns support the vertical loads of the SG. Each RCP support system consists of a lateral support structure, and three pinned-end structural columns. Both support structures were designed considering thermal expansion of connected piping. Figures 5-7 and 5-8 show the FE models utilized to develop the support stiffnesses of the upper and intermediate shell supports of the SGs.

5.2 Seismic Analysis of Coupled RCL-Building Model

(1) Analysis Method

Figure 5-9 shows the analytical model of the entire RCL including the individual components of the four loops and the support representation. This model was connected to the building model by attaching the support springs of RCL to the appropriate building nodes to result in the coupled model shown in Figure 3-2. The fixed end nodes of RCL support springs were attached to the nodes associated with the internal concrete by rigid links. For example, fixed end nodes which represent the ends of RV support springs at RV inlet and outlet nozzle were all connected by rigid links to IC03 of the CIS at that elevation.

The seismic analysis of the coupled RCL-Building model utilizes direct integration of the equations of motion. The analysis was performed for three orthogonal (two horizontal and one vertical) components of earthquake ground motion. Because of different damping between RCL and building models with the different elements, such as RCL components, structural concrete of the buildings and SSI elements, the equations of motion were expanded to include the full stiffness, damping and mass matrices. A fully populated damping matrix was developed by matrix transformation utilizing stiffness and mass matrices and the mode shapes. The resulting equations of motion were solved by direct integration for the three orthogonal seismic ground motion time histories applied separately. Response analysis was performed by the direct integration; Newmark β method ($\beta=0.25, \gamma=0.5$). The time step (Δt) 0.001 sec, was determined to be small enough so that the use of $1/2\Delta t$ does not change the response by more than 10%.

The response of a multi degree-of-freedom linear system subjected to seismic excitation is represented by the following equation of motion:

$$[M] \ddot{\bar{x}} + [C] \dot{\bar{x}} + [K] \bar{x} = -[M] \bar{u}_b \ddot{u}_g \quad (5-1)$$

where

$[M]$ = mass matrix ($n \times n$), $[C]$ = damping matrix ($n \times n$)

$[K]$ = stiffness matrix ($n \times n$)

\bar{x} = column vector of relative displacements ($n \times 1$)

$\dot{\bar{x}}$ = column vector of relative velocities ($n \times 1$)

$\ddot{\bar{x}}$ = column vector of relative accelerations ($n \times 1$)

\bar{u}_b = influence vector; displacement vector of the structural system when the support undergoes a unit displacement in the direction of the earthquake motion ($n \times 1$)

\ddot{u}_g = ground acceleration

Equation of motion (5-1) is expressed in the following form, in the case where the mass points concerned to the soil springs are expressed with the suffix 'c' and the other mass points are expressed with suffix 's'.

$$\begin{bmatrix} [M_s] & 0 \\ 0 & [M_c] \end{bmatrix} \begin{Bmatrix} \ddot{\bar{x}}_s \\ \ddot{\bar{x}}_c \end{Bmatrix} + \begin{bmatrix} [C_{ss}] & [C_{sc}] \\ [C_{cs}] & [C_{cc}] + [C_c] \end{bmatrix} \begin{Bmatrix} \dot{\bar{x}}_s \\ \dot{\bar{x}}_c \end{Bmatrix} + \begin{bmatrix} [K_{ss}] & [K_{sc}] \\ [K_{cs}] & [K_{cc}] + [K_c] \end{bmatrix} \begin{Bmatrix} \bar{x}_s \\ \bar{x}_c \end{Bmatrix} = -[M] \bar{u}_b \ddot{u}_g \quad (5-2)$$

where

$[K_c], [C_c]$; the stiffness and the damping matrix of the soil springs and dashpots

The damping matrix of the structure was treated as the modal damping. The modal damping ratio was obtained by the following equation as the stiffness-weighted formula.

$$h_j = \frac{\bar{\phi}_j^T [\bar{K}] \bar{\phi}_j}{\bar{\phi}_j^T [K] \bar{\phi}_j} \quad (5-3)$$

where

$[K]$; stiffness matrix of RCL, Buildings and soil-structure system

h_j ; equivalent modal damping ratio of the j^{th} mode

$[\bar{K}]$; the modified stiffness matrix constructed from element matrices by the product of the damping ratio for the element and its stiffness or mass matrix

$\bar{\phi}_j$; j^{th} normalized mode shape vector

The damping matrix $[C_s]_i$ of the structure is derived from the modal damping ratios as follows.

$$[C_s]_i = [\bar{\phi}^T]^{-1} \begin{bmatrix} \ddots & 0 & 0 \\ 0 & 2h_i \omega_i & 0 \\ 0 & 0 & \ddots \end{bmatrix} [\bar{\phi}]^{-1} \quad (5-4)$$

where

$[\bar{\phi}]$; normalized mode shape matrix of RCL, Buildings and soil-structure system

$[\bar{\phi}]^T [M] [\bar{\phi}] = [I]$ (identity matrix)

$[M]$; mass matrix of the total soil-structure system;

$[\bar{\phi}]^{-1} = [\bar{\phi}]^T [M]$

$[\bar{\phi}^T]^{-1} = [M] [\bar{\phi}]$

h_i ; equivalent modal damping ratio of i^{th} mode;

ω_i ; frequency of i^{th} mode of the total soil-structure system (rad/s);

(2) Time History Analysis and Response Combination

SSE excitation waves (Referred to Figure 3-5 through Figure 3-7)

Horizontal two directions ; H1,H2 Vertical Direction ; V

Maximum Acceleration ; 0.3 G
Duration ; 22.09 sec, Time pitch ; 0.005 sec

Soil conditions (Four Site Independent Subgrade Conditions ; Referred to Table 3-1)

Soft, Medium1, Medium2, Hard Rock

For each of soil profiles, building stiffness was varied to account for the widening of spectral peak of -15%, 0%, 15%.

Combined response (Acceleration, Velocity, Displacement, Support Load or Element Force) for each excitation direction for the soil condition and building stiffness, is as follows;

$$R_i = \text{SQRT} [(F_{i\text{max}})_{\text{NS}}^{**2} + (F_{i\text{max}})_{\text{EW}}^{**2} + (F_{i\text{max}})_{\text{UD}}^{**2}] \quad (5-5)$$

where

i ; suffix for the degree of freedom of each x, y, z, θ_x , θ_y , θ_z direction
 R_i ; combined response for i-th direction (ex. F_x , F_y , F_z , M_x , M_y , M_z)
 $(F_{i\text{max}})_{\text{NS}}$; Maximum i-th directional response for N-S excitation
 $(F_{i\text{max}})_{\text{EW}}$; Maximum i-th directional response for E-W excitation
 $(F_{i\text{max}})_{\text{UD}}$; Maximum i-th directional response for Vertical excitation

The enveloped loads cover the combinations over the three cases of building stiffness and the four kinds of soil condition that were applied as the design values.

5.3 Accident Analysis of RCL

The postulated pipe break conditions for the RCS loop are as follows

- Hot Leg Branch Line break at the 10 inches RHR/SI line nozzle
- Cold Leg Branch Line break at the 14 inches accumulator line nozzle
- FW Line break at SG FW nozzle
- MS Line break at SG MS nozzle

The design loads were set based on the dynamic analysis of RCS loop for these pipe break conditions. The dynamic analysis method is shown below.

5.3.1 Forcing Function of Dynamic Analysis

Hydraulic forcing functions considered in the postulated RCS pipe break events are as follows,

- thrust forces that include the jet force at the break point and system internal hydraulic forces
- jet impingement force from the ruptured piping
- asymmetric compartment pressure force based on the compartment pressure analysis

Additionally, since the RV is oscillated by the internal hydraulic forces in case of the pipe break at the branch line nozzle of hot leg and cold leg, RV dynamic motion is also considered for these cases in RCS loop dynamic analysis.

a. Calculation of thrust force

Hydraulic forces acts on each part of the RCL system by jet thrust force from the break location, or flow change in a system.

The time history hydraulic forces were calculated using the pressure transient, flow rate, and other coolant property obtained by blowdown analysis described in the section 4.2.1. the jet blowdown force is calculated by the following equation.

$$F_j = (P - P_a) \cdot A + \rho u^2 \cdot A = (P - P_a) \cdot A + \frac{G^2}{\rho} \cdot A$$

where:

- F_j : jet force
- P : fluid pressure at the break plane area
- P_a : ambient pressure
- A : break plane area
- u : flow rate
- ρ : mass density
- G : mass flow rate . G = ρ · u

The system internal hydraulic forces were calculated at various locations of the RCS loop, such as elbow, RCP, SG plenum using time history hydraulic property of P, G, ρ and control volume surface area.

b. Calculation of jet impingement force

The jet impingement force is calculated according to the equation given in Appendix D of ANSI/ANS-58.2-1988. (Reference 6)

$$F_{imp} = K_{\phi} F_j = K_{\phi} C_T P_0 A_e$$

where:

F_{imp} = jet impingement force

$F_j = C_T P_0 A_e$

K_{ϕ} = shape factor

C_T = steady state thrust coefficient

P_0 = initial pressure

A_e = break plane area

c. Asymmetric compartment pressure force

The asymmetric compartment pressure force acting on the SG and the RCP was calculated based on the pressure time history result of the compartment pressurization analysis described in section 4.2.2. This force was applied to the broken loop of four loop RCL model.

d. RV dynamic motion

The RV was oscillated by the internal hydraulic forces in the pipe break cases at the branch line nozzle of hot leg and cold leg.

Therefore RV dynamic motion was also considered for these pipe break cases. Time history displacement data at RV center was loaded in the RCS loop dynamic analysis.

5.3.2 RCL Dynamic Analysis

The RCL was vibrated by the hydraulic force which acts at the piping rupture. The analysis method used to calculate the load is as follows.

The RCL structural model was created using the ANSYS code. A four loop structural model centering on RV model was developed. Considering the symmetry of the four loops, the break can be postulated in any one loop. Therefore, the broken loop was defined as B-loop in the analysis.

RCL model consists of the following structures.

- Reactor vessel (RV)
- Steam generator (SG)
- Reactor coolant pump (RCP)
- Main coolant pipes (MCP)
- Primary component support

Three-dimensional beam element and pipe element was used in the model. The support structures were modeled by spring elements. The four loop RCL model is shown in Figure 5-10. Non-linear spring element was used for SG lower lateral support considering those bumper support structures as shown in Figure 5-11.

Time history direct integration method was applied to obtain the dynamic load of the RCL in the analysis. Forcing functions described in section 5.3.1 were assumed to act on the structural model.

- Direct integration : Newmark beta method
- Break opening time : 0.001 second
- Integration time interval : 0.0001 second
- Analysis time : 2.0 seconds for Steam Line break condition and about 0.5 seconds for other break conditions

Rayleigh damping was applied to the model. Critical damping ratios were set 3% to the applicable RG 1.61 Rev.1 (Reference 7)

5.4 Nozzle Loads from Piping Reaction Force

The RCL components/piping nozzle loads were conservatively determined as estimated loads. These estimated loads will be confirmed, in the technical reports (Reference 8), to be submitted in March 2009 to envelope the actual loads obtained from the analysis of RCL branch piping and MS piping.

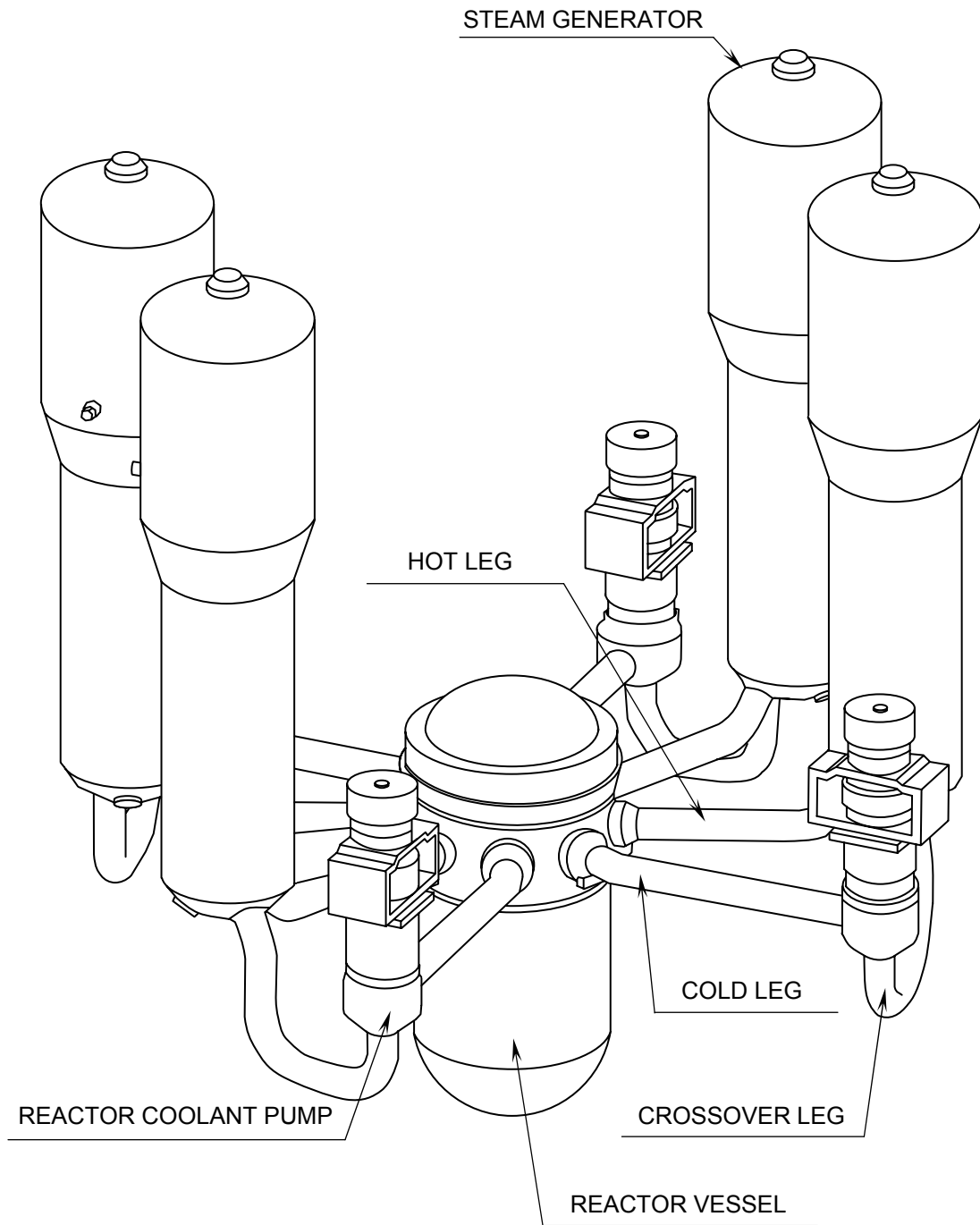


Figure 5-1 US-APWR RCL

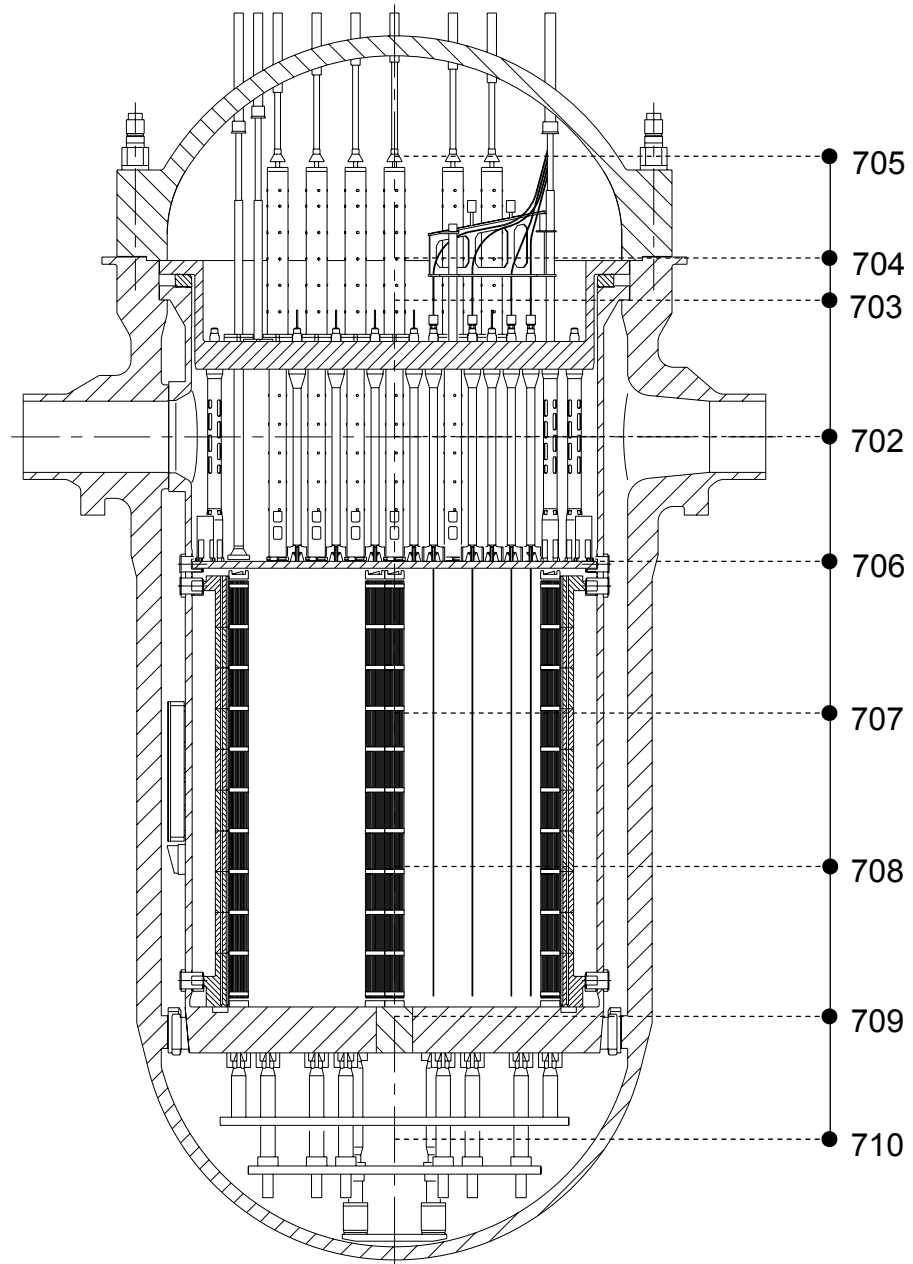


Figure 5-2 Stick Mass Model for RV with Internals

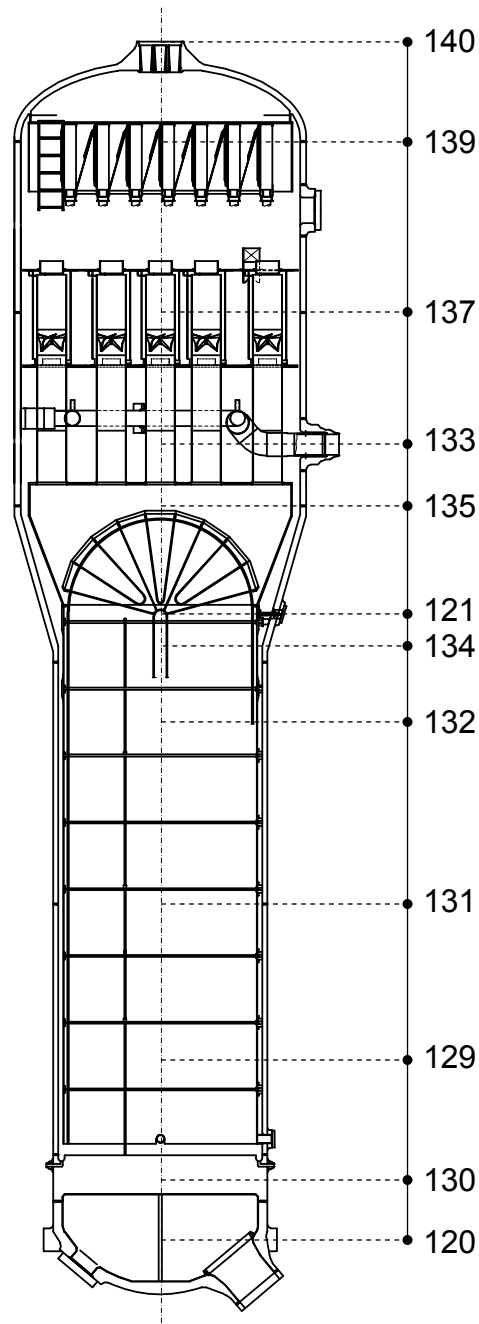


Figure 5-3 Stick Mass Model for SG with Internals

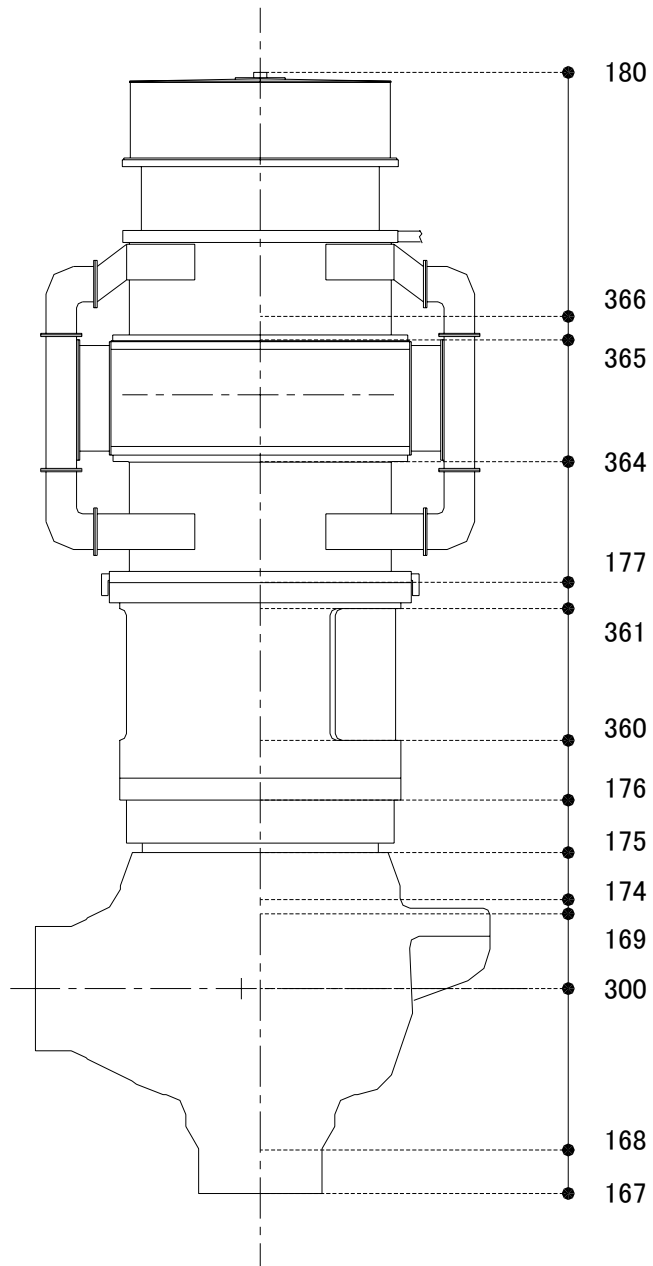


Figure 5-4 Stick Mass Model for RCP with Internals

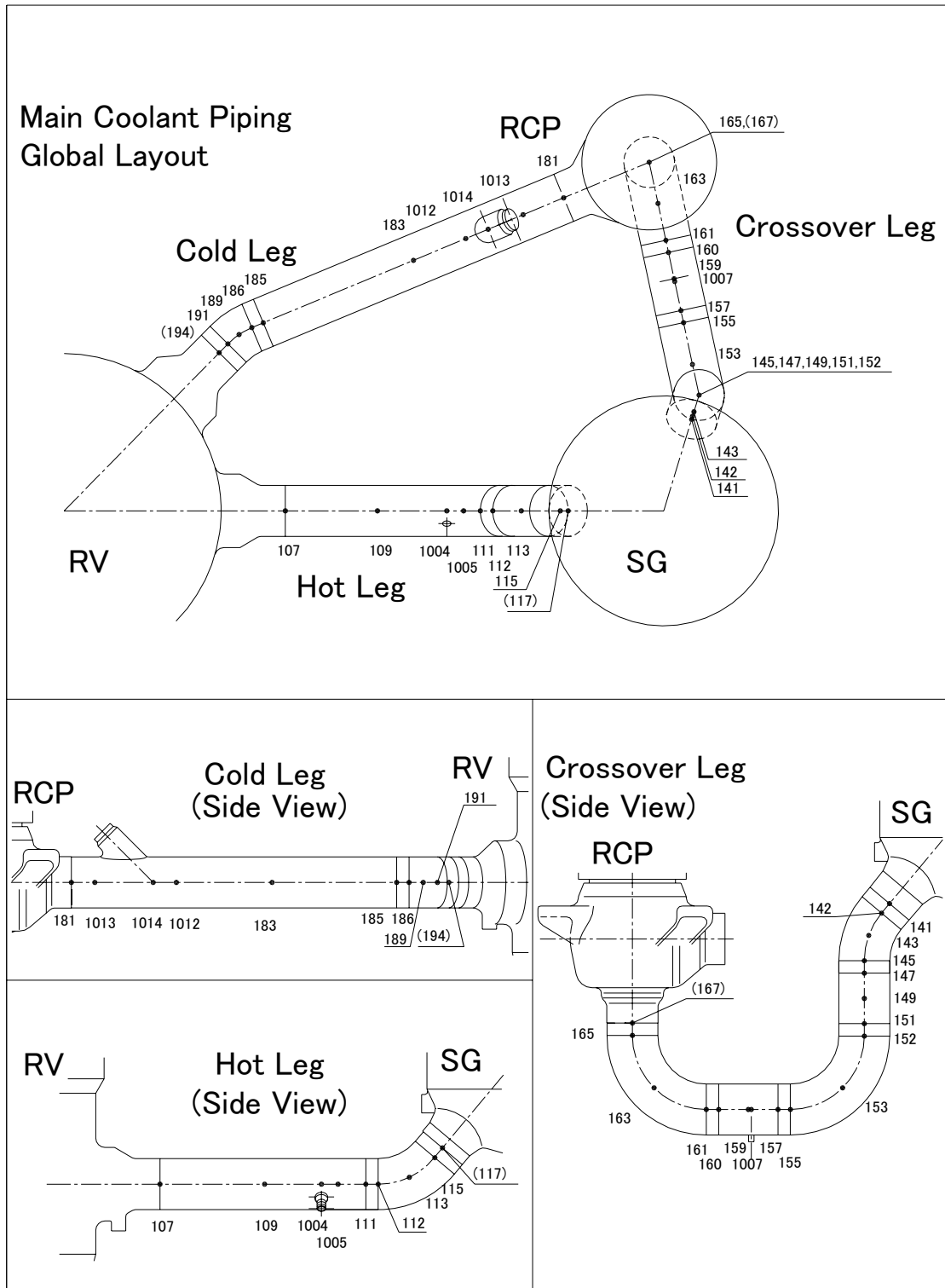


Figure 5-5 RCL Piping Model

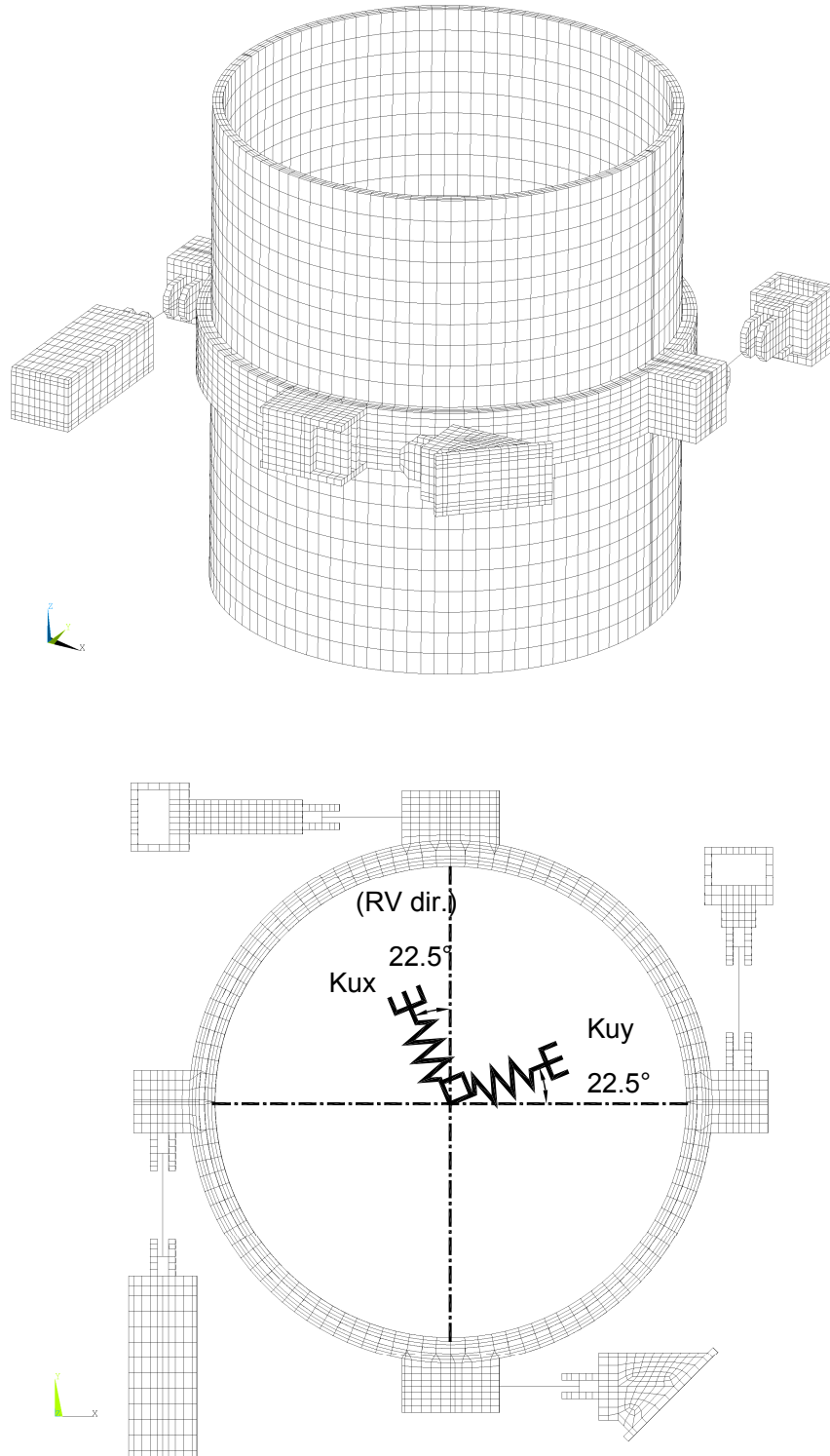


Figure 5-7 Spring Model of SG Upper Shell Support

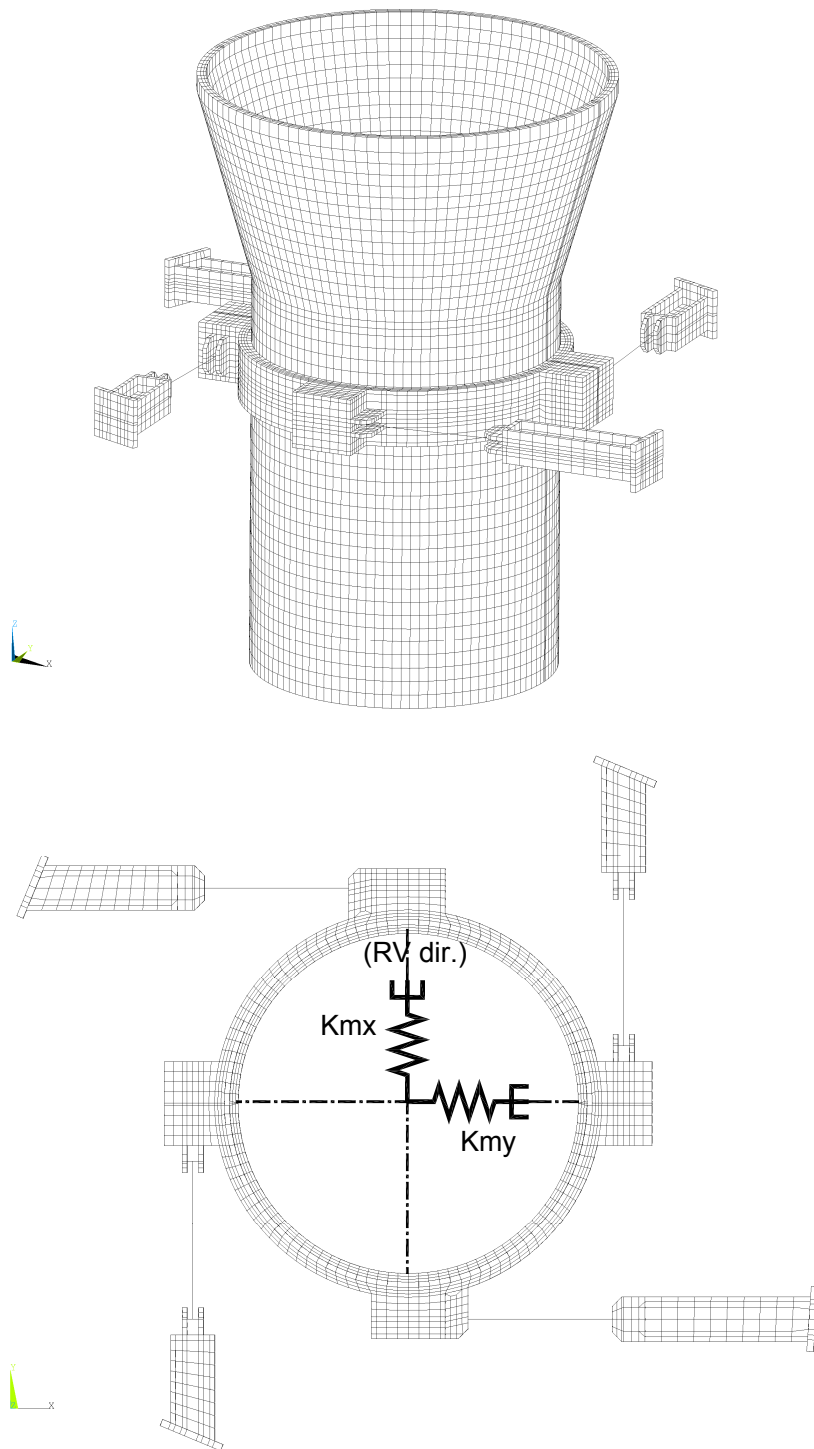


Figure 5-8 Spring Model of SG Intermediate Shell Support

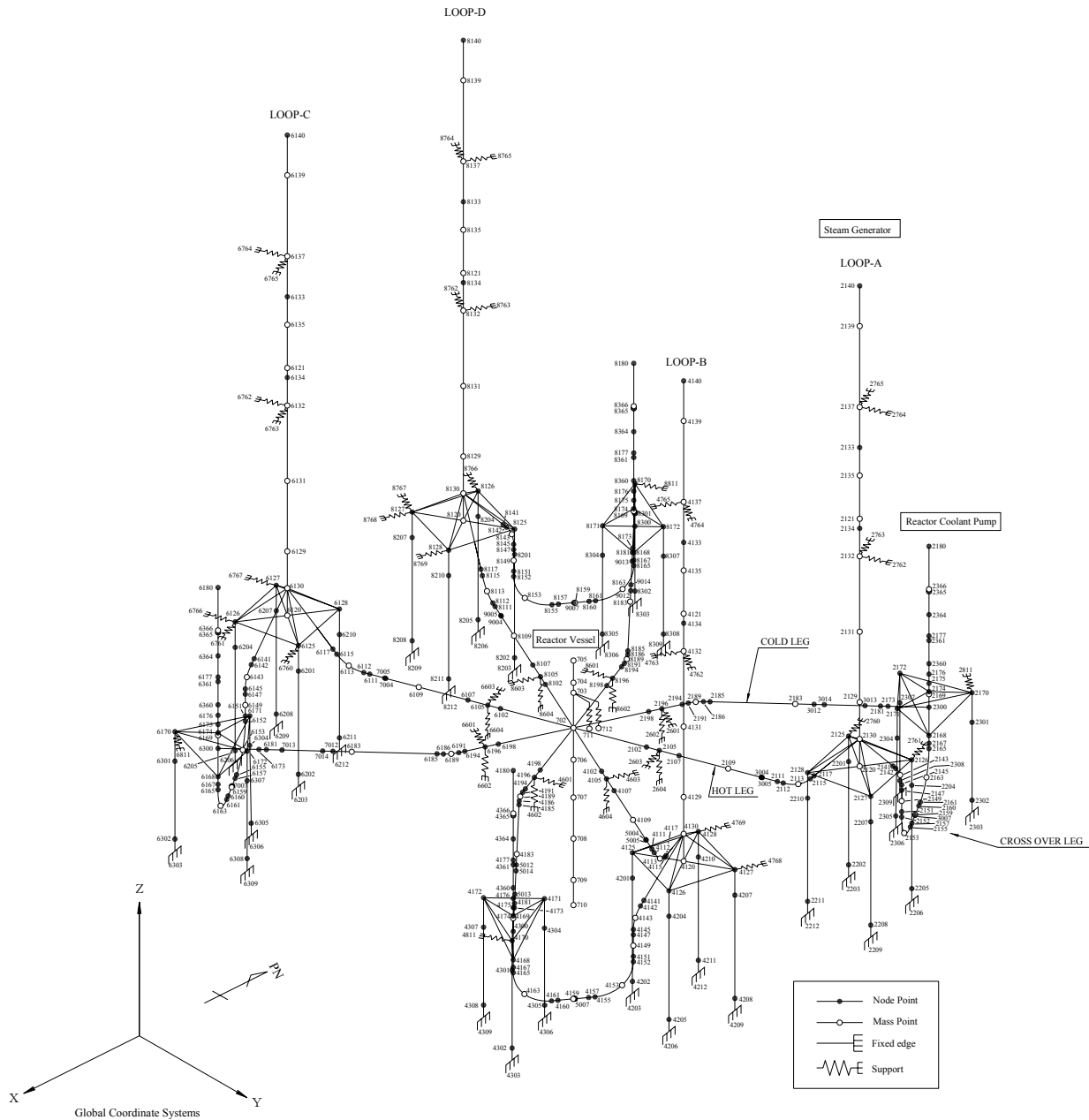


Figure 5-9 Stick Mass Spring Model for RCL

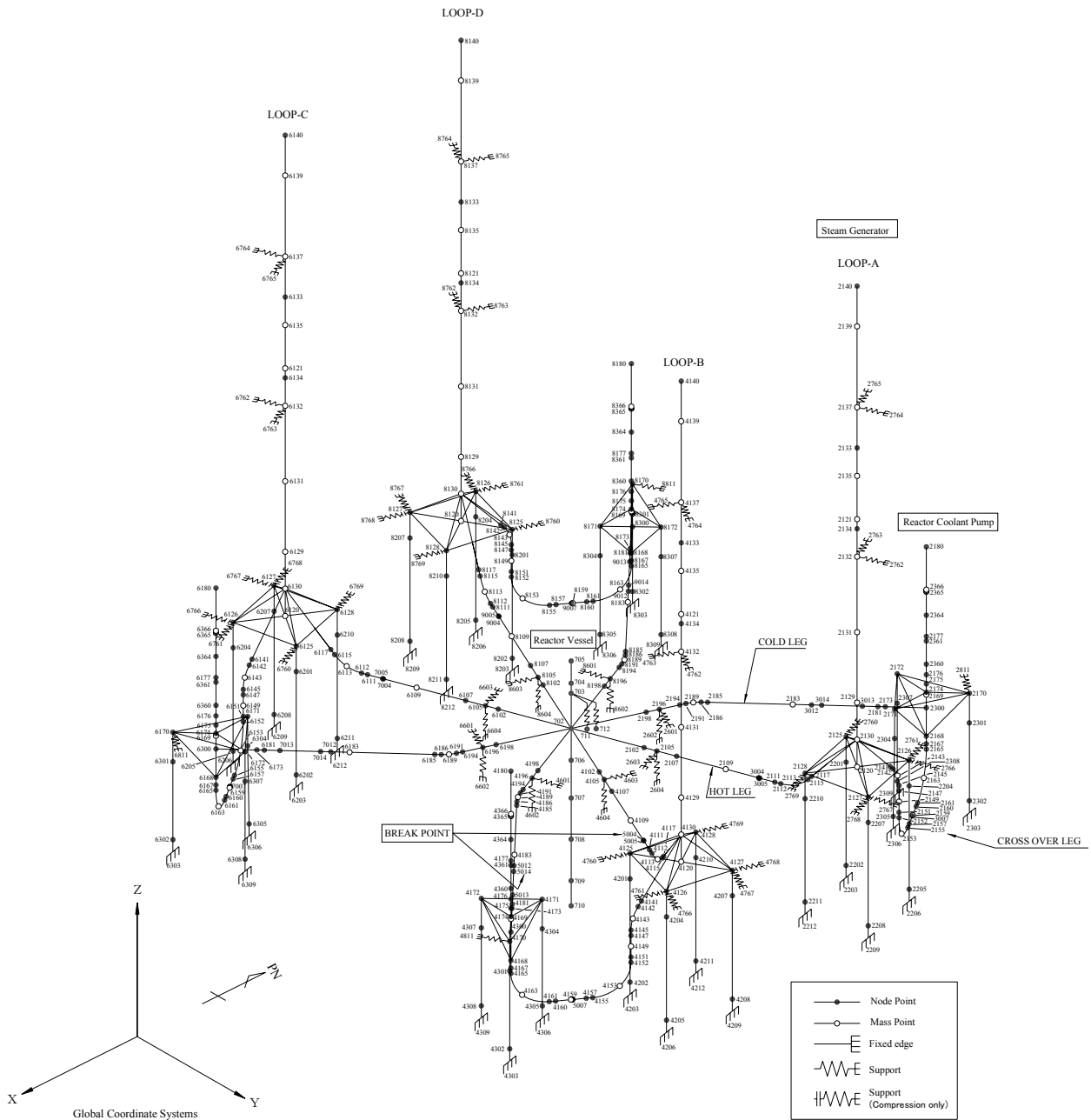


Figure 5-10 RCL Model for Accident Analysis

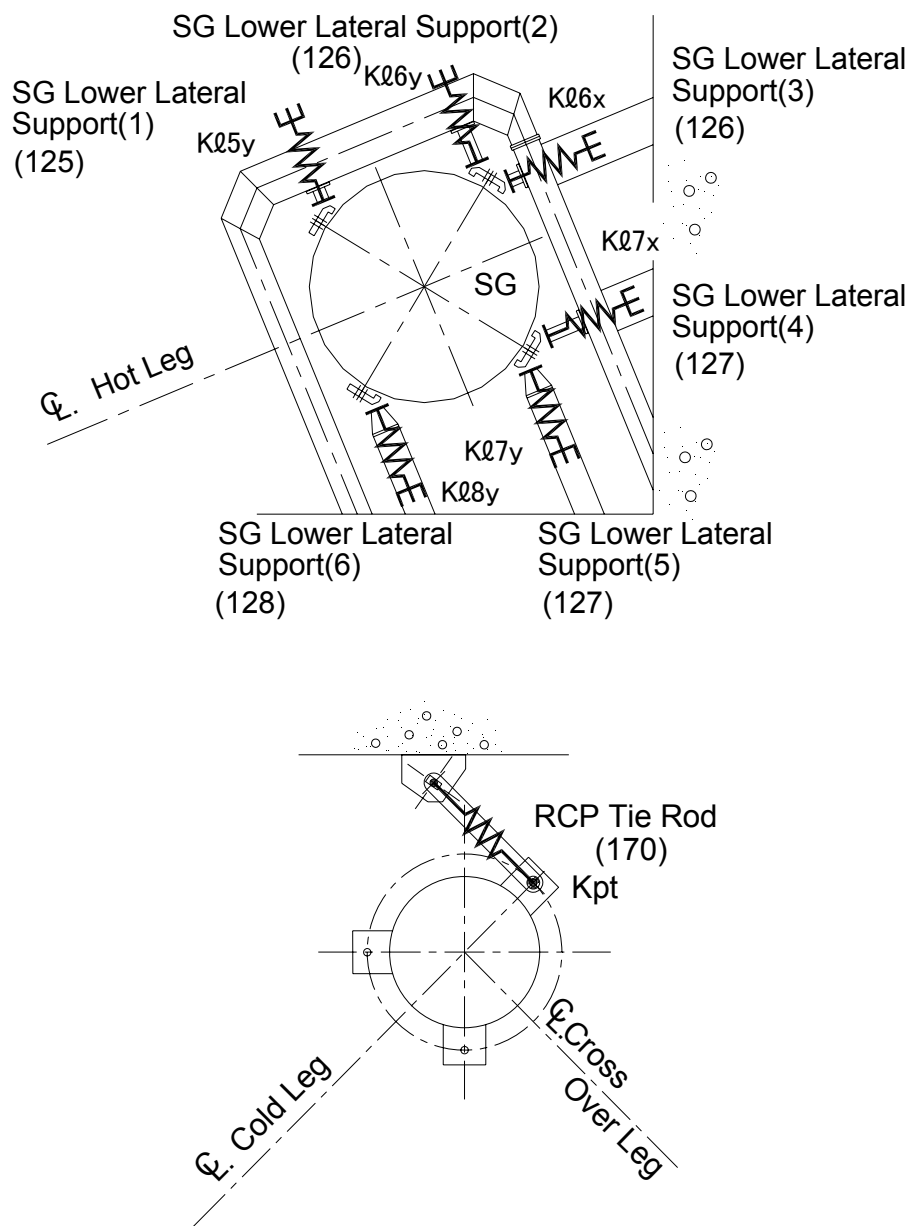


Figure 5-11 SG Lower Support and RCP Tie Rod

6.0 ANALYSIS OF REACTOR EQUIPMENT

6.1 Introduction

The review requirements of SRP 3.9.2, Rev. 3 (Reference 9), create a need for a detailed discussion of the reactor internals, design criteria and dynamic analyses methodology for the combined the seismic and postulated pipe rupture events under the ASME Level D (faulted) service conditions. The results of the analyses are required to meet the stress limits of the ASME Code, Section III (Reference 2), Subsection NG for the core support structures, and the functional requirements of the reactor internals design specification. Meeting the requirements of the ASME Code, Section III (Reference 2) and the design specification provides assurance of the structural and functional integrity of the reactor internals under the ASME Level D service conditions, combined loads of the seismic and pipe rupture events.

The time history displacements of RV obtained by this analysis were used as the input of the RCS, and Direct Vessel Injection (DVI) piping dynamic response analysis described in Section 5. The time histories of reactor internals acceleration response were used to dynamic analysis of the fuel assembly. The maximum element forces and reaction forces on the RV, the reactor internals and the control rod drive mechanism (CRDM) were used for the stress analysis of the core support structures, RV and CRDM.

6.2 Seismic Loads

The seismic loads for the reactor equipments were obtained from the time history analysis with the finite element model of the coupled RCL-Building as discussed in Section 5.2. The time history data of the earthquake response at the vessel support and operating floor level nodes were used as the inputs. The analysis was performed for three orthogonal (two horizontal and one vertical) components of earthquake ground motion. As for the site variations, combinations of four kinds of soil conditions ; Soft, Medium1, Medium2, Hard Rock (Referred to Table 3-1) and three variation of the building stiffness (spectral peak of -15%, 0%, 15%).

The enveloped loads cover the combinations over the three cases of building stiffness and the four kinds of soil condition that were applied as the design values.

Additional loading input to the seismic analysis were vertical pressure loadings converted to nodal point external loads, and the vertical weights of the reactor internals and interfacing components, as inputs of density on the beams with spring effects or mass nodal points.

6.3 Hydraulic Loads in LOCA Events

The Hydraulic loads on the RV and internals during the blowdown phase of the LOCA events were calculated from the dynamic pressure inside the vessel obtained by MULTIFLEX code as discussed in Section 4.2. The calculation methods of the horizontal and vertical part for hydraulic loads are discussed below. In addition, the thrust forces from the RCL analysis were combined with the hydraulic loads as the input.

(1) Horizontal Loads

At the beginning of blow-down phase of the LOCA events, the region of the downcomer annulus close to the break depressurizes rapidly, but because of the finite speed of sound, the opposite side of the core barrel remains at a high pressure. This pressure difference in the downcomer causes asymmetric horizontal loads on the RV and the core barrel. The depressurization wave propagates around the downcomer annulus and goes up through the core, causing the core barrel differential pressure to be reduced and decreasing, the resulting hydraulic forces.

For the forces calculation, the core barrel was divided into [] force segments in the axial direction and the [] in the circumferential direction. The horizontal time history force on each segment was calculated by the circumferential integration of the downcomer pressure distribution around the core barrel obtained from the blowdown analysis. Dynamic loads on the RV were also calculated in the same manner of the core barrel.

The result of total horizontal force on the core barrel is shown in Figure 6-1 for the LOCA event of the 14 inches pipe rupture connecting to the cold leg.

(2) Vertical Loads

The depressurization wave also causes the vertical differential pressure across the reactor internals and fuel assemblies.

The vertical dynamic loads on each structural element were calculated by multiplying the pressure time histories obtained from the blow-down analysis and the projection area of each element.

The results of total vertical force on the RV and its internals are shown in Figure 6-2 for the LOCA event of the 14 inches pipe rupture connecting to the cold leg.

6.4 Reactor Internals Dynamic Response Model

The dynamic analysis methodology was based on the models using the general purpose FE computer code ANSYS. The reactor equipment model was a three-dimensional non linear dynamic FE computer model representing the reactor internals and the support system and was used to determine the maximum accelerations, displacements, and member forces. The details of the seismic and LOCA dynamic analysis model are discussed below.

The model includes representation of the RV support system, inlet and outlet piping nozzles, the CRDM, integrated head package, in-core instrumentation columns, and fuel assembly nozzles and grids.

Figures 6-3 and 6-4 show a typical model of the reactor internals used for the seismic and the LOCA dynamic analysis. The physical geometry and the material properties (density, modulus of elasticity, Poisson's ratio) of the reactor internals were represented by the beam elements. The reactor internals and interfacing structures were connected or represented by the mass inertia effects, stiffness matrices, and hydro-dynamic matrices, springs, and/or impact elements including gap and damping (including coexistence of viscous and Coulomb damping).

The nodal point DOFs, and the damping coefficients of the reactor internals and surrounding structures were selected such that the most dominant frequencies were represented in the dynamic response.

Fluid-structure interaction effects were accounted for by matrices developed for that purpose.

6.5 Response Analysis

(1) Calculation Method

The time history analysis with the direct time integration method was applied to both SSE and the LOCA response analysis. The 4% of critical damping ratio was used with the Raleigh damping method. The dead weights of structures and vertical interface loads such as the hold down spring force were also taken into the response analyses.

(2) Response Combination

The outputs of the SSE and the LOCA response analysis are time-history accelerations, displacements (absolute and relative), and member forces (forces and moments). The maximum member forces and displacements were input into reactor internals component static FE models and the maximum stress intensities and displacements were compared to the ASME Code, Section III (Reference 2) and the allowable interface load and displacement limits. The LOCA dynamic system analyses results confirm that the adequacy of the structural design of the reactor internals can withstand the dynamic loadings of the most severe LOCA in combination with the SSE.

(3) Results of Response Analysis

The horizontal and vertical displacements at the elevation of inlet nozzle center are shown in Figure 6-5 and Figure 6-6 as examples of the RV response analysis result.

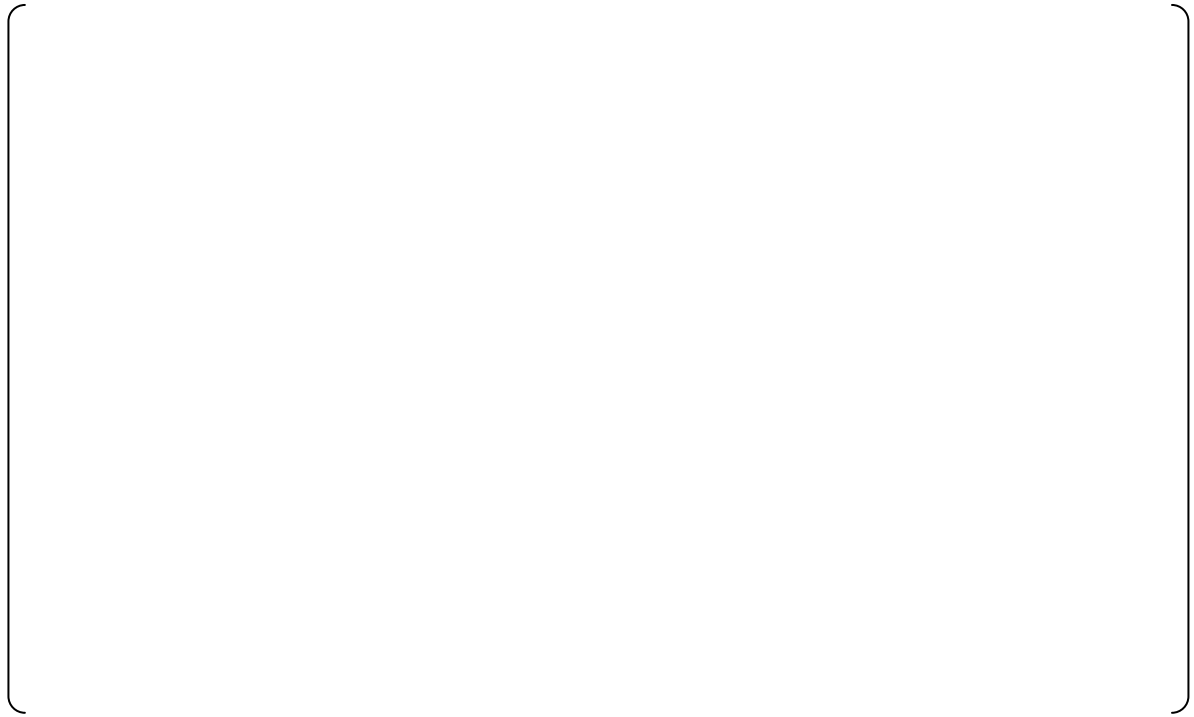


Figure 6-1 Horizontal Hydraulic Loads on RV during LOCA



Figure 6-2 Vertical Hydraulic Loads on RV during LOCA

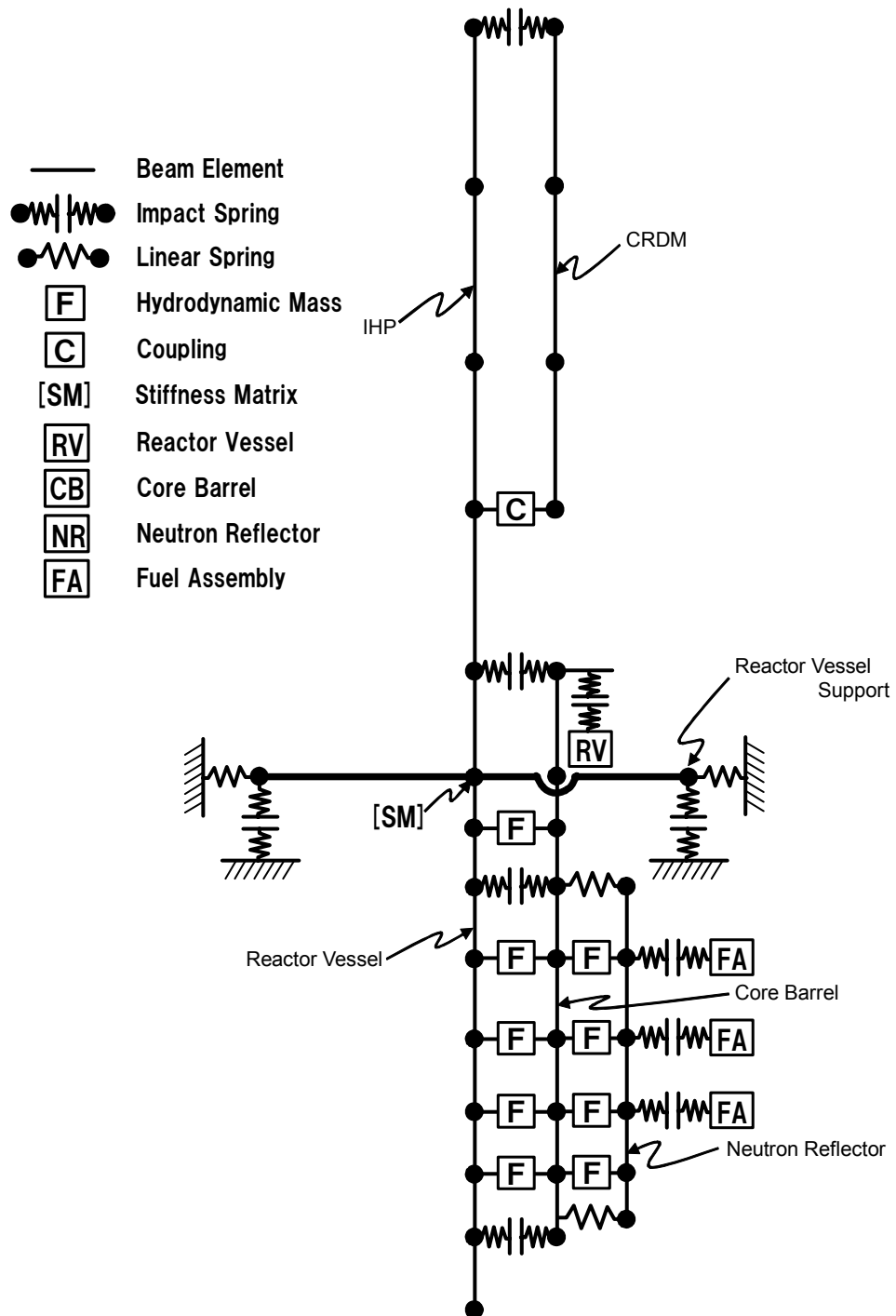


Figure 6-3 RV and Internals Dynamic Analysis Model

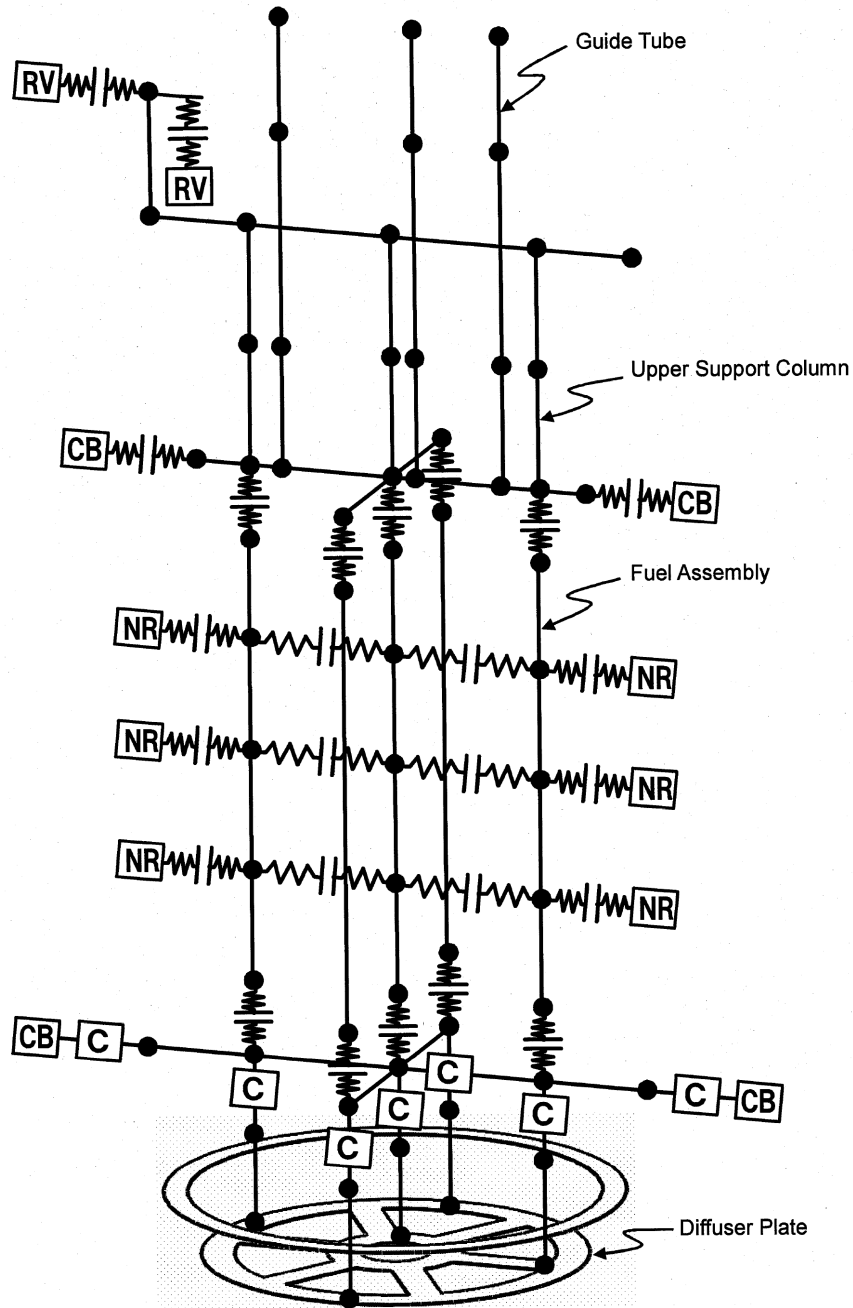


Figure 6-4 Model Details Inside The Core Barrel and Lower Plenum



Figure 6-5 Horizontal Displacement of RV during LOCA



Figure 6-6 Vertical Displacement of RV during LOCA

7.0 ANALYSIS OF PRESSURIZER

The PZR stick mass spring model consists of lumped masses, pipe elements, beam elements and spring elements, as shown in Figure 7-1. The structural model in the figure is a three dimensional two-stick model. The numbers in the figure shows the node numbers. One stick represents the stiffness and mass properties of the PZR pressure boundary shell, and the second stick at the bottom represents the skirt. Both sticks were tied in the double line between node 3 and node 113, which represents the rigid connection. The total number of DOFs is adequate to represent the dynamic behavior of the PZR component. The model includes spring elements at the interface point of the upper lateral support at node 11, which represents the bumper stiffness and the local shell flexibility, as shown in Figure 7-2.

7.1 Seismic Analysis

This section summarizes the seismic analysis of the PZR component to obtain the SSE earthquake loadings for the element stress evaluation. Seismic loadings of the PZR component were evaluated by the response spectrum analysis method, using the PZR structural model shown in Figure 7-1. In the response spectrum analysis, three orthogonal earthquakes components(X, Y, Z directions) were applied with square root of the sum of the squares (SRSS) combination. Combination of periodic modal responses and rigid modal responses were considered in accordance with the guideline of RG 1.92 Rev.2 (Reference 10).

The in-structure response spectra (ISRS) at IC15 and IC18 referred to the CIS model of Figure 3-1, was developed with a 3 % damping for the analysis, as shown in Figure 7-3.

7.2 Accident Analysis

This section summarizes the accident analysis of the PZR component. Pipe rupture at RCL accident condition are postulated in the RCL branch piping, MS piping or FW piping considering LBB methodology as stated in Section 4.1. Significant Accident load of the PZR is generated by surge line vibration caused by MCP dynamic response in the LOCA and other reaction force such as the PZR spray line is negligible small. Consequently component loads other than surge line nozzle do not occur in accident condition.

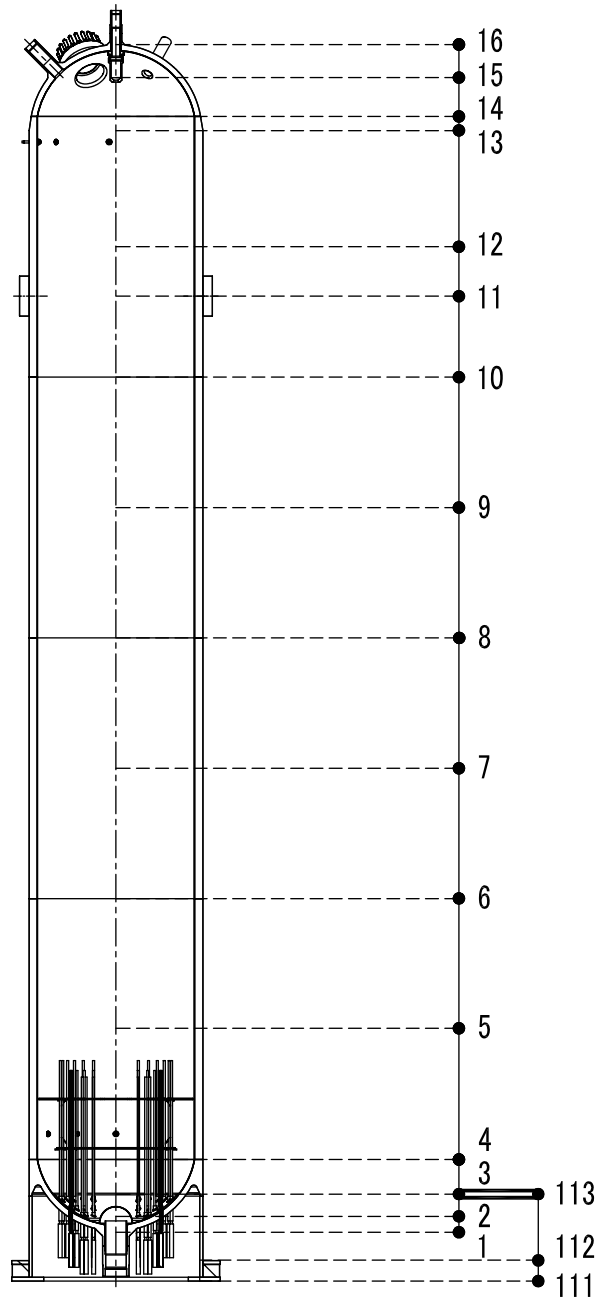


Figure 7-1 Stick Mass Model for PZR

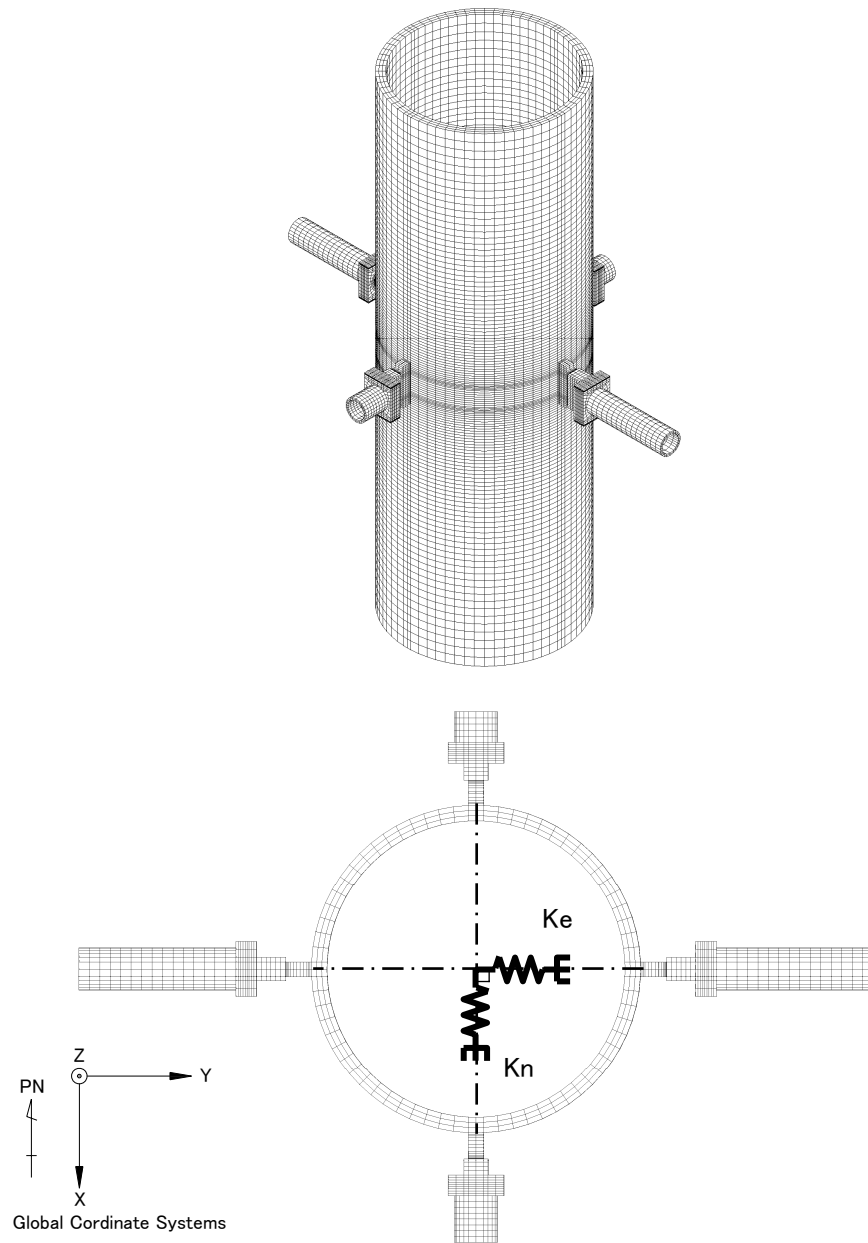
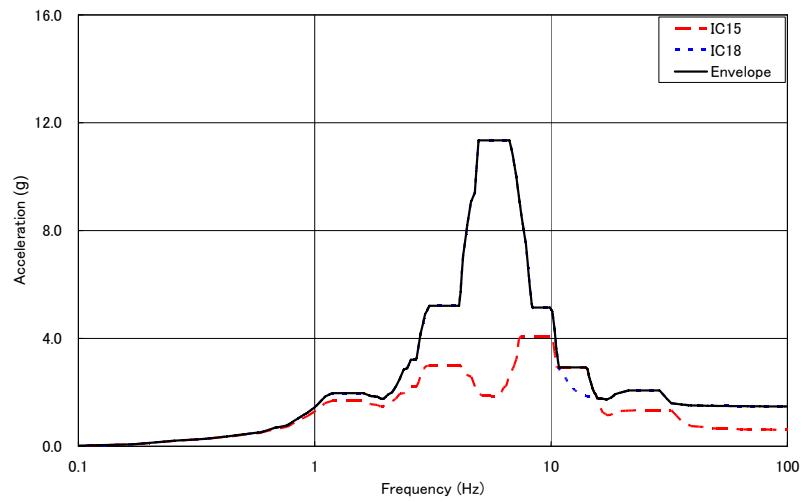
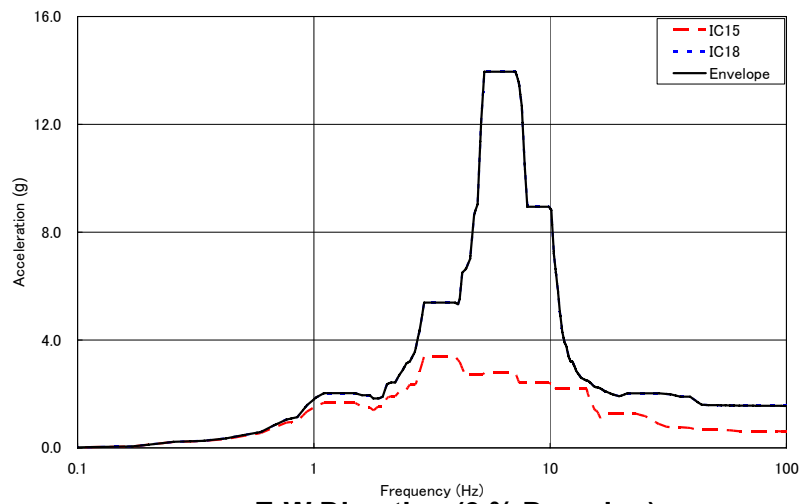


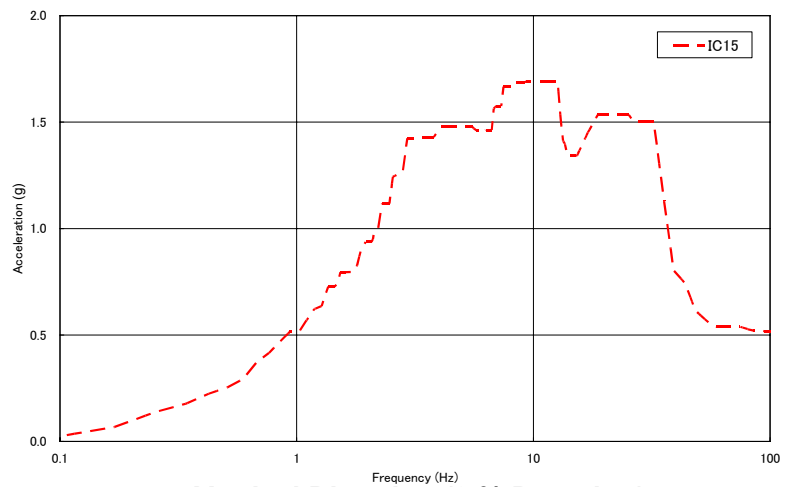
Figure 7-2 Spring Model of PZR Upper Supports



N-S Direction (3 % Damping)



E-W Direction (3 % Damping)



Vertical Direction (3 % Damping)

Figure 7-3 ISRS for PZR

8.0 SUMMARY OF PRIMARY COMPONENTS LOADS

8.1 RCL Member Forces and Support Loads

(1) Seismic Loads

The component nozzle load, the reaction force of support point, and the member forces of the MCP at SSE design condition are presented in the tables and figures of Table 8-1.

(2) Accident Loads

The force tables for the accident loads are presented in a same manner in Table 8-1. The accident design loads were determined conservatively based on the result of RCS loop dynamic analysis described in the section 5.3. The accident design loads are presented by the Table 8-6 through Table 8-9.

The row of 'Design Load 1' in each table is presented as the maximum umbrella design load for the following break conditions.

- Hot Leg pipe break at the 10 inches RHR/SI line nozzle on the Hot Leg
- Cold Leg pipe break at the 14 inches accumulator line nozzle on the Cold Leg
- FW pipe break at SG FW nozzle

The row of 'Design Load 2' is presented as the design load for the postulated MS pipe break at SG MS nozzle.

8.2 Loads Related to RV and Reactor Equipment Dynamic Response

The general assembly of the RV and reactor internals is shown in Figure 8-11. The SRSS of the SSE and the LOCA loads obtained from the dynamic analysis of the RV are summarized as follows.

(1) Member Forces of Core Support Structures

The member forces on core support structures are summarized in from Table 8-10 to Table 8-12. Locations for load the definitions are shown in Figure 8-12 and Figure 8-13.

(2) The RV and reactor internals Interface Loads

The interface loads between the RV and reactor internals are summarized in Table 8-13.

(3) Member Forces on the RV Head

The Member forces on the RV Head for the CRDM and instrumentation systems are summarized in Table 8-14.

(4) Member Forces on CRDM

The CRDM assembly is shown in Figure 8-14. The member force on the CRDM are summarized in Table 8-15. The distributions of the axial force, the shear force and the bending moment on the CRDM are shown in Figure 8-15 through Figure 8-17.

(5) Fuel Assembly Loads

The accelerations of the upper core plate and the lower core support plate during SSE are shown in Figure 8-18 and Figure 8-19.

The horizontal accelerations of the upper core plate and the lower core support plate during the LOCA event are shown in Figure 8-20 and Figure 8-21.

8.3 Component Loads of PZR

(1) Seismic Loads

Seismic loads of the PZR consist of component load and nozzle load. Component loads are shown in Table 8-16, is provided from dynamic analysis results of the PZR stick model described in section 7.1. Nozzle loads are shown in Table 8-17, is determined as design loads described in section 5.4.

(2) Accident Loads

Accident loads of the PZR consist of nozzle load at postulated pipe rupture. Nozzle loads are shown in Table 8-18, is determined as design loads described in section 5.4.

Table 8-1 List of Tables and Figures of RCL Seismic and Accident Loads

Load Type	Location	Seismic Load	Accident Load	Coordinate
Nozzle Load	RV Inlet and Outlet Nozzle	Table 8-2	Table 8-5	Figure 8-1
	SG Inlet and Outlet Nozzle			Figure 8-2
	RCP Inlet and Outlet Nozzle			Figure 8-3
Reaction Force of Support Point	SG Lower Support	Table 8-3	Table 8-6	Figure 8-4
	SG Intermediate Shell Support			
	SG Upper Shell Support			
	RCP Lower Support			Figure 8-5
Member Forces of MCP	Hot Leg	Table 8-4	Table 8-7	Figure 8-6
	Cross Over Leg			
	Cold Leg			
Nozzle Load	RV Vent Nozzle	Table 8-5	Table 8-9	Figure 8-7
	RV DVI Nozzle			Figure 8-8
	SG MS Nozzle			
	SG FW Nozzle			Figure 8-9
	RCP Seal Water Injection Nozzle			
	MCP Pressurizer Surge Nozzle			
	MCP Pressurizer Spray Nozzle			Figure 8-10
	MCP CVCS Letdown and Loop Drain Nozzle			
	MCP Charging Nozzle			
	MCP RHRS/SIS Nozzle			
MCP Accumulator Tank Nozzle				

Table 8-2 Seismic Loads of Inlet and Outlet Nozzle on RV, SG, RCP

Node	Location	Coordinate	Force (kips)			Moment (kips-in)		
			Fx	Fy	Fz	Mx	My	Mz
194	RV Inlet Nozzle	Figure 8-1						
107	RV Outlet Nozzle							
117	SG Inlet Nozzle	Figure 8-2						
141	SG Outlet Nozzle							
167	RCP Inlet Nozzle	Figure 8-3						
181	RCP Outlet Nozzle							

Table 8-3 Seismic Reaction Forces of Support Points

Node	Location	Coordinate	Force (kips)			Moment (kips-in)		
			Fx	Fy	Fz	Mx	My	Mz
125	SG Lower Support Point(1)	Figure 8-4						
126	SG Lower Support Point(2)							
127	SG Lower Support Point(3)							
128	SG Lower Support Point(4)							
132	SG Intermediate Shell Support Point							
137	SG Upper Shell Support Point							
170	RCP Lower Support Point(1)	Figure 8-5						
171	RCP Lower Support Point(2)							
172	RCP Lower Support Point(3)							

Table 8-4 Seismic Member Forces of MCP

Node	Location	Coordinate	Force (kips)			Moment (kips-in)		
			Fx	Fy	Fz	Mx	My	Mz
107	Hot Leg	Figure 8-6						
109	Hot Leg							
111	Hot Leg							
112	Hot Leg							
113	Hot Leg							
115	Hot Leg							
117	Hot Leg							
141	Cross Over Leg							
142	Cross Over Leg							
143	Cross Over Leg							
145	Cross Over Leg							
147	Cross Over Leg							
149	Cross Over Leg							
151	Cross Over Leg							
152	Cross Over Leg							
153	Cross Over Leg							
155	Cross Over Leg							
157	Cross Over Leg							
159	Cross Over Leg							
160	Cross Over Leg							
161	Cross Over Leg							
163	Cross Over Leg							
165	Cross Over Leg							
167	Cross Over Leg							
181	Cold Leg							
183	Cold Leg							
185	Cold Leg							
186	Cold Leg							
189	Cold Leg							
191	Cold Leg							
194	Cold Leg							

Table 8-5 Seismic Loads of Nozzles on RV, SG, MCP

Location	Coordinate	Force (kips)			Moment (kips-in)		
		Fx	Fy	Fz	Mx	My	Mz
RV Vent Nozzle	Figure 8-7						
RV DVI Nozzle							
SG MS Nozzle	Figure 8-8						
SG FW Nozzle							
RCP Seal Water Injection Nozzle	Figure 8-9						
MCP Pressurizer Surge Nozzle	Figure 8-10						
MCP Pressurizer Spray Nozzle							
MCP CVCS Letdown and Loop Drain Nozzle							
MCP Charging Nozzle							
MCP RHRS/SIS Nozzle							
MCP Accumulator Tank Nozzle							

Table 8-6 Accident Loads of Inlet and Outlet Nozzle on RV, SG, RCP

Node	Location	Loading Condition	Force (kips)			Moment (kips-in)		
			Fx	Fy	Fz	Mx	My	Mz
194	RV Inlet Nozzle	Design Load 1						
		Design Load 2						
107	RV Outlet Nozzle	Design Load 1						
		Design Load 2						
117	SG Inlet Nozzle	Design Load 1						
		Design Load 2						
141	SG Outlet Nozzle	Design Load 1						
		Design Load 2						
167	RCP Inlet Nozzle	Design Load 1						
		Design Load 2						
181	RCP Outlet Nozzle	Design Load 1						
		Design Load 2						

Table 8-7 Accident Reaction Force of Support Points

Node	Location	Loading Condition	Force (kips)			Moment (kips-in)		
			Fx	Fy	Fz	Mx	My	Mz
125	SG Lower Support Point(1)	Design Load 1						
		Design Load 2						
126	SG Lower Support Point(2)	Design Load 1						
		Design Load 2						
127	SG Lower Support Point(3)	Design Load 1						
		Design Load 2						
128	SG Lower Support Point(4)	Design Load 1						
		Design Load 2						
132	SG Intermediate Shell Support Point	Design Load 1						
		Design Load 2						
137	SG Upper Shell Support Point	Design Load 1						
		Design Load 2						
170	RCP Lower Support Point(1)	Design Load 1						
		Design Load 2						
171	RCP Lower Support Point(2)	Design Load 1						
		Design Load 2						
172	RCP Lower Support Point(3)	Design Load 1						
		Design Load 2						

Table 8-8 (1/2) Accident Member Force of MCP

Node	Location	Loading Condition	Force (kips)			Moment (kips-in)		
			Fx	Fy	Fz	Mx	My	Mz
107	Hot Leg	Design Load 1						
		Design Load 2						
109	Hot Leg	Design Load 1						
		Design Load 2						
111	Hot Leg	Design Load 1						
		Design Load 2						
112	Hot Leg	Design Load 1						
		Design Load 2						
113	Hot Leg	Design Load 1						
		Design Load 2						
115	Hot Leg	Design Load 1						
		Design Load 2						
117	Hot Leg	Design Load 1						
		Design Load 2						
141	Cross Over Leg	Design Load 1						
		Design Load 2						
142	Cross Over Leg	Design Load 1						
		Design Load 2						
143	Cross Over Leg	Design Load 1						
		Design Load 2						
145	Cross Over Leg	Design Load 1						
		Design Load 2						
147	Cross Over Leg	Design Load 1						
		Design Load 2						
149	Cross Over Leg	Design Load 1						
		Design Load 2						
151	Cross Over Leg	Design Load 1						
		Design Load 2						
152	Cross Over Leg	Design Load 1						
		Design Load 2						
153	Cross Over Leg	Design Load 1						
		Design Load 2						
155	Cross Over Leg	Design Load 1						
		Design Load 2						
157	Cross Over Leg	Design Load 1						
		Design Load 2						

Table 8-8 (2/2) Accident Member Force of MCP

Node	Location	Loading Condition	Force (kips)			Moment (kips-in)		
			Fx	Fy	Fz	Mx	My	Mz
159	Cross Over Leg	Design Load 1						
		Design Load 2						
160	Cross Over Leg	Design Load 1						
		Design Load 2						
161	Cross Over Leg	Design Load 1						
		Design Load 2						
163	Cross Over Leg	Design Load 1						
		Design Load 2						
165	Cross Over Leg	Design Load 1						
		Design Load 2						
167	Cross Over Leg	Design Load 1						
		Design Load 2						
181	Cold Leg	Design Load 1						
		Design Load 2						
183	Cold Leg	Design Load 1						
		Design Load 2						
185	Cold Leg	Design Load 1						
		Design Load 2						
186	Cold Leg	Design Load 1						
		Design Load 2						
189	Cold Leg	Design Load 1						
		Design Load 2						
191	Cold Leg	Design Load 1						
		Design Load 2						
194	Cold Leg	Design Load 1						
		Design Load 2						

Table 8-9 Accident Loads of Nozzles on RV, SG, MCP

Location	Coordinate	Force (kips)			Moment (kips-in)		
		Fx	Fy	Fz	Mx	My	Mz
RV Vent Nozzle	Figure 8-7						
RV DVI Nozzle							
SG MS Nozzle	Figure 8-8						
SG FW Nozzle							
RCP Seal Water Injection Nozzle	Figure 8-9						
MCP Pressurizer Surge Nozzle	Figure 8-10						
MCP Pressurizer Spray Nozzle							
MCP CVCS Letdown and Loop Drain Nozzle							
MCP Charging Nozzle							
MCP RHRS/SIS Nozzle							
MCP Accumulator Tank Nozzle							

Table 8-10 Seismic and Accident Loads on Lower Reactor Internal Assembly

Member	Load	Force (lbf)		Moment (lbf-in)	Memo
		Shear	axial		
Lower Core Support Plate	Seismic				Vertical Force on LCSP
	Accident				
	SRSS				
Core Barrel Flange	Seismic				
	Accident				
	SRSS				
Core Barrel Middle	Seismic				
	Accident				
	SRSS				
Core Barrel Bottom	Seismic				CB/LCSP Discontinuity
	Accident				
	SRSS				

Table 8-11 Seismic and Accident Loads on Upper Reactor Internal Assembly

Member	Load	Force (lbf)		Moment (lbf-in)	Memo
		Shear	axial		
Upper Core Plate	Seismic				Vertical Direction
	Accident				
	SRSS				
Upper Core Support (Plate)	Seismic				Vertical Direction
	Accident				
	SRSS				
Upper Core Support (Flange)	Seismic				
	Accident				
	SRSS				
Upper Core Support (Bottom of Skirt)	Seismic				
	Accident				
	SRSS				
Upper Core Support Column (Top)	Seismic				
	Accident				
	SRSS				
Upper Core Support Column (Bottom)	Seismic				
	Accident				
	SRSS				
Top Slotted Column (Top)	Seismic				
	Accident				
	SRSS				
Top Slotted Column (Bottom)	Seismic				
	Accident				
	SRSS				

Table 8-12 Seismic and Accident Loads on Radial Support Keys

Member	Load	Force (lbf)	
		Horizontal	Vertical
Radial Support Key	Seismic	[]
	Accident		
	SRSS		

Note: Horizontal Force per One Key

Table 8-13 Seismic and Accident Loads between Vessel / Reactor Internals Interface Loads

Member	Load	Force (lbf)	
		Horizontal	Vertical
Core Barrel Flange I / F	Seismic	[]
	Accident		
	SRSS		
Radial Support	Seismic		
	Accident		
	SRSS		
USP Flange I / F	Seismic	[]
	Accident		
	SRSS		

Note: Contact surface angle []

Table 8-14 Seismic and Accident Loads on RV Head Nozzles and IHP Lug

Member	Load	Force (lbf)			Moment (lbf-in)		
		Fx	Fy	Fz	Mx	My	Mz
CRDM Nozzle	Seismic						
	Accident						
	SRSS						
ICIS Nozzle	Seismic						
	Accident						
	SRSS						
TC Nozzle	Seismic						
	Accident						
	SRSS						
RV Water Level Instrumentation Nozzle	Seismic						
	Accident						
	SRSS						
IHP Lug	Seismic						
	Accident						
	SRSS						

Note: Loads for RV Head nozzles are defined at the elevation on the outer surface of the vessel head.

Table 8-15 Seismic and Accident Loads on CRDM

Member	Load	Force (lbf)		Moment (lbf-in)
		Shear	axial	
Bottom of Rodtravel Housing	Seismic			
	Accident			
	SRSS			
Bottom of Latch Housing (Weld Junction)	Seismic			
	Accident			
	SRSS			

Table 8-16 Seismic Loads of PZR Component

Part	Node	Forces (kips)			Moment (kips-in)		
		Fx	Fy	Fz	Mx	My	Mz
Upper Support Point	11						
Lower Head	3						
Skirt	111						

Note : Location of Upper Support Point of Node 11 is presented in Figure 7-1.

Table 8-17 Seismic Loads of PZR Nozzles

Part	Coordinate	Forces (kips)			Moment (kips-in)		
		Fx	Fy	Fz	Mx	My	Mz
Surge Nozzle	Figure 8-23						
Spray Nozzle							
Safety Valve Nozzle							
Relief Valve Nozzle							

Table 8-18 Accident Loads of PZR Nozzles

Part	Coordinate	Forces (kips)			Moment (kips-in)		
		Fx	Fy	Fz	Mx	My	Mz
Surge Nozzle	Figure 8-23						
Spray Nozzle							
Safety Valve Nozzle							
Relief Valve Nozzle							

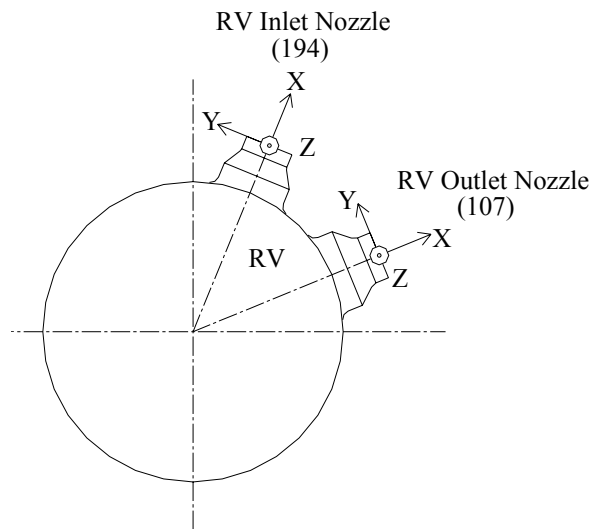


Figure 8-1 RV Nozzle Load

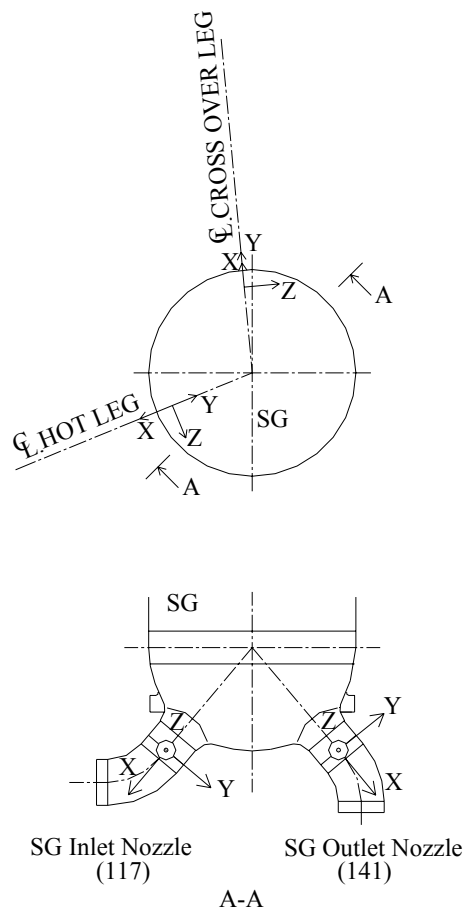


Figure 8-2 SG Nozzle Load

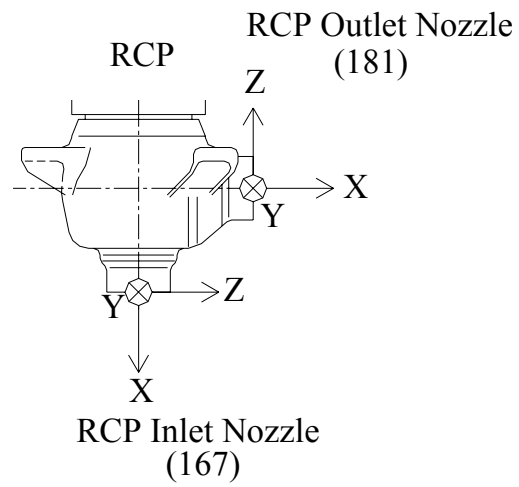
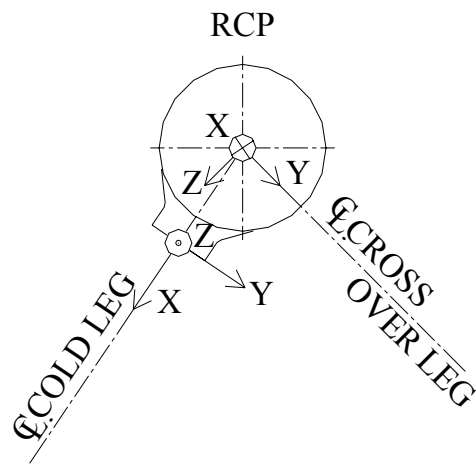
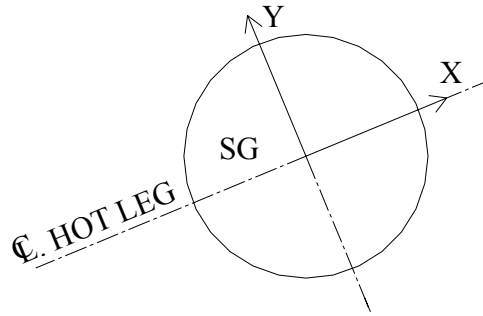
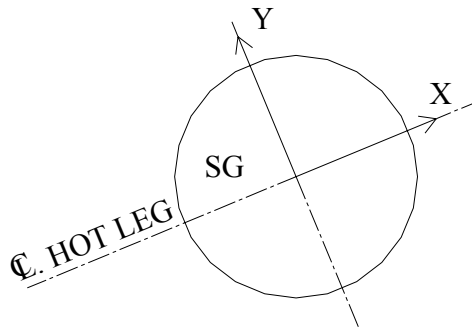


Figure 8-3 RCP Nozzle Load



SG Upper Shell Support Point
(137)



SG Intermediate Shell Support Point
(132)

SG Lower Support
Point(2)
(126)

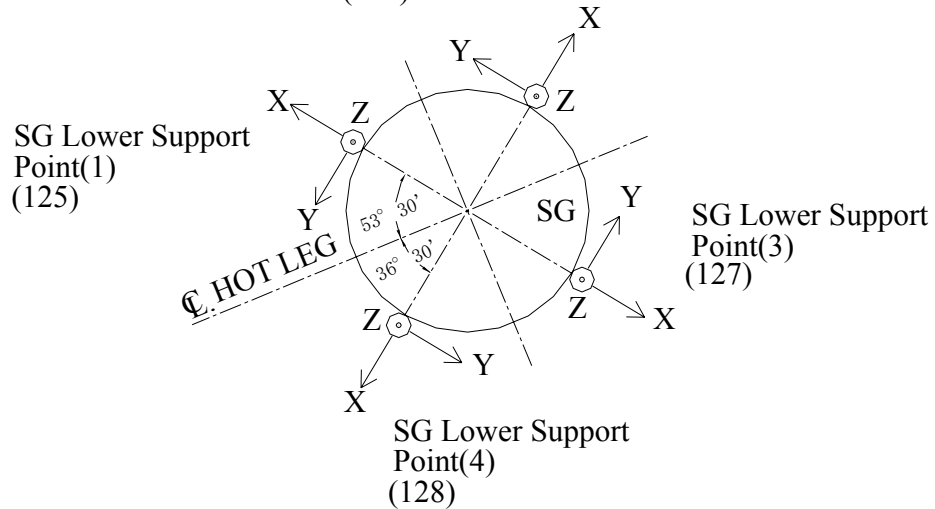


Figure 8-4 Reaction Force of SG Support Points

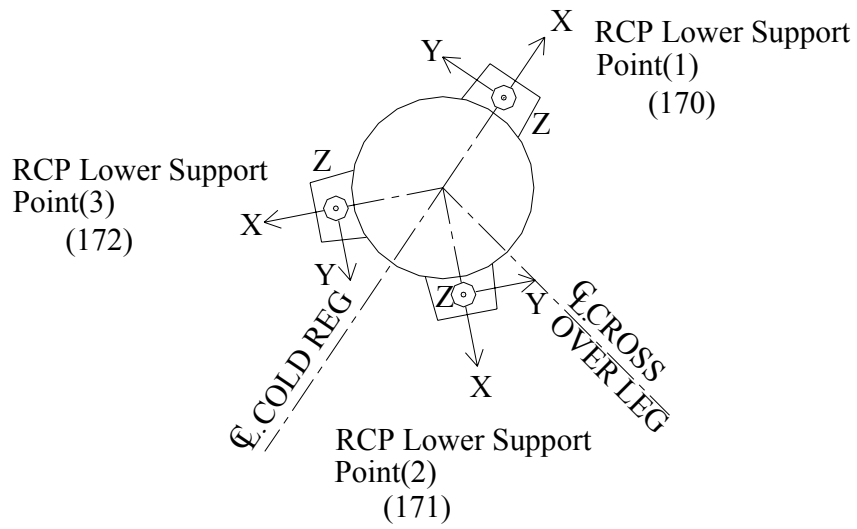


Figure 8-5 Reaction Force of RCP Lower Support Points

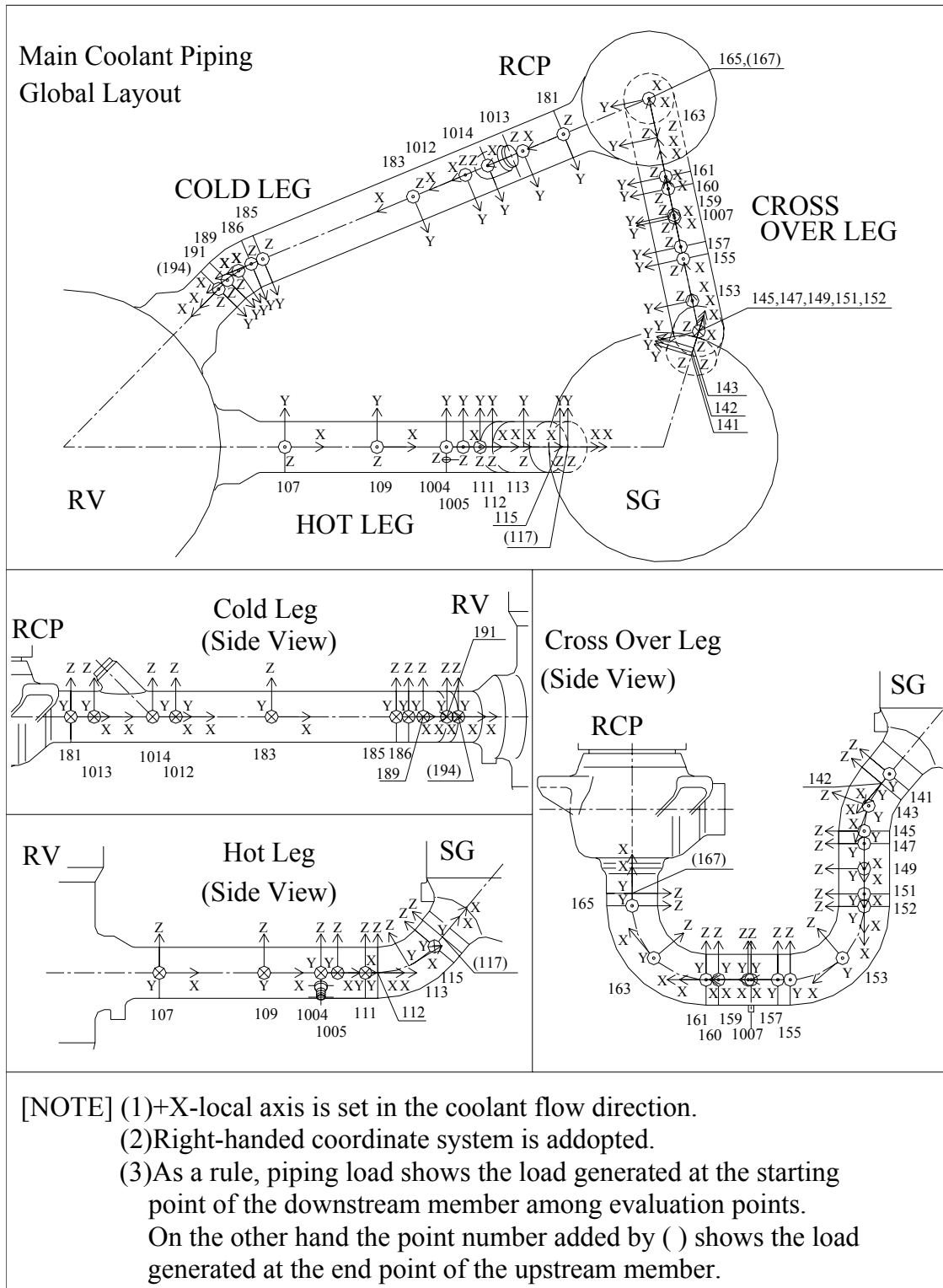


Figure 8-6 MCP Member Forces

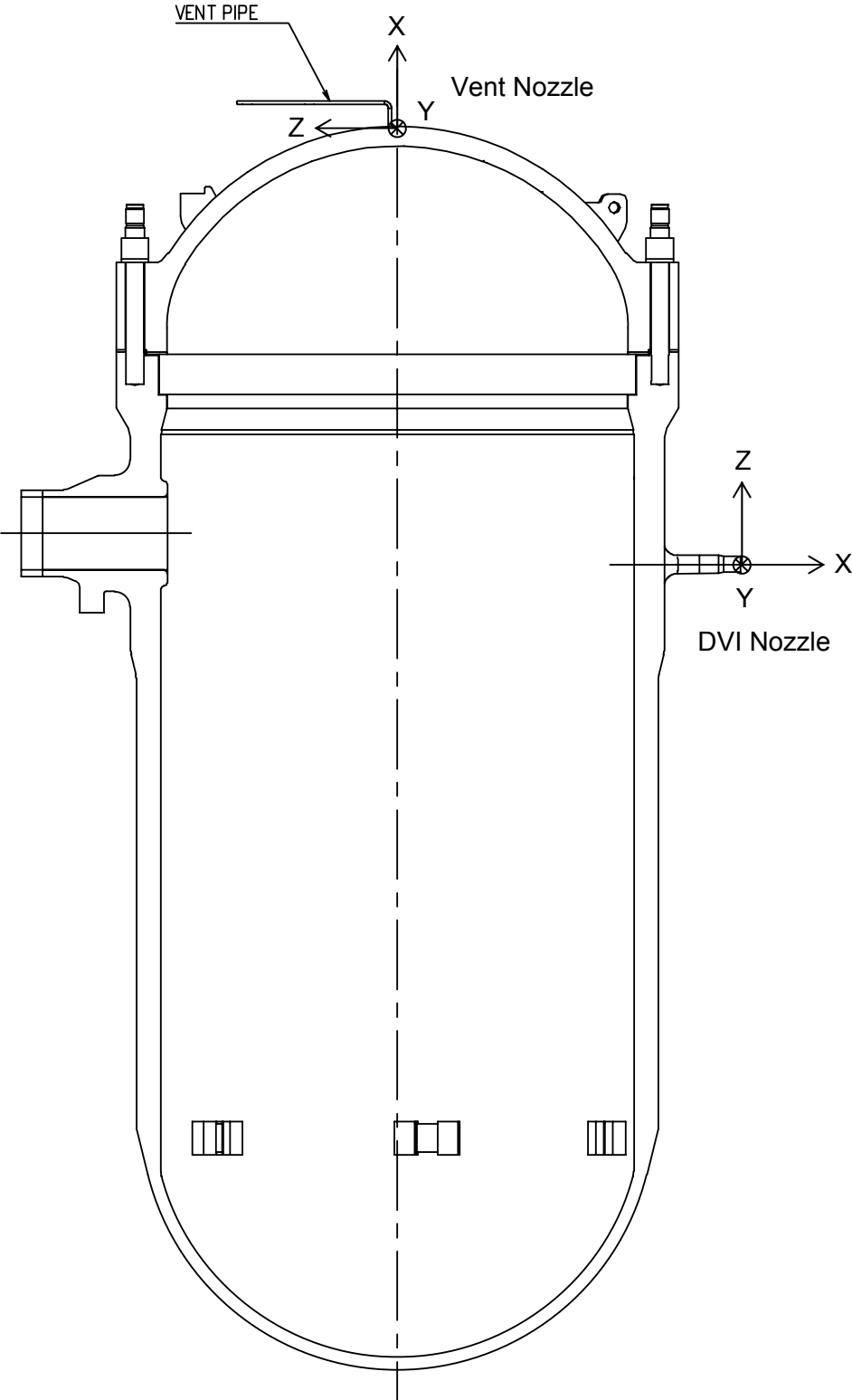


Figure 8-7 RV Nozzles

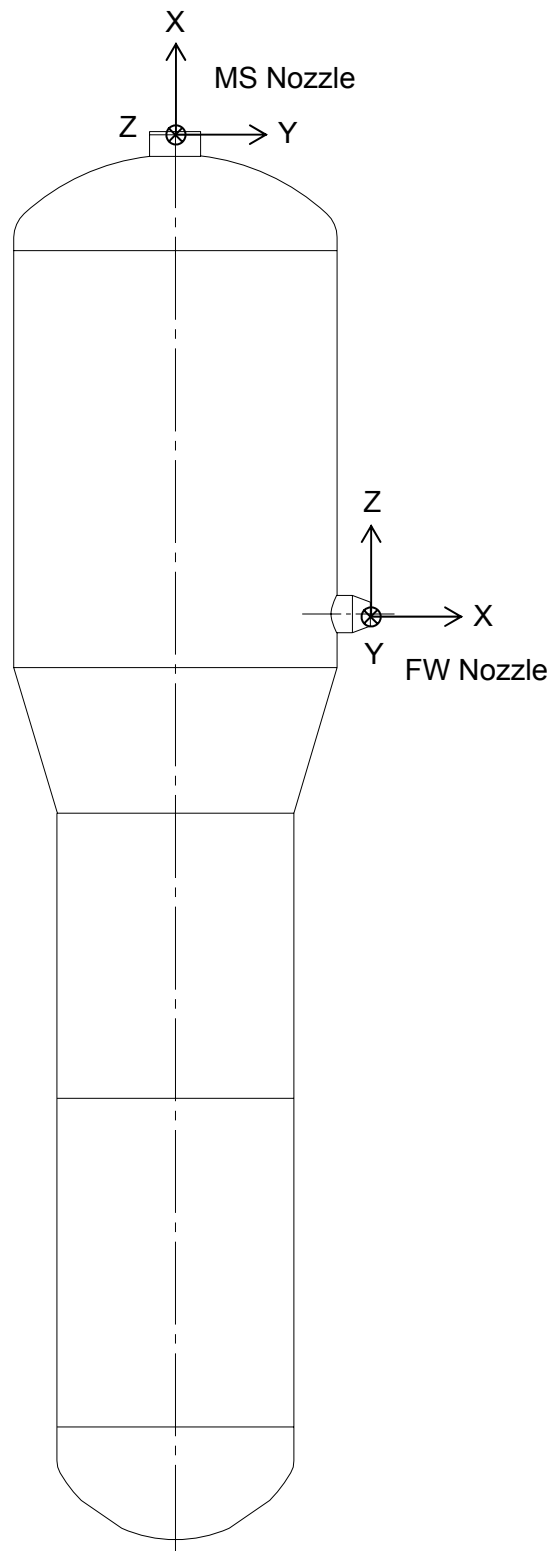


Figure 8-8 SG Nozzles

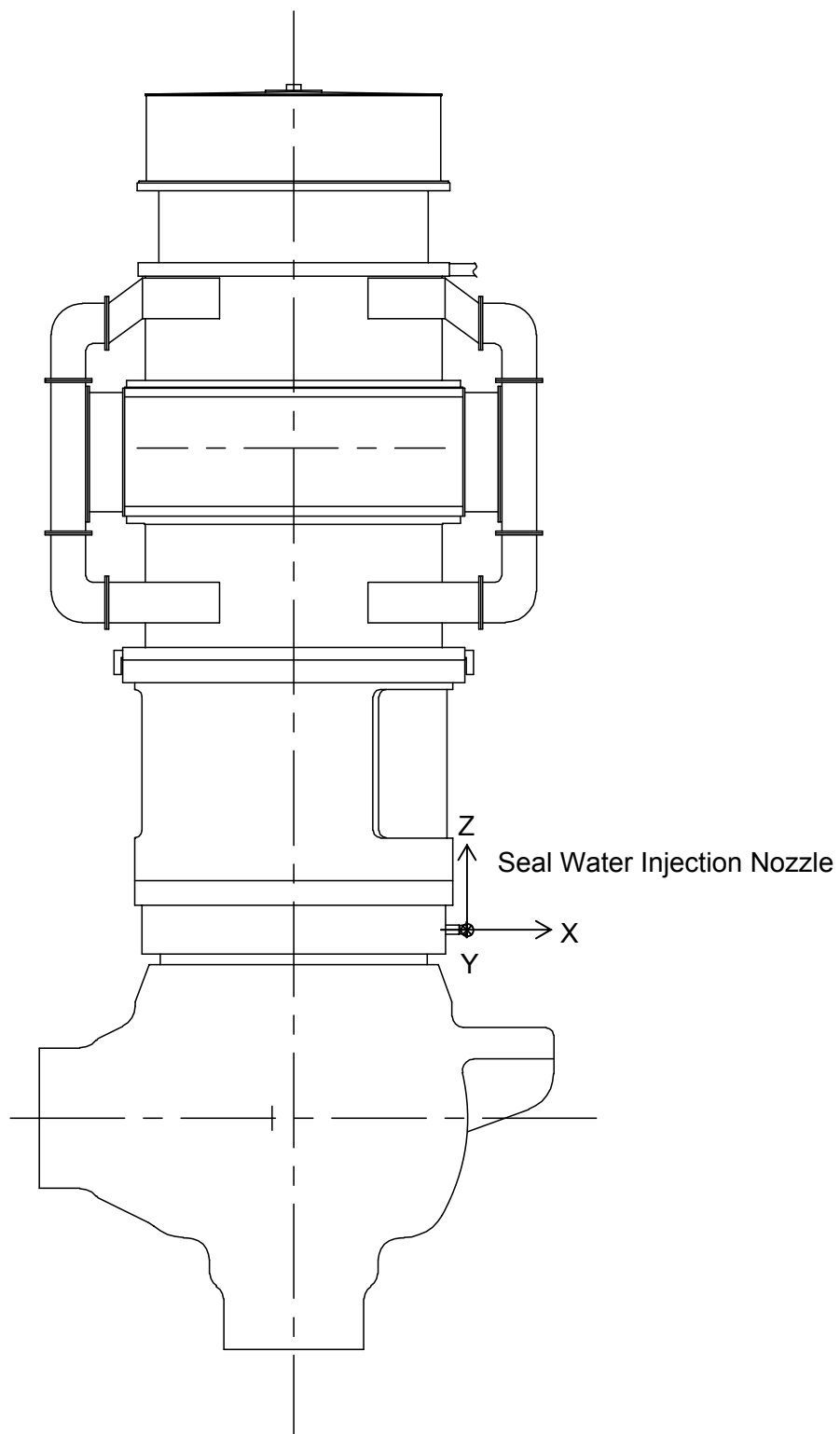


Figure 8-9 RCP Nozzle

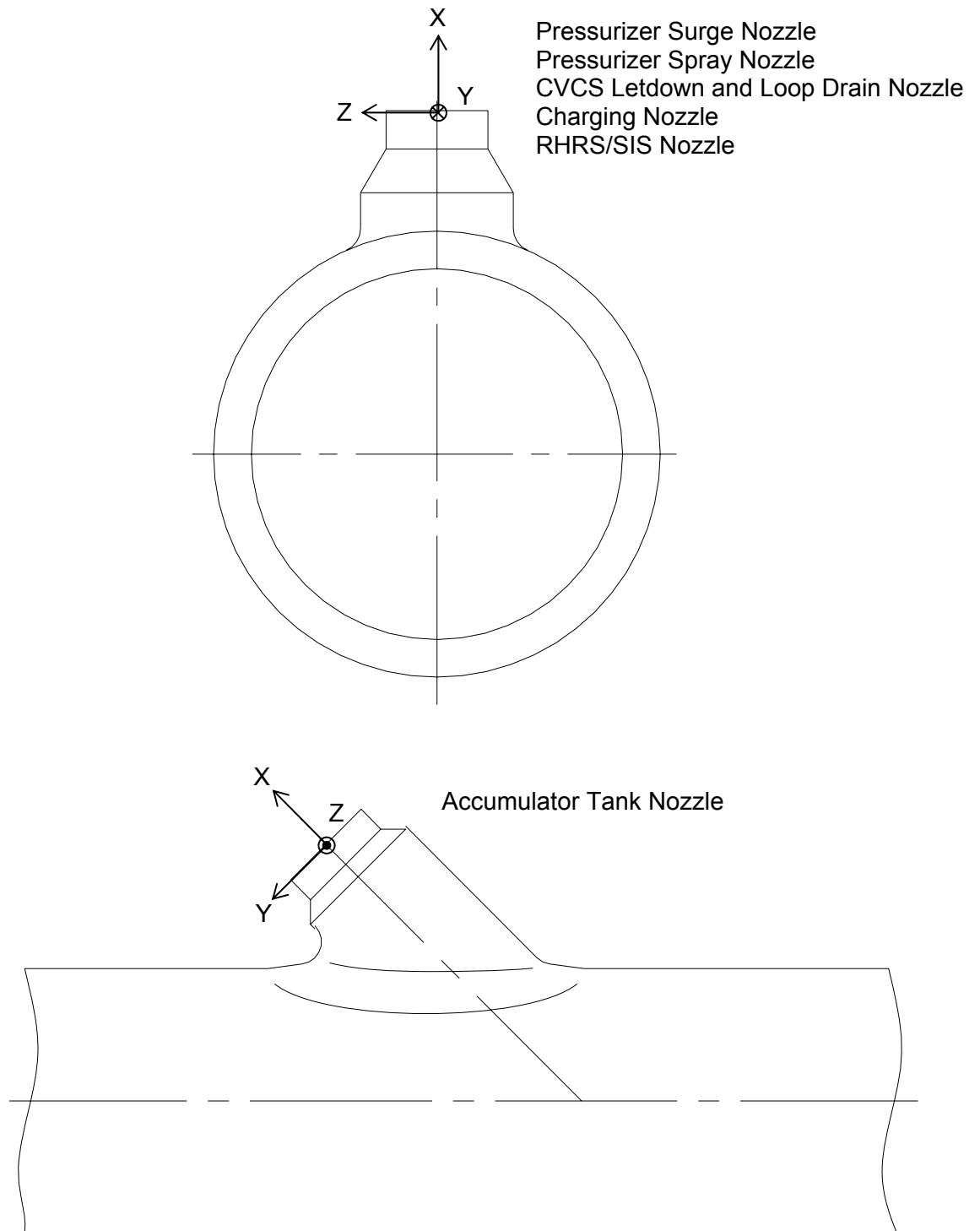


Figure 8-10 MCP Nozzles

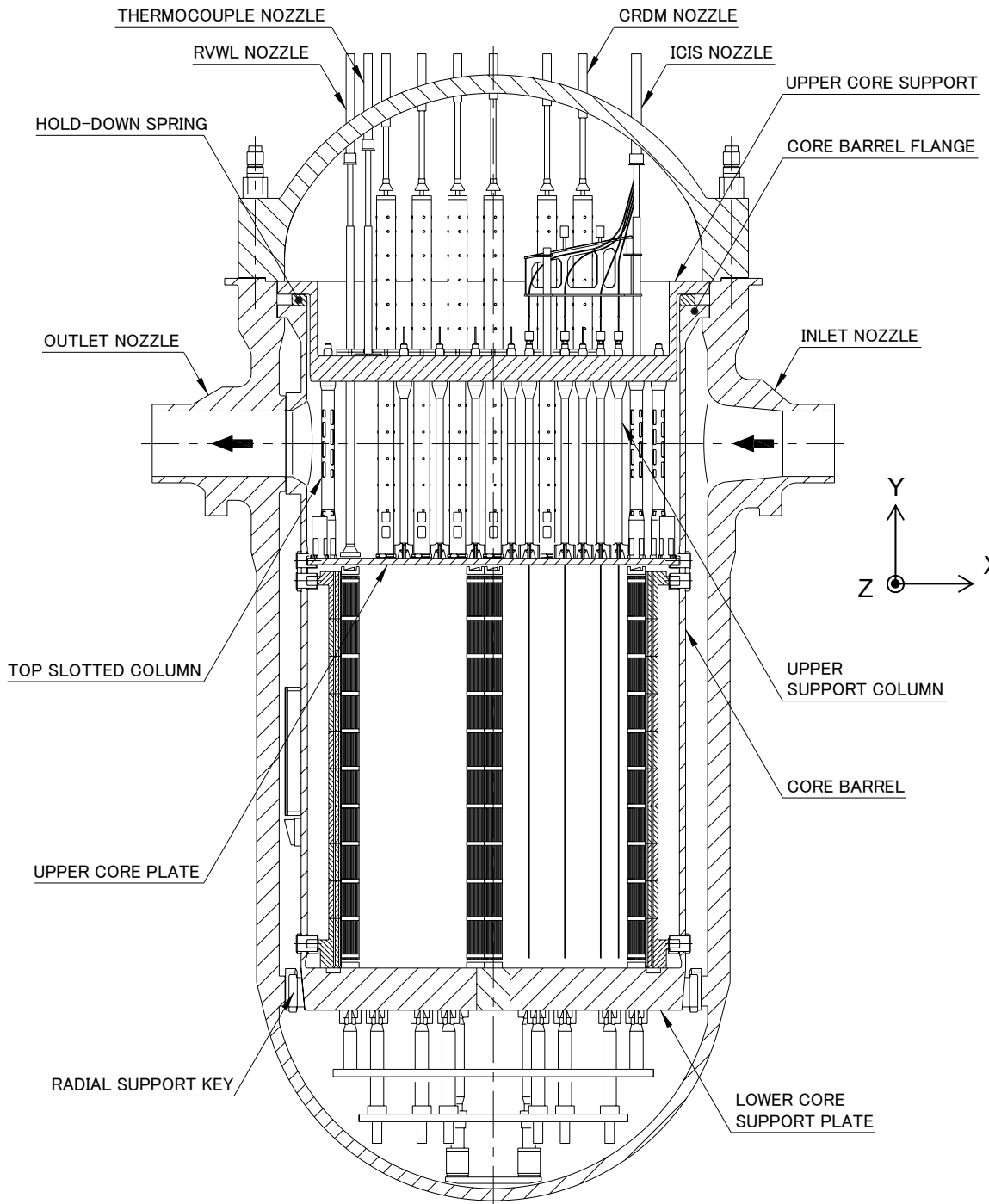


Figure 8-11 RV and Reactor Internals

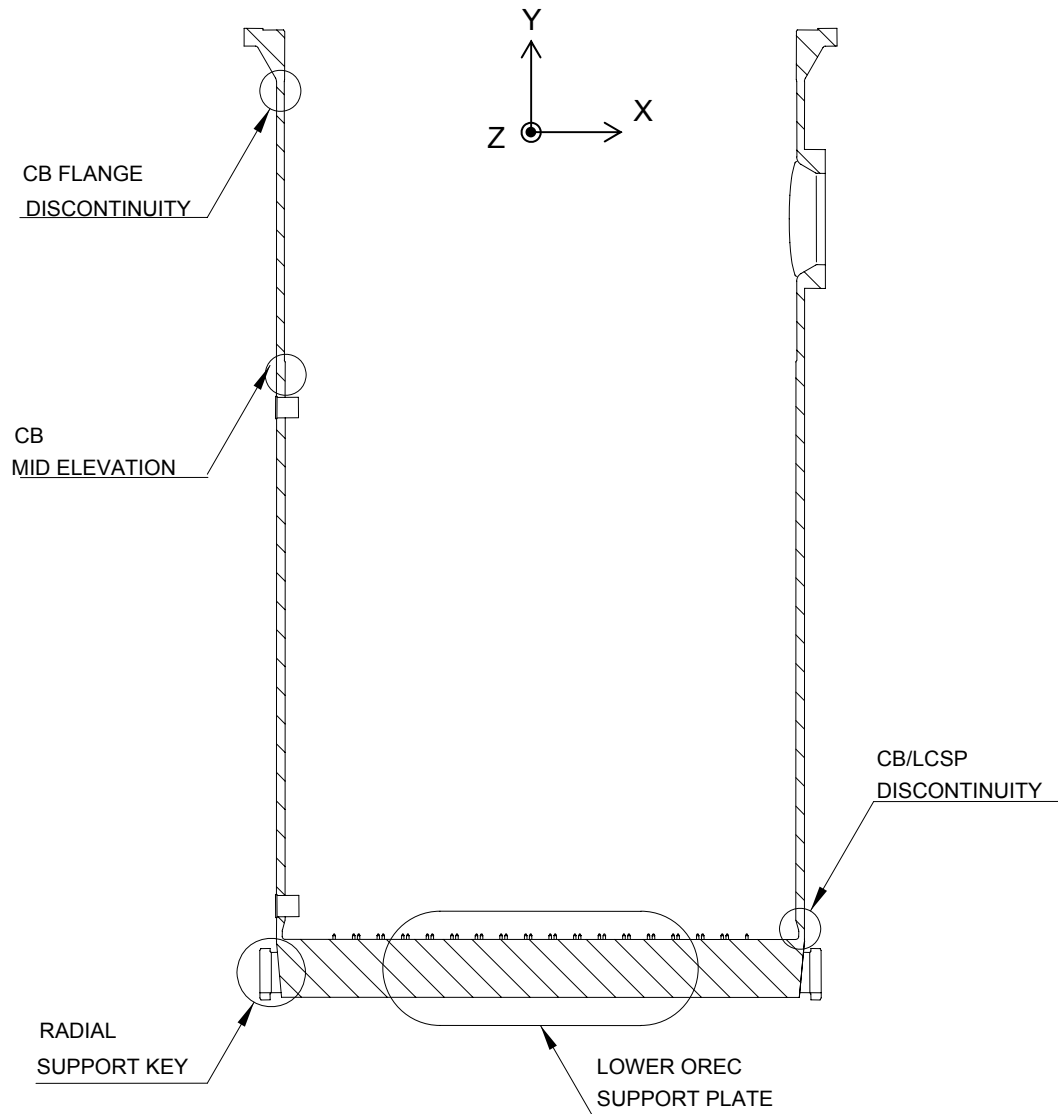


Figure 8-12 Locations of Stress Evaluation on Lower Reactor Internal Assembly

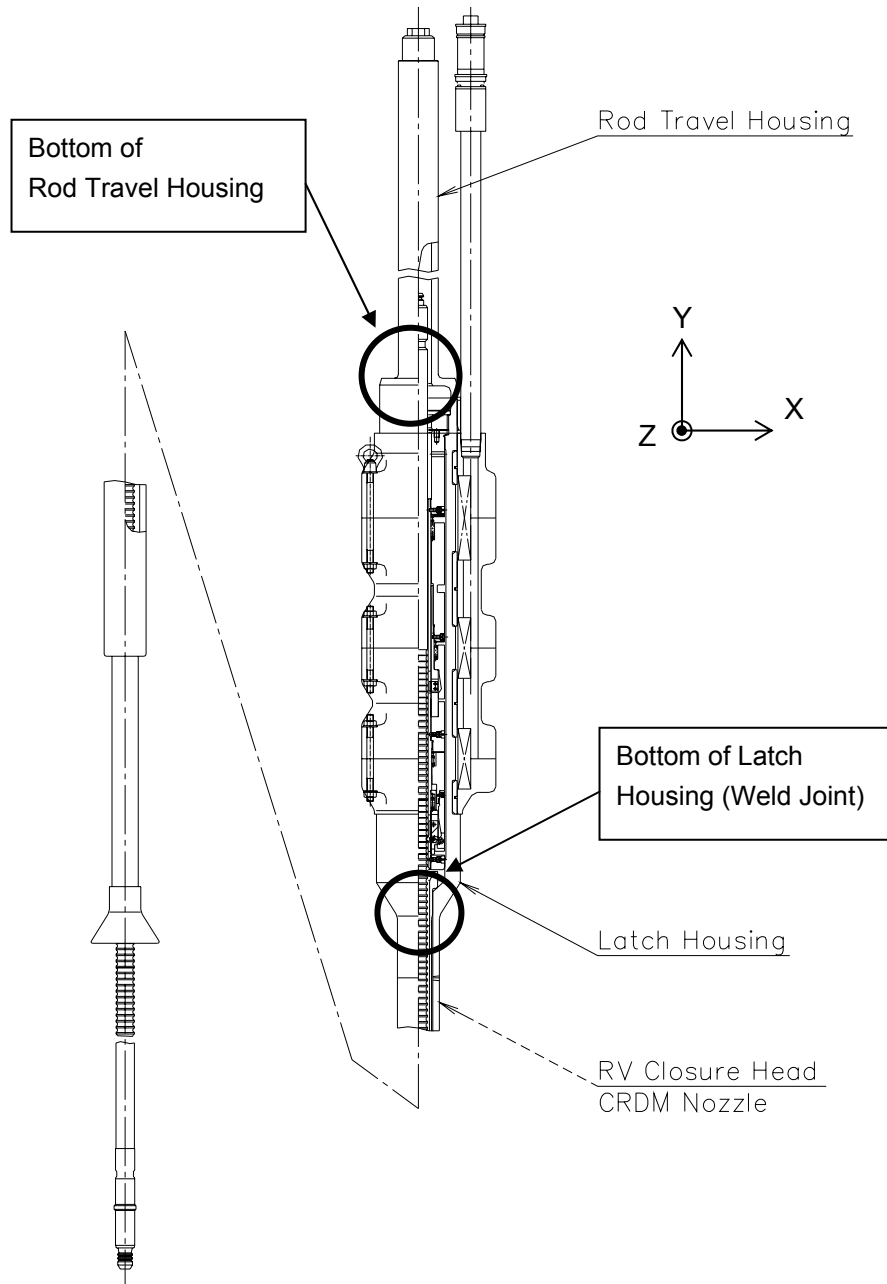


Figure 8-14 CRDM Assembly



Figure 8-15 Axial Force vs Elevation on CRDM (SSE+LOCA)



Figure 8-16 Shear Force vs Elevation on CRDM (SSE+LOCA)



Figure 8-17 Bending Moment vs Elevation on CRDM (SSE+LOCA)



Figure 8-18 Horizontal UCP Acceleration during SSE



Figure 8-19 Horizontal LCSP Acceleration during SSE



Figure 8-20 Horizontal UCP Acceleration during LOCA



Figure 8-21 Horizontal LCSP Acceleration during LOCA

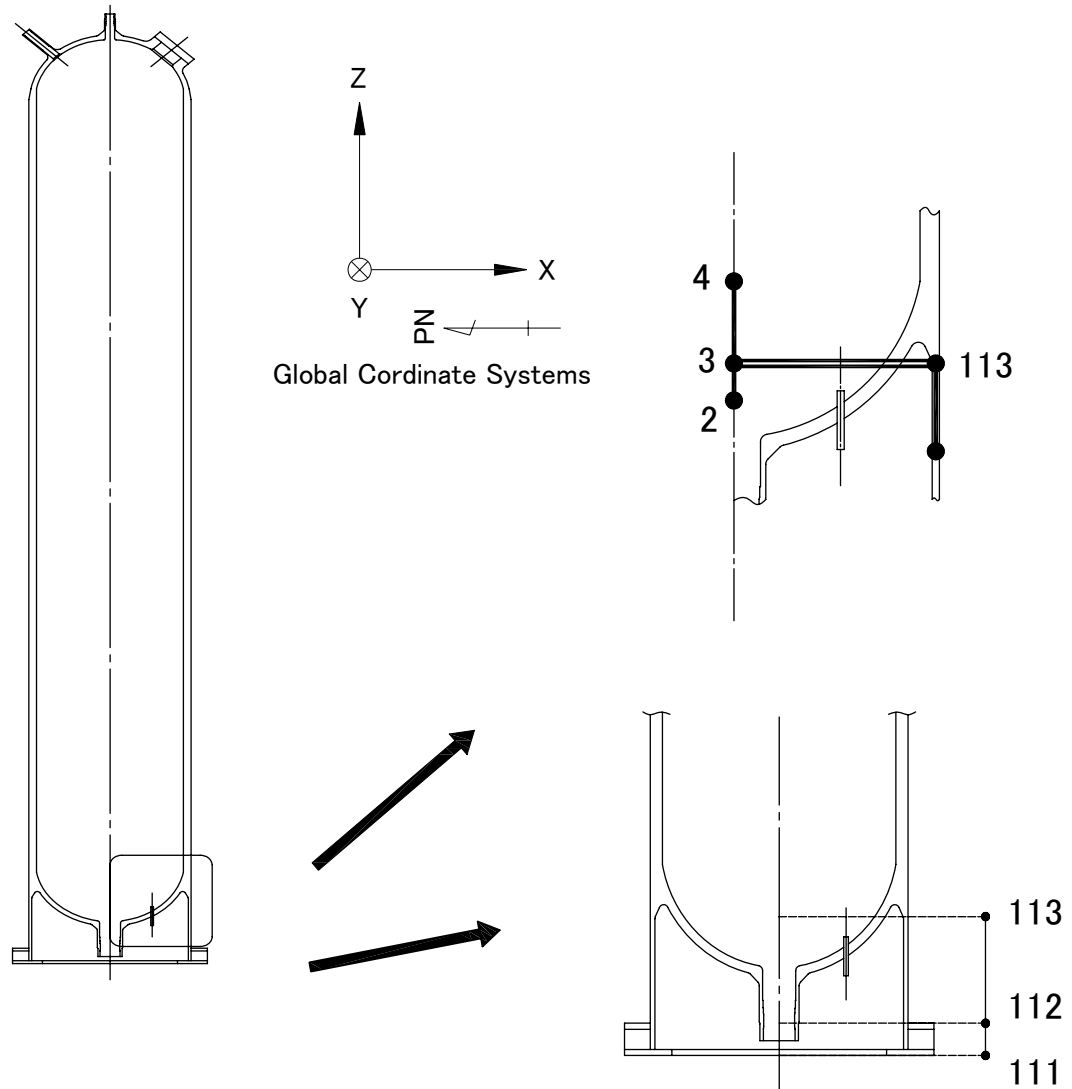


Figure 8-22 Reaction Force of PZR Lower Elements

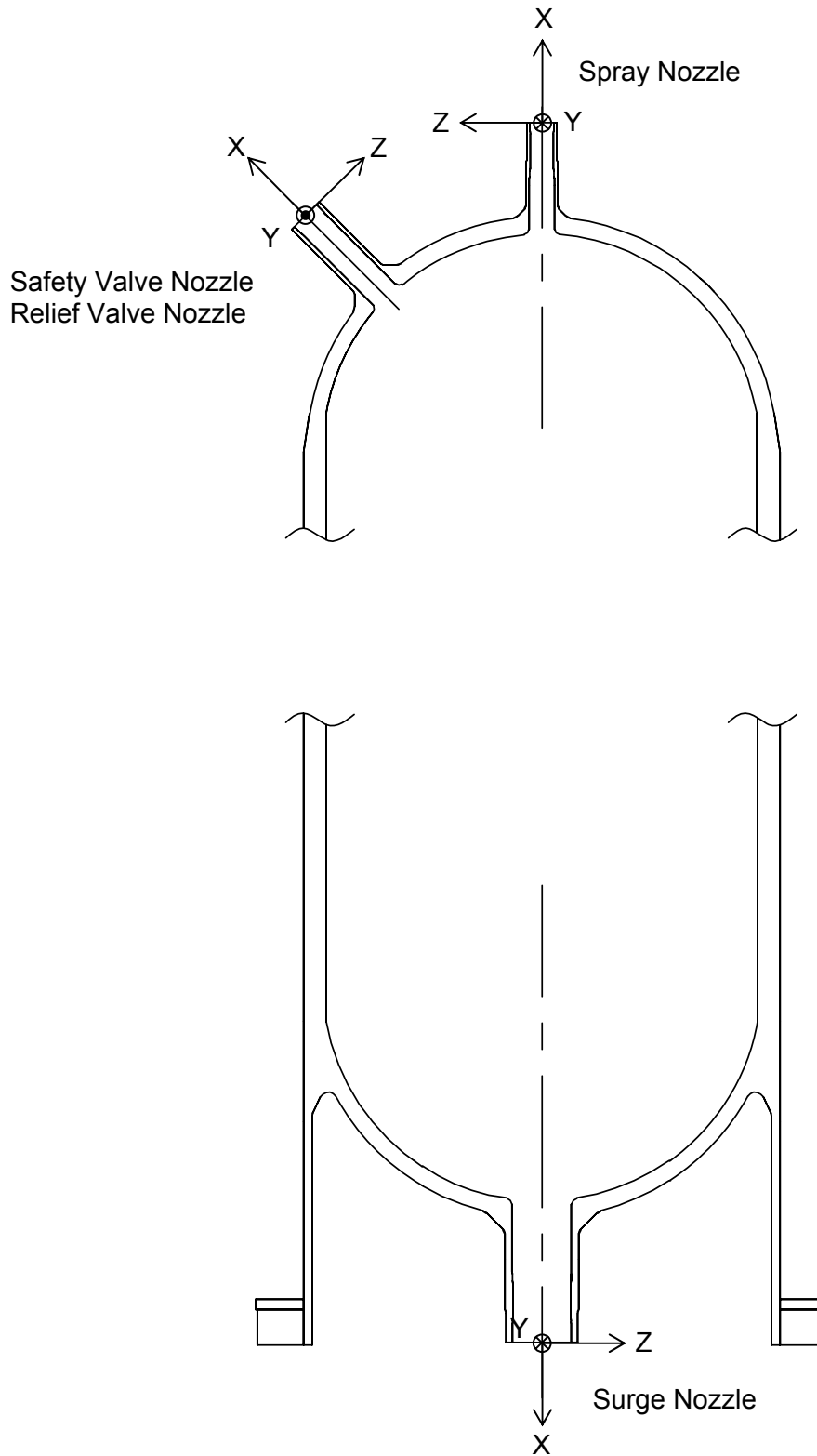


Figure 8-23 PZR Nozzles

9.0 COMPUTER PROGRAM

- MULTIFLEX Code

The MULTIFLEX computer code was used for the blowdown analysis in the primary system hydraulic load evaluation of the postulated pipe break. MULTIFLEX code is a computer program which calculates the transient of pressure, flow rate and density during the initial phase of the blowdown in a complex system such as the primary coolant system of a PWR. MULTIFLEX code includes mechanical structure models and their interactions with thermal hydraulic system. The general characteristics of MULTIFLEX are shown in the following;

- (a) The complex system is modeled with one-dimensional hydraulic piping.
- (b) The flow conditions within the system are calculated by solving the method of characteristics.
- (c) MULTIFLEX includes heat transfer models of the core and the SG, and also simulates various boundary condition of the PWR system including the core.

The calculated results of MULTIFLEX (pressure, flow rate and so on) are used in the RV internals load evaluation and the RCL mechanical load evaluation. MULTIFLEX code includes the fluid-structure interaction model, which enable to simulate the effect of flow path area change due to the motion of the core barrel. During blowdown phase of the LOCA, the core barrel walls surrounding a hydraulic flow path deviate from their neutral position depending on the force differential on the wall. In the calculation, the wall displacements are represented by those of 1-dimensional mass points which are described by mechanical equations of vibration. Ten of the mass points are used for modeling of the core barrel.

MULTIFLEX code had been approved by NRC (Reference 11), and the analysis model described in this report is the same as that of US conventional plants evaluated by Westinghouse.

- M-RELAP5 Code

The M-RELAP5 computer code was used for the SB-LOCA blowdown analysis. This code model is described in Reference 12.

The M-RELAP5 is a code improved by MHI from RELAP5-3D code. One of the main improvements is an addition of Moody's critical flow model. The Moody's critical flow model is used in the calculation of the break flow out of the highly pressurized the RV during the blowdown phase of the postulated pipe break. The Moody's model is acceptable to critical flow phenomena, which is shown in ANSI/ANS-58.2-1988. (Reference 6)

RELAP5-3D code, which is the original source of M-RELAP5, has been developed at Idaho National Laboratory. RELAP5 is a highly generic code that, in addition to calculating the behavior of the RCS during a transient, can be used for simulation of a wide variety of hydraulic and thermal transients in both nuclear and nonnuclear systems involving mixtures of vapor, liquid, noncondensable gases, and nonvolatile solute.

The code models the coupled behavior of the RCS and the core for the LOCA and operational transients such as anticipated transient without scram, loss of offsite power, loss of feedwater, and loss of flow.

The code includes many generic component models from which general systems can be simulated. The component models include pumps, valves, pipes, heat releasing or absorbing structures, reactor kinetics, electric heaters, jet pumps, turbines, separators, annuli, PZR's, feedwater heaters, ECC mixers, accumulators, and control system components. In addition, special process models are included for effects such as form loss, flow at an abrupt area change, branching, choked flow, boron tracking, and noncondensable gas transport.

A set of equation of RELAP5 gives a two-fluid system simulation using a nonequilibrium, nonhomogeneous, six-equation representation. The presence of boron and noncondensable gases is also simulated using separate equations for each. Constitutive models represent the interphase drag, the various flow regimes in vertical and horizontal flow, wall friction, and interphase mass transfer.

- GOTHIC Code

The GOTHIC computer code was used for the asymmetric pressurization analysis. GOTHIC is a general purpose thermal-hydraulics code for performing design, licensing, safety and operating analysis of nuclear power plant containments and other confinement buildings (Reference 13).

GOTHIC solves the conservation equations for mass, momentum and energy for multi-component, multi-phase flow in lumped parameter and/or multi-dimensional geometries. The phase balance equations are coupled by mechanistic models for interface mass, energy and momentum transfer that cover the entire flow regime from bubbly flow to film/drop flow, as well as single phase flows. The interface models allow for the possibility of thermal non-equilibrium between phases and unequal phase velocities, including countercurrent flow. GOTHIC includes full treatment of the momentum transport terms in multi-dimensional models, with optional models for turbulent shear and turbulent mass and energy diffusion.

The principal element of a model is a control volume, which is used to model the space within a building or subsystem that is occupied by fluid. The fluid may include non-condensing gases, steam, drops or liquid water. GOTHIC features a flexible nodal scheme that allows computational volumes to be treated as lumped parameter (single node) or one-, two- or three-dimensional, or any combination of these within a single model.

Flow paths model hydraulic connections between any two computational cells, which includes lumped parameter volumes and cells in subdivided volumes. Flow paths are also used to connect boundary conditions to computational cells where mass, momentum and energy can be added or removed. A separate set of momentum equations (one for each phase) is solved for each flow path.

Initial conditions allow the user to specify the state of the fluid and solid structures within the modeled region at the start of a transient. These include the initial temperature and composition of the atmosphere.

Additional resources available to expand the realm of situations that can be modeled by GOTHIC include functions, control variables, trips and material properties.

Using a conservative model prescription, GOTHIC predicts the time dependent compartment differential pressure.

- ANSYS Code

The ANSYS code is a general purpose finite element analysis program for linear and nonlinear, static and dynamic, structural, thermal, or other various problems, and the code has the excellent capability of pre-processing, solver, and post-processing with a comprehensive graphical user interface of the interactive access to program functions, commands, documentation, and reference material (Reference 14).

ANSYS was used for the structural analysis of RCL, RV, and PZR in this report.

10.0 CONCLUSION

This report has presented the analysis of the load conditions for primary components and piping. Load values will be applied external mechanical load to stress analysis for components and piping. Stress analysis will be performed in accordance with ASME Code, Section III (Reference 2) requirements, and applied criteria of the service Level C and D service conditions. The combination of seismic load (SSE) and accident load (LOCA) will be set in conformance with SRP 3.9.3 Rev. 2 (Reference 4).

Based on these load combinations, technical reports will be shown summary of stress analysis results for primary components and piping and submit on March 2009.

11.0 REFERENCES

1. Dynamic Analysis of the Coupled RCL-R/B-PCCV-CIS, Mitsubishi Heavy Industries, Technical Report MUAP-08005 Rev.0, April 2008.
2. ASME Boiler and Pressure Vessel Code, Section III. 2001 Edition through the 2003 Addenda, American Society of Mechanical Engineers.
3. Design Response Spectra for Seismic Design of Nuclear Power Plants. Regulatory Guide 1.60, Rev.1, U.S. Nuclear Regulatory Commission, Washington, DC, December 1973.
4. ASME Code Class 1, 2 and 3 Components and Component Supports, and Core Support Structures. NUREG-0800 SRP Section 3.9.3, Rev.2, U.S. Nuclear Regulatory Commission, Washington, DC, March 2007.
5. Determination of Rupture Locations and Dynamic Effects Associated with The Postulated Rupture of Piping. NUREG-0800, SRP 3.6.2, Rev.2, U.S. Nuclear Regulatory Commission, Washington, DC, March 2007.
6. Design Bases for Protection of Light Water Nuclear Power Plants Against Effects of Postulated Pipe Rupture. ANSI/ANS-58.2-1988, American National Standards Institute/American Nuclear Society.
7. Damping Values for Seismic Design of Nuclear Power Plants. Regulatory Guide 1.61, Rev.1, U.S. Nuclear Regulatory Commission, Washington, DC, March 2007.
8. Summary of Stress Analysis Results for Reactor Coolant Loop Branch Piping. Mitsubishi Heavy Industries, Technical Report, LATER
9. Dynamic Testing and Analysis of Systems, Structures, and Components. NUREG-0800, SRP 3.9.2, Rev.3, U.S. Nuclear Regulatory Commission, Washington, DC, March 2007.
10. Combining Modal responses and Spatial Components in Seismic Response Analysis. Regulatory Guide 1.92, Rev.2, U.S. Nuclear Regulatory Commission, Washington, DC, July 2006.
11. Evaluation of Westinghouse Topical Reports WCAP-8708(P) and WCAP-8709(NP). Letter from John F. Stolz (NRC) to C. Elicheldinger (Westinghouse) dated JUN 17, 1977.
12. Small Break LOCA Methodology for US-APWR. Mitsubishi Heavy Industries, Topical Report MUAP-07013-P Rev.0, July 2008.
13. GOTHIC Containment Analysis Package User Manual. Version 7.2a(QA), NAI 8907-02, Rev.17, Numerical Applications Inc., Richland, WA, January 2006.
14. ANSYS, Finite Element Structural Analysis Program, Release 11.0, ANSYS, Inc., Canonsburg, PA, 2007.